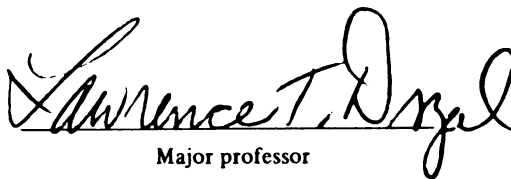This is to certify that the

thesis entitled

EFFECT OF POLYMER MODIFICATION ON THE PROPERTIES

OF ASPHALT CONCRETE

presented by

ALEKH S. BHURKE

has been accepted towards fulfillment
of the requirements for

____M.S.____degree in _MATERIALS_SCIENCE

Major professor

Date __11/12/99__

**PLACE IN RETURN BOX** to remove this checkout from your record.
**TO AVOID FINES** return on or before date due.
**MAY BE RECALLED** with earlier due date if requested.

| DATE DUE | DATE DUE | DATE DUE |
|----------|----------|----------|
|          |          |          |
|          |          |          |
|          |          |          |
|          |          |          |
|          |          |          |
|          |          |          |
|          |          |          |
|          |          |          |
|          |          |          |
|          |          |          |

11/00  c:/CIRC/DateDue.p65-p.14

# EFFECT OF POLYMER MODIFICATION ON THE
# PROPERTIES OF ASPHALT CONCRETE

By

Alekh S. Bhurke

A THESIS

Submitted to
Michigan State University
In partial fulfillment of the requirements
For the degree of

MASTER OF SCIENCE

Department of Materials Science & Mechanics

1999

El

A:

degradatio

a method

binder an

of this res

Fi

Styrene (S

used to m

morpholog

asphalt bi

asphalt co

microstruc

enhance b

asphalt con

# ABSTRACT

## EFFECT OF POLYMER MODIFICATION ON THE PROPERTIES OF ASPHALT CONCRETE

By

Alekh S. Bhurke

Asphalt pavements fail due to variety of reasons ranging from climatic changes to degradation of material properties. Polymer modification of asphalt has been evaluated as a method to enhance pavement performance. The interfacial adhesion between asphalt binder and aggregate and its effect on the final properties of asphalt concrete is the focus of this research.

Five polymers, Styrene Butadiene Styrene (SBS), Styrene Ethylene Butylene Styrene (SEBS), Styrene Butadiene Rubber (SBR), Elvaloy AM and Crumb Rubber were used to modify two viscosity graded asphalt binders, AC5 and AC10. The microstructure, morphology, failure mechanisms and locus of failure were identified in polymer modified asphalt binder and concrete. Fracture toughness and lap-shear adhesive strength of asphalt concrete were measured. Asphalt binder was found to have an intrinsic network microstructure which plays a role in fracture process. Polymer modification was found to enhance binder-aggregate adhesion, engineering properties and resistance to aging in asphalt concrete.

To
My loving parents

And

Sir Pelham Grenville Wodehouse
Whose writings never fail to
Gruntle me.

I wi

directed thi

guidance: th

results prese

Dr. Joon Le

I also

research and

not have bee

# ACKNOWLEDGEMENTS

# TABLE OF CONTENTS

# LIST OF TABLES

# LIST OF FIGURES

Th

the rest of

required

developme

across the

pavements

of paveme

extremes s

40°C durir

problem of

Tha

States Cor

performanc

Some of th

polymers a

As

(crushed s

60°C) ar

aggregate

concrete

# CHAPTER ONE

## INTRODUCTION

The vast network of asphalt concrete pavements in the State of Michigan, as in the rest of the United States, is showing signs of premature distress. The frequent repairs required by failed pavements is a concern for the authorities charged with the development and maintenance of road transport. Various Departments of Transportation across the country are looking at methods for improving the lifetime and performance of pavements in an effort to reduce the overall costs. In the State of Michigan, this problem of pavement failure is particularly serious due to the geographical location and climatic extremes seen in the state. Temperatures vary widely during the course of a year, nearing 40°C during the summer and drop well below -20°C during the winters, which makes the problem of pavement distress even more acute.

The Strategic Highway Research Program (SHRP) was established by the United States Congress in 1987 as a 5-year, $150 million research program to improve the performance and durability of the nation's roads and to make them safer for motorists. Some of the studies undertaken by SHRP indicate that the modification of asphalt with polymers and other additives can improve the lifetime of asphalt concrete pavements.

Asphalt concrete is a mixture of asphalt binder (asphalt cement) and aggregate (crushed stone). Asphalt binder is a black, viscous liquid at high temperatures (~ 40-60°C) and becomes a hard and very brittle solid at low temperatures (~0°C). The aggregates are the load-bearing phase held together by the asphalt binder, making asphalt concrete a composite material. Asphalt binder is a mixture of hydrocarbons left over from

1

the refinir

depending

binder car

variations

in the sam

enhance t

[1]. For th

although c

their struc

different.

modificati

specificati

of asphalt

account an

set of speci

Wh

the case o

added to a

may be va

application

asphalt c

(MDoT)

binders, e

the refining of crude oil. It consists of the last remaining fractions of processed crude and depending on the quality of the crude, the composition and properties of the asphalt binder can change. Asphalt binder thus produced rarely has uniform properties; subtle variations in properties are detectable in different batches produced from the same crude in the same process facility. Modifiers are typically added to the asphalt binder phase to enhance the properties of asphalt binder which in turn enhance pavement performance [1]. For this reason, asphalt binders are characterized on the basis of their viscosity and although different binders with the same viscosity grade can be said to behave similarly, their structure, chemical, physical and thermodynamic properties may be entirely different. It is this variability that adds to the difficulty of evaluating different methods of modification of asphalt. As a result, SHRP recommended a set of performance based specifications based on chemical and thermodynamic properties for the characterization of asphalt binders used in pavements [2]. The SHRP specifications do not take into account any modifications that may be made to the asphalt binder, recommending that the set of specifications be applied to the final asphalt binders.

While this approach may be pragmatic, it may prove to be inadequate by itself in the case of modified asphalts. Various types of modifiers, especially polymers, when added to asphalt can cause different properties to change in different ways [3-5]. There may be various ways in which different modifiers can work to improve properties and the application of one set of standards may not be able to predict all the properties of the asphalt concrete. Keeping this in mind, the Michigan Department of Transportation (MDoT) has initiated research into the use of SHRP specifications for modified asphalt binders, especially polymer modified asphalt binders. As part of this study at Michigan

State Uni

physical a

properties

concrete.

morpholog

## 1.1   Ty

Th

cracking.

these failt

different n

expansion

can enter

expansion

in the form

temperatur

fracture un

binder and

viscosity

loads.  A

accelerate

State University, a three pronged program was founded to characterize: i) chemical, physical and thermodynamic properties of asphalt; ii) microstructural and morphological properties of asphalt binder and asphalt concrete and iii) engineering properties of asphalt concrete. This thesis presents some of the investigations into the microstructural and morphological properties of polymer modified asphalt binder and asphalt concrete.

## 1.1 Types of Pavement Distresses

The main types of pavement distresses found in asphalt concrete are thermal cracking, fatigue cracking, rutting, ravelling, stripping and aging [6-8]. The causes for these failures are summarized in Table 1.1. Thermal cracking can result from three different mechanisms which are not mutually exclusive. Different coefficients of thermal expansion can cause thermal strains leading to cracking of the asphalt concrete. Water can enter the existing cracks and during winters, the freeze-thaw cycling can lead to expansion and widening of these cracks. Catastrophic failures of this nature can be seen in the form of eruption of pavements. The third cause for thermal cracking is the low temperature brittleness during winter which makes the pavement more susceptible to fracture under applied traffic loads. Aging of the asphalt occurs due to oxidation of the binder and the loss of oils due to volatilization during service. This can increase the viscosity of the asphalt, making it very brittle, hard and susceptible to fracture under loads. Aging of asphalt occurs over years during normal service and the process is accelerated by high temperatures and other environmental factors.

Pave

Ther

Agin

Fatig

Rutti

Ravel

Fa

is essenti

grow ove

the asphal

microstru

under loa

due to r

Ravelling

aggregate

temperatu

deformati

increases

binder-ag

as the we

**Table 1.1 Typical pavement distresses and their causes**

| Pavement Distress | Cause |
|---|---|
| Thermal Cracking | - Freeze-thaw cycling<br>- Low temperature embrittlement during winter<br>- Different coefficients of thermal expansion |
| Aging | - Embrittlement caused by oxidation |
| Fatigue Cracking | - Tensile failure due to cyclic loading |
| Rutting | - Microstructural rearrangement of asphalt due to<br>  plastic flow under load at high temperatures |
| Ravelling/Stripping | - Adhesive fracture due to poor asphalt-aggregate adhesion |

Fatigue cracking is caused by cyclic stresses. The nature of loading on pavements is essentially cyclic and with the passage of every vehicle, a small initiating flaw can grow over time into a large crack. Fatigue failure is generally initiated at the bottom of the asphalt layers where tensile strain is greatest. Rutting is a type of failure caused by the microstructural rearrangement of the asphalt binder due to plastic deformation (flow) under load. This is typically a high temperature failure; a common indication of failure due to rutting being tire tracks left in the pavement surface during summer. Ravelling/stripping is a failure of the concrete caused by poor adhesion between the aggregate and the asphalt binder. This type of failure is particularly disastrous at low temperatures. At high temperatures, the asphalt binder is sufficiently soft to allow deformation of the binder phase, but at low temperatures when the binder modulus increases and it becomes brittle, the applied strain is transferred more efficiently to the binder-aggregate interface. With poor adhesion between the two phases, the interface acts as the weak link and cracks in the pavement can easily propagate.

The

asphalt bind

low creep

resistance t

polymers ca

adhesion an

particles en

The

characteriz

into two co

modulii de

Polymers

performanc

At high te

modulus an

low glass

blend, mas

Most of

Polymers.

affect the

cracks[25

## 1.2    Need for Polymer Modification of Asphalt

The various types of failures in asphalt can be overcome by modification of the asphalt binder with polymers [9-21]. Polymer modifiers offer several advantages such as low creep at high temperatures, high ductility at low temperatures, high toughness, resistance to moisture and temperature, high cohesive and adhesive strength. Blended polymers can modify the binder properties such as complex modulus, ductility, interfacial adhesion and cohesive strength while binders modified with heterogeneous fibers and particles enhance the final properties by changing the locus and mechanism of failure.

The complex modulus ($G^*$) of the binder is a convenient parameter to characterize the asphalt binder rheologically [22].  The complex modulus can be resolved into two components, the elastic modulus, $G'$, and the viscous modulus, $G''$ [20]. These modulii determine the behaviour of the asphalt during deformation and fracture. Polymers can increase both the elastic and viscous modulii and thus extend the performance envelope of the asphalt binders at high as well as low temperatures [23-24]. At high temperatures, the polymer modifier can toughen the binders due to their high modulus and viscosity, preventing failures such as rutting while at low temperatures, the low glass transition ($T_g$) of the polymer phase can depress the $T_g$ of the polymer-asphalt blend, making the asphalt binder softer and thus prevent brittle low temperature cracking. Most of the pavement distresses ultimately lead to fracture by various mechanisms. Polymers, whether blended with binder or particulate reinforcement, have the ability to affect these fracture processes by altering the initiation, locus and propagation of cracks[25].

Anot

distribution

propagation

expansion ar

sufficient air

crack initiato

void size and

also alleviate

One o

the asphalt bir

The strength o

role in the low

modulus increa

tough interface

*interface* is a n

not a simple tw

than the bulk o

region forming

should be used

occurs. A schen

the interphase

dependent on

chemical comp

Another factor affecting the performance of asphalt concrete is the size and distribution of air voids. Void microstructure and morphology is related to initiation and propagation of cracks [18, 25]. Voids are necessary in asphalt concrete to provide for expansion and flow of the binder at high temperatures as well as water drainage. Without sufficient air voids, asphalt binder can bleed to the surface, while large voids can act as crack initiators. The addition of polymer modifiers to asphalt can cause changes in the void size and distribution and these changes must be studied. Polymer modification can also alleviate the effects of aging in asphalt [26].

One of the objectives of this research is to study the effect of adhesion between the asphalt binder and aggregate on the properties of polymer modified asphalt concrete. The strength of the asphalt binder-aggregate interface is believed to play an important role in the low temperature behavior of asphalt concrete. At low temperatures, the binder modulus increases and failure proceeds along the relatively weaker interface. A strong, tough interface can thus enhance the low temperature properties. The asphalt-aggregate *interface* is a misnomer since the boundary between the asphalt and aggregate phases is not a simple two dimensional boundary but a region with different physical properties than the bulk of the two phases. The asphalt-aggregate *interphase*, the three-dimensional region forming the boundary between the two bulk phases, is a more accurate term that should be used to describe the region where asphalt binder and aggregate interaction occurs. A schematic model of an adhesive interphase was proposed by Drzal [27] where the interphase between a viscoelastic adhesive and solid substrate is shown to be dependent on the surface chemistry, morphology, topography, microstructure, local chemical composition as well as the bulk properties of the two adhering phases. Figure

1.1 shows a

must take in

this schema

& binder ph

in the aggr

interphase a

asphalt conc

Poly

thermoplasti

particulate p

basis of the

reactive poly

Figure 1.3 sh

(PMAC) that

## 1.3 Autom

Automc

Every year mo

million tons of r

The process co

the size by shre

for shredding a

amount of non-

1.1 shows a schematic of such an interphase. The study of any interfacial phenomenon must take into account all these factors. In the case of polymer modified asphalt concrete, this schematic model can be extended to include aggregate surface properties, interfacial & binder phase voids, asphalt binder & polymer phase morphology and binder absorption in the aggregate. Figure 1.2 is a schematic model of the asphalt binder-aggregate interphase and shows the various factors that can affect the interfacial properties in asphalt concrete.

Polymer modifiers for asphalt can be classified into five categories: dispersed thermoplastic polymers, network thermoplastic polymers, reactive polymers, fibers and particulate polymers. Asphalts modified with these polymers can be classified on the basis of the final morphology as homogeneous asphalts (thermoplastic, network and reactive polymers) and non-homogeneous asphalts (fiber and particulate polymers). Figure 1.3 shows a schematic of the various types of polymer modified asphalt concretes (PMAC) that can be obtained.

## 1.3    Automobile Shredder Residue (ASR)

Automobiles are the most recycled high-volume consumer product in the US. Every year more than 10 million American cars are shredded, producing nearly 10 million tons of metallic scrap, 50 million tires, and 2.5 million tons of non-metallic scrap. The process consists of dismantling and stripping of vehicles followed by reduction of the size by shredding and separation of metals Recovery of metals is the primary motive for shredding automobiles, but due to the increasing use of plastics and composites, the amount of non-metallic residue is significant.

7

$\Sigma$

T
c
v

Pol
mo

Poly
surfa
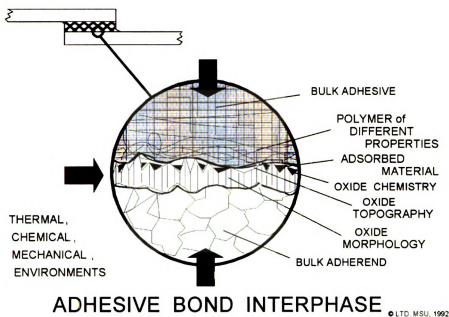
Figure 1.2 S

Figure 1.1 Schematic of the adhesive bond interphase
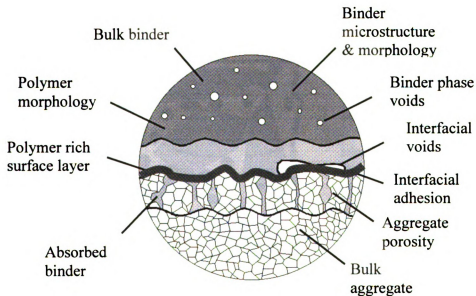


Figure 1.2 Schematic of the polymer modified asphalt binder-aggregate interphase
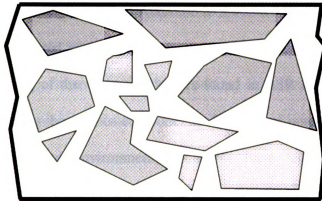
Homogeneous Asphalt

Modifiers :
Dispersed Thermoplastics
Network Thermoplastics
Reacting Polymers
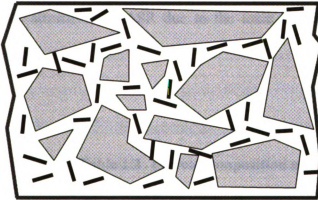
Non-homogeneous
Asphalt

Modifier :
Fibers
(organic and inorganic)
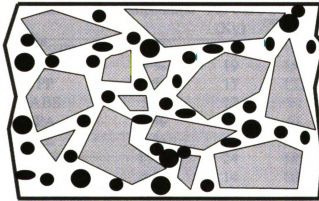
Non-homogeneous
Asphalt

Modifier :
Particulate polymer
(Rubber particles)

**Figure 1.3  Different types of Polymer Modified Asphalt Concrete (PMAC)**

The

paper, fabric

is collectivel

and is treated

recycling of

separating the

landfills and

alternative, va

are not attrac

produced.

| Material |
|---|
| PU Foam |
| PVC |
| PP |
| ABS |
| PA |
| PE |
| PUR |
| Elastomer |
| Other Plast |
| Fibers |
| Wood, Metal |
| Total |

The non-metallic residue comprising of various kinds of plastics, rubber, wood, paper, fabrics, glass, sand, dirt, metal pieces and traces of automotive fluids such as oils, is collectively termed as Automobile Shredder Residue (ASR). ASR has no direct value and is treated as a hazardous waste product which is usually disposed in landfills. Direct recycling of the various polymers found in ASR is hampered by the difficulty faced in separating the various components. The loss of potentially usable material, rising cost of landfills and environmental concerns have led to research focussing on finding alternative, value added uses for ASR. Traditional means of disposal, like incineration, are not attractive for ASR due to the toxic by-products of combustion that may be produced.

**Table 1.2  Typical composition and production of ASR**

| Material | Composition | Amount Per Car (Kg) | Annual Production of ASR (1995) (x $10^3$ Metric Tonnes) | | | |
|---|---|---|---|---|---|---|
| | | | Europe | USA | Other | Total |
| PU Foam | 9 % | 20 | 154 | 121 | 165 | 440 |
| PVC | 9 % | 19 | 150 | 118 | 161 | 430 |
| PP | 8 % | 17 | 132 | 103 | 141 | 378 |
| ABS | 5 % | 12 | 92 | 72 | 99 | 264 |
| PA | 4 % | 8 | 61 | 48 | 65 | 174 |
| PE | 2 % | 5 | 38 | 30 | 41 | 110 |
| PUR | 11 % | 24 | 189 | 148 | 202 | 540 |
| Elastomers | 6 % | 14 | 108 | 85 | 116 | 310 |
| Other Plastics | 11 % | 23 | 182 | 143 | 195 | 522 |
| Fibers | 18 % | 39 | 308 | 242 | 330 | 880 |
| Wood, Metals, etc. | 18 % | 39 | 308 | 242 | 330 | 880 |
| Total | 100 % | 220 | 1,725 | 1,355 | 1,848 | 4,929 |

The c

Polyurethane

Acrylonitrile-

Polyurethane

gives a typica

USA and the

## 1.4 ASR

Cemen

applications a

been shown to

[28-29]. Vario

improved by

particulate ad

material. The

cost modifiers

concrete. has a

The me

cement concre

failure in ceme

unique propert

absorbing the

Different poly

The composition of ASR varies constantly and some of the constituents are Polyurethane foam (PU foam), Polyvinylchloride (PVC), Polypropylene (PP), Acrylonitrile-Butadiene-Styrene (ABS), Polyamides (PA), Polyethylene (PE), Polyurethane rubber (PUR) and various other materials including dirt and oil. Table 1.2 gives a typical composition of ASR and the approximate amounts produced in Europe, USA and the rest of the world.

## 1.4    ASR Modified Cement Concrete

Cement concrete is commonly used for slab-on-grade applications. These applications are generally pavement and building construction. Polymer modification has been shown to be an effective method for improving the properties of cement concrete [28-29]. Various properties such as tensile, flexural, compressive, fatigue, etc. can be improved by the addition of specific polymers. The use of a polymer rich ASR as particulate additive to cement concrete is an attractive and value-added use for a waste material. The large volume of cement concrete used every year demands the use of low cost modifiers and ASR, if shown to maintain or improve the properties of cement concrete, has a high potential for widespread use.

The mechanisms by which particulate polymer additives enhance the properties of cement concrete are similar to those seen in asphalt concrete [43]. The manifestation of failure in cement concrete is fracture, or cracking of the material. Polymers, due to their unique properties such as high toughness and ductility, can act as crack inhibitors by absorbing the fracture energy or by changing the locus and mechanism of failure. Different polymer modifiers may have different mechanisms by which they work, but

11

one of the

polymer w

asphalt) co

material is

wettability

interfacial a

adequately.

act as a flaw

potential fail

polymer and

interface betw

Figure 1.3 sh

matrix interfac

water based m

ASR-cement in

   The int

concrete by sur

abrasion and ch

be used to imp

improvements

in the improve

one of the essential properties of a good polymer modifier is the interaction of the polymer with the bulk material. In the case of particulate modification of cement (or asphalt) concrete, the interaction of the surface of the polymer particle with the matrix material is critical. This interaction can be quantified in terms of interfacial adhesion or wettability of the particle surface by the matrix [30]. A high wettability indicates high interfacial adhesion which is necessary for any particulate reinforcement to perform adequately. If the interface of a particulate inclusion in a matrix is weak, the particle can act as a flaw and the stress transfer that can occur via the interface is limited making it a potential failure site. A strong interface allows stress transfer from the matrix to the polymer and is necessary for dissipation of fracture energy. Thus the need for a strong interface between the additive and the matrix material is an important consideration. Figure 1.3 shows a schematic representation of crack propagation along the polymer-matrix interface. The addition of ASR may present problems in this regard. Cement is a water based material and the oils and dirt on the ASR surface may lead to a very weak ASR-cement interface and cause the properties of the concrete to deteriorate.

The interfacial properties of ASR can be improved prior to addition to cement concrete by surface treatments. Various methods such as detergent washing, mechanical abrasion and chemical modification of the surface by processes such as sulphonation can be used to improve the wettability and surface energy of the ASR. The effect of these improvements in the interaction between the polymer particles and the matrix can result in the improvement of the final properties of cement concrete.
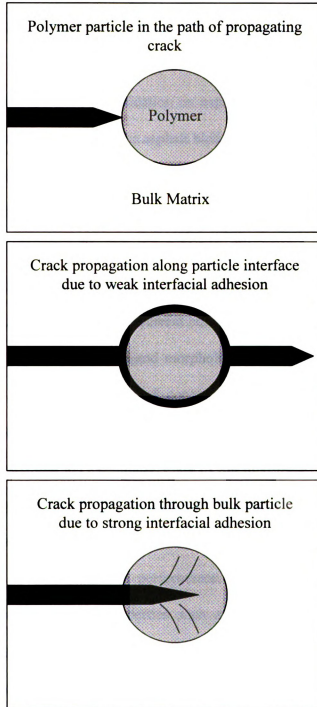
Figure 1.4  **Crack propagation in a particle modified/reinforced matrix.**

Asphal

cracking. agin

of asphalt bin

access the eff

adhesion and f

should be cha

polymer modi

which ultimate

modification or

has not been th

take into accou

properties of t

asphalt paveme

It is pro

changes occurr

techniques to m

mechanisms th

developed to

morphology. p

mechanisms.

characterizatic

along with the

## 1.5    Problem Statement

Asphalt concrete pavements fail due to a variety of distresses such as thermal cracking, aging, fatigue cracking, rutting and ravelling/stripping. Polymer modification of asphalt binder has the potential to improve the performance of these pavements. To access the effects of polymer modification on asphalt, the microstructure, morphology, adhesion and fracture toughness of the asphalt binder and concrete are key properties that should be characterised. The microstructure and morphology of the polymer and the polymer modified binder are controlled by the mix ingredients and mixing procedures which ultimately have an effect on pavement performance. The effect of polymer modification on the interfacial properties, or the role of interfacial adhesion is an area that has not been thoroughly explored and current building practices and specifications do not take into account the microstructure and morphology of the asphalt binder used. Bulk properties of the binder, aggregate and concrete are commonly used to characterise asphalt pavements.

It is proposed that the systematic study of the microstructural and morphological changes occurring due to polymer modification can lead to development of evaluation techniques to measure the effectiveness of asphalt additives and an understanding of the mechanisms that enhance pavement performance. Several laboratory tests have been developed to measure specific properties such as: asphalt binder microstructure and morphology, polymer phase morphology, void analysis, fracture morphology, fracture mechanisms, fracture toughness and lap-shear adhesion. These tests allow the characterization of polymer modified asphalt binder and concrete which, when studied along with the chemical [31,32] and engineering [33] properties, provide a set of tools for

14

the charac

polymer m

evaluated a

discussed.

The

changes in t

concrete spe

by the applic

on the surfac

The f

properties of

properties of

study. Chapte

on ASR modi

theories used t

presents the re

properties of

respectively in

obtained. The

presented alor

the understand

cement concr

the characterization and specification for polymer modified asphalt concrete. Five polymer modifiers: SBS, SEBS, SBR latex, Elvaloy AM and Crumb Rubber were evaluated and the optimum compositions and their effect on key properties will be discussed.

The effect of addition of ASR to cement concrete were characterized by the changes in the tensile strength and fracture morphology of cured ASR modified cement concrete specimen. The role of interfacial adhesion in ASR modified cement was studied by the application of various mechanical and chemical surface treatments and their effect on the surface energy and wettability of the ASR.

The focus of this research is to study the effect of polymer modification on the properties of asphalt and cement concrete. Chapter Two describes the nature and properties of various polymer modifiers, asphalt binders and cement concrete used in the study. Chapter Three describes in detail the experiments and results obtained from studies on ASR modified cement concrete. Chapter Four describes the different experiments and theories used to characterize polymer modified asphalt binder and concrete. Chapter Five presents the results of investigations into the microstructural, morphological and adhesive properties of polymer modified asphalt binder and concrete. Chapter Six and Seven respectively include the discussions and conclusions that can be drawn from the results obtained. The advantages and disadvantages of different polymer systems will be presented along with recommendations for future work that can be undertaken to promote the understanding of the role of the interface in composite systems such as asphalt and cement concrete.

This c

wide variety c

concrete  hav

morphology a


## 2.1    Cem

Asphal

stone)  as  the

composite can

crosslinked. el

this study the

and "asphalt cc


M
(asphalt bind

# CHAPTER TWO

## MATERIALS

This chapter provides an overview of the various materials used in this study. A wide variety of materials such as asphalt cement, aggregate, various polymers and cement concrete have been studied and brief descriptions of their microstructures and morphology are provided in the following sections.

### 2.1 Cement and Asphalt Concrete

Asphalt and cement concretes are composite materials with aggregate (crushed stone) as the discontinuous load bearing component. The continuous matrix of the composite can be of different types ranging from thermoplastic, viscoelastic bitumens to crosslinked, elastic cements. Figure 2.1 shows a schematic representation of concrete. In this study the term used to refer to bituminous binders and concrete is "asphalt binder" and "asphalt concrete" respectively.
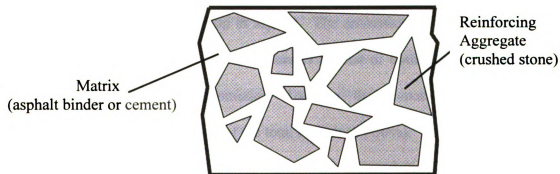


**Figure 2.1  Schematic representation of concrete**

Aspha

distillation of

asphalt.  An

approximately

amounts of n

analysis of th

have been wi

asphalts  are

aromatics, an

of the four g

Asphaltenes c

of 1.1:1.  As

naphthenic rir

size is on the

dispersing age

the lightest m

weight naphth

and alkyl-na;

phase) const;

## 2.2    Asphalt Binder

Asphalt binders are complex mixtures of hydrocarbons derived from the fractional distillation of crude oil where the heaviest residue is processed into different grades of asphalt.    An elemental analysis of asphalt shows that the composition by weight is approximately 82-86% carbon, 8-11% hydrogen, 0-1.5% oxygen, 0-6% sulfur, with trace amounts of nitrogen, vanadium, nickel, and iron [34].    Table 2.1 shows the elemental analysis of three different viscosity graded asphalt binders.    Chromatographic techniques have been widely used in the evaluation of asphalt constitution; based on these studies asphalts are typically divided into four major groups, namely: asphaltenes, resins, aromatics, and saturates [35].    Asphaltenes are the highest molecular weight constituent of the four groups and are considered highly polar and complex aromatic materials. Asphaltenes constitute 5% to 25% of the total asphalt and have a hydrogen / carbon ratio of 1.1:1.    Asphaltenes are believed to be stacks of plate-like sheets of aromatic and naphthenic ring structures held together by hydrogen bonds [36].    The asphaltene particle size is on the order of 5-30nm.    Resins are also very polar in nature and act as a dispersing agent or peptisers for the asphaltenes.    Finally, the aromatics and saturates are the lightest molecular weight group in asphalt.    The aromatics are the lowest molecular weight naphthenic compounds and the saturates consist of both aliphatic hydrocarbons and alkyl-napthenes and alkyl aromatics.    Together, the aromatics and saturates (oily phase) constitute the major portion of the total asphalt (40-50%).

| Ca... |
| --- |
| *Hyc...* |
| Oxy... |
| Nitr... |
| Sulp... |
| *Vana...* |
| *Nick...* |
| Iron... |
| Arom... |
| Arom... |
| Molec... |

Asph...

asphaltene re...

shows a sch...

considered to...

mixture. The...

dispersed as di...

oils. Experim...

demonstrated...

the constituent...

degree of as...

influence the...

between asph...

governs the r...

**Table 2.1 Elemental analysis of asphalt binders [34].**

|  | AC-5 | AC-10 | AC-20 |
|---|---|---|---|
| Carbon (%) | 85.7 | 82.3 | 84.5 |
| Hydrogen (%) | 10.6 | 10.6 | 10.4 |
| Oxygen (%) | -- | 0.8 | 1.1 |
| Nitrogen (%) | 0.54 | 0.54 | 0.55 |
| Sulphur (%) | 5.4 | 4.7 | 3.4 |
| Vanadium (ppm) | 163 | 220 | 87 |
| Nickel (ppm) | 36 | 56 | 35 |
| Iron (ppm) | -- | 16 | 100 |
| Aromatic Carbon (%) | 32.5 | 31.9 | 32.8 |
| Aromatic Hydrogen (%) | 7.24 | 7.12 | 8.66 |
| Molecular Weight | 570-890 | 810-930 | 840-1300 |

Asphalt is often regarded as a colloidal system consisting of high molecular asphaltene/resin micelles dispersed in a lower molecular weight oily medium. Figure 2.2 shows a schematic of this three phase structure of asphalt binders. The micelles are considered to be an ensemble of asphaltenes with a sheath of resins which stabilizes the mixture. The asphalt and resins may be linked in an open network but may also be dispersed as discrete particles depending on the relative amounts of resin, asphaltene, and oils. Experiments involving systematic blending of resins, oils, and asphaltenes have demonstrated that the rheological properties of the asphalt cements depend strongly on the constituents, especially the asphaltene content in the mixture. Thus, the interaction or degree of association between the asphaltene, as well as their size and shape, will influence the viscosity of the binder [37]. The arrangement and degree of association between asphaltene particles within the oily phase is important since this ultimately governs the rheological properties of the asphalt cement binder [35,38,39].

Figure
\sho
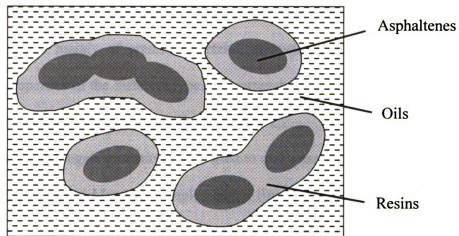
**Figure 2.2  Schematic representation of 3-phase model of asphalt binder
\showing the asphaltene, resin and low molecular weight oil phases.**

The as

were classified

according to s

to minimize th

## 2.3    Aggre

The ag

quarries and

sandstone. Th

used in the asp

Two di

gradation [40]

fracture tough

tests is discus

shown in Tab

aggregate grad

5.7%(w w) asp

The asphalt samples used in this study were supplied by Amoco Corporation and were classified as the low viscosity (AC-5) grade or a moderate viscosity (AC-10) grade according to standard pen tests. The asphalts were stored at -10°C, which is near the Tg, to minimize the effects of aging. No emulsifiers were added to the binders.

## 2.3    Aggregates Used in Asphalt Concrete

The aggregate used for making asphalt concrete was obtained from Michigan quarries and consisted mainly of granite, quartzite, greenstone, limestone, basalt and sandstone. The properties of the different types of aggregate and the relative proportions used in the asphalt concrete mix are summarized in Table 2.2.

Two different aggregate gradations were used to make asphalt concrete mixes: G7 gradation [40] for preparing Marshall samples and a fine mix gradation for preparing fracture toughness samples. The rationale for using a fine mix for fracture toughness tests is discussed in Chapter 5. Marshall samples were made with the G7 gradation shown in Table 2.3 while fracture toughness test beams were prepared using a finer aggregate gradation as shown in Table 2.4. Mixes made with both gradations had 5.7%(w/w) asphalt binder content.

| Type | | |
| --- | --- | --- |
| Granite | | |
| Basalt | | |
| Quartzite | | |
| Greenstone | | |
| Sandstone | | |
| Limestone | | |

**Table 2.2 Types of aggregates used in asphalt concrete [40]**

| Type | Volume in mix (%) | Compressive Strength ($10^8$ N/m$^2$) | Schmidt Hardness | Composition/Description |
|------|------|------|------|------|
| Granite | 28 | 2.5 – 5.5 | 52 - 90 | Coarse crystalline igneous rocks. |
| Basalt | 19 | 2.0 – 3.5 | 50 - 90 | Fine grained igneous rocks. |
| Quartzite | 23 | 2.9 – 5.0 | 30 - 70 | Tough but brittle rock, fully or partially metamorphosed quartz sandstone. |
| Greenstone | 10 | 2.0 – 3.0 | 60 - 80 | Dense fine crystalline basaltic rock. |
| Sandstone | 11 | 0.3 – 2.0 | 20 - 60 | Highly variable distribution ranging from lithic fragments to quartz sands. |
| Limestone | 9 | 0.2 – 2.0 | 30 - 60 | Varies from limy mudstones to crystalline carbonate rocks. $CaCO_3$ and $CaMg(CO_3)_2$. |

Size (r

| 19 |
| 12.5 |
| 9.5 |
| 7.7 |
| 4.75 |
| 2.37 |
| 1.18 |
| 0.6 |
| 0.3 |
| 0.15 |
| 0.075 |
| Fly as |

**Tabl**

Size (mr

| 19 |
| 12.5 |
| 9.5 |
| 7.7 |
| 4.75 |
| 2.37 |
| 1.18 |
| 0.6 |
| 0.3 |
| 0.15 |
| 0.075 |
| Fly ash |

**Table 2.3 Aggregate gradation (G7) used for Marshall samples**

| Size (mm) | Passing % | Retained % | Weight (gm) | Cumulative weight (gm) |
|:---:|:---:|:---:|:---:|:---:|
| 19 | 100 | 0 | 0 | 0 |
| 12.5 | 99 | 1 | 54 | 54 |
| 9.5 | 81 | 18 | 972 | 1026 |
| 7.7 | 63 | 18 | 972 | 1998 |
| 4.75 | 35 | 28 | 1512 | 3510 |
| 2.37 | 22 | 13 | 702 | 4212 |
| 1.18 | 16 | 6 | 324 | 4536 |
| 0.6 | 11 | 5 | 270 | 4806 |
| 0.3 | 9 | 2 | 108 | 4914 |
| 0.15 | 7 | 2 | 108 | 5022 |
| 0.075 | 5 | 2 | 108 | 5130 |
| Fly ash | 0 | 5 | 270 | 5400 |

**Table 2.4 Fine Mix Gradation (FMG) used for fracture toughness tests**

| Size (mm) | Passing % | Retained % | Weight (gm) | Cumulative weight (gm) |
|:---:|:---:|:---:|:---:|:---:|
| 19 | 100 | 0 | 0 | 0 |
| 12.5 | 100 | 0 | 0 | 0 |
| 9.5 | 100 | 0 | 0 | 0 |
| 7.7 | 99 | 1 | 32.5 | 32.5 |
| 4.75 | 68 | 31 | 1007.5 | 1040 |
| 2.37 | 38 | 30 | 975 | 2015 |
| 1.18 | 26 | 12 | 390 | 2405 |
| 0.6 | 14 | 12 | 390 | 2795 |
| 0.3 | 10 | 4 | 130 | 2925 |
| 0.15 | 7 | 3 | 97.5 | 3022.5 |
| 0.075 | 4 | 3 | 97.5 | 3120 |
| Fly ash | 0 | 4 | 130 | 3250 |

prope

conter

their b

temper

normal

time, e

and per

improvi

viscosity

flexible

applicati

relative

propertie

temperat

Polymer

modified

temperatu

An

is by mod

concrete is

## 2.4 Role of Polymer Modifiers in Improving Asphalt Concrete Properties

The performance of asphalt concrete is greatly influenced by the rheological properties of the asphalt binder as well as the mix composition, aggregate properties, void content, and other parameters [31-33, 35]. Asphalt binders are visco-elastic materials and their behavior ranges from purely elastic to completely viscous depending on the service temperature and time of loading. Pavement grade asphalts undergo cyclic loads under normal service conditions and a large accumulation of permanent strain develops over time, eventually leading to failure [33]. Other failures may be caused by loss of adhesion and permanent plastic deformation.

In recent years polymer modifiers have been added to asphalts with the goal of improving the resistance to failure at extreme service temperatures. Conventionally low viscosity (soft) asphalts are used for low temperature service due to their ability to remain flexible at lower temperatures and high viscosity (hard) asphalts used in high temperature applications to prevent plastic flow (rutting). This leads to pavements performing well relative to one type of failure, but poorly relative to others. Polymers have unique properties such as low glass transition temperatures and high viscosities at elevated temperatures. Asphalts benefit from the unique properties imparted by polymers. Polymer modification can increase the storage and loss moduli of asphalt, making modified asphalts more flexible at low temperatures and more viscous at high temperatures.

Another mechanism by which polymers can enhance the properties of pavements is by modifying the binder-aggregate interface [15-19, 25]. The interface in asphalt concrete is an area that has not been studied widely and yet it is critical to the failure of

pavements

interphase (

and the agg

phases and

generally re

temperatures

brittle and t

resistance. t

binder modu

the interface

known as adl

The presence

cycling which

these problem

binder and ag

better wetting

propagation of

behaviour is se

    Particu

rubber does n

the toughenin

the viscosity

pavements at low temperatures. The binder-aggregate interface (2 dimensional) or interphase (3 dimensional) is the region surrounding the boundary of the asphalt binder and the aggregate. This region can have very different properties than the bulk of either phases and can play a critical role in the fracture process. The strength of the interface generally relates to the level of adhesion between the two bulk phases. At low temperatures (below or near the Tg of the asphalt binder), the binder becomes more brittle and the modulus increases. Since any failure process follows the path of least resistance, the weakest region of the concrete acts as the locus of failure. With a high binder modulus and the high strength of aggregate, the weaker region is generally along the interface and cracks proceed along the aggregate boundaries. This type of failure is known as adhesive failure and accounts for cracking occurring at very low temperatures. The presence of cracks along the interface can be further complicated by freeze-thaw cycling which tend to widen and grow cracks. Polymers added to the binder can alleviate these problems to a great degree by creating independent networks that associate with the binder and aggregate or by changing the surface energy of the binder and allowing for better wetting of the aggregate. This can lead to a tougher interface that resists the propagation of cracks and alleviates low temperature cracking in asphalt concrete. This behaviour is seen in homogeneous polymer modified asphalts.

Particulate modifiers like crumb rubber act in a different way. Although the rubber does not interact chemically with the asphalt, at low temperatures it can serve as the toughening elastomeric phase in a brittle matrix. At high temperatures, it can increase the viscosity of the asphalt making it resistant to rutting [42].

Po

[41]. This

oxidation

also absorb

the case of

imagined a.

replenish th

Due

is possible

those relatin

application c

## 2.5   Descr

Five

descriptions o

Dispersed The

Network Ther

Reacting Poly

Particulate P(

Polymers can also retard the natural oxidative aging of asphalt binders in service [41]. This may be due to a variety of mechanisms such as provision of sacrificial oxidation sites and reaction with unsaturated sites in the asphalt. Many polymers can also absorb the low molecular weight oils in asphalt. This can be observed very easily in the case of crumb rubber particles which swell due to absorption of oils. These can be imagined as in-situ reservoirs of oils which initially protect them from oxidation and can replenish the asphalt binder with oils as natural aging processes occur.

Due to the various types of polymers available, tailoring the properties of asphalt is possible with judicious selection of modifiers. The different mechanisms, especially those relating to the binder-aggregate interface need to be studied carefully to aid proper application of polymer modifiers in asphalt concrete.

## 2.5    Description of Polymer Modifiers

Five polymers representing four different polymer types were used. Brief descriptions of the polymers are presented in this section.

Dispersed Thermoplastic      : SBS (Kraton D1101; Shell Chemical Co.)

SEBS (Kraton G1650; Shell Chemical Co.)

Network Thermoplastic      : SBR latex (Ultrapave; UP70)

Reacting Polymer      : Epoxy based reacting polymer (Du Pont; Elvaloy AM®)

Particulate Polymer      : Crumb Rubber (Rouse Rubber, GF-80A);

25

S

monomer

can consi

a two ph

polystyre

common

SBS  pol

Compatib

polymer

oxidize d

help the a

the viscoe

to degrad

used for

weight of

## 2.5.1 Styrene-Butadiene-Styrene (SBS)

SBS block copolymers consist of segments of styrene and butadiene rubber monomer units with a styrene:butadiene monomer ratio of 30:70. Each block segment can consist of many monomer units and the common morphology at room temperature is a two phase structure as shown in Figure 2.3. The styrene blocks segregate into hard polystyrene domains which are connected by soft polybutadiene segments The most common form used in asphalt modification is a linear styrene-butadiene-styrene structure. SBS polymers are physically dispersed in asphalt, but do not react chemically. Compatibility of the SBS with the binder is important to prevent segregation of the polymer during processing. The butadiene midblock in SBS is unsaturated and it can oxidize during processing or service in the pavement. This sacrificial aging of SBS can help the asphalt resist aging initially, but once oxidation of the rubber midblock occurs, the viscoelastic properties of the polymer can be adversely affected. The polymer begins to degrade at temperatures above 380°F due to oxidation. Typical SBS concentrations used for modification of asphalt range from 1-5 % by weight (w/w). The molecular weight of the SBS used was approximately 30,000 [31].

## 2.5.2 Styre

Styrer

ethylene buty

domains con

poly(ethylene

temperature to

form of pellet

weight of the

used for mod:
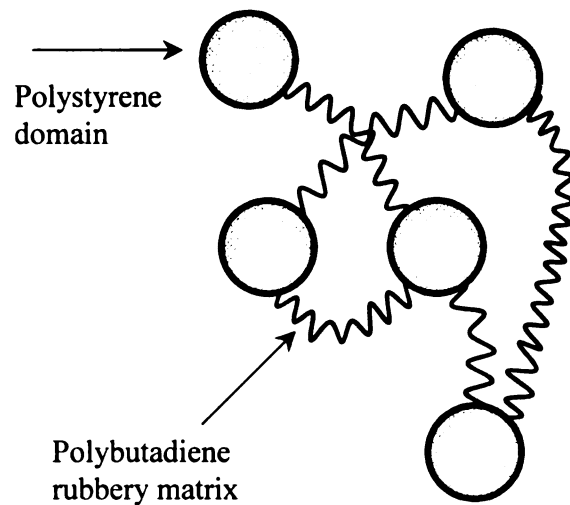
**Figure 2.3  Schematic representation of the Styrene and Butadiene
phase segregation in SBS**

### 2.5.2   Styrene-Ethylene-Butylene-Styrene (SEBS)

Styrene-Ethylene-Butylene-Styrene (SEBS) is a block copolymer of styrene and
ethylene/butylene. The physical structure is similar to that of SBS with hard styrene
domains connected by rubbery ethylene-butylene midblocks. The fully saturated
poly(ethylene-butylene) rubbery blocks are less susceptible to oxidation and thus the high
temperature tolerance of the polymer is better than that of SBS. SEBS is obtained in the
form of pellets and the polymer is dispersed physically in the asphalt. The molecular
weight of the SEBS used was approximately 30,000 [31]. Typical SEBS concentrations
used for modification of asphalt range from 1-5 % (w/w).

S

butadien

(~0.5μm

achieved

in the asp

solvating

network w

UP-70 (UT

24:76. Typ

1-5 % (w w

## 2.5.4 Elva

Elval

EGA (ethyle

and glycidyl

modified with

reaction site w

the chain. Si

resistant to o

responsible f

The epoxide

groups in

## 2.5.3 SBR Latex

SBR latex is an emulsion polymerized random copolymer of styrene and butadiene in a water-based system. In latex form, the SBR particles are very small (~0.5μm) and as a result, physical dispersion of the polymer particles in asphalt can be achieved easily. Heat and mechanical agitation produces a homogenous blend of polymer in the asphalt. As the latex is added, the polymer particles swell from the heat and solvating effects of the resins and oils in the asphalt. After mixing, the SBR forms a network within the asphalt binder. The latex used in this study was an anionic emulsion, UP-70 (Ultrapave/Goodyear) with 70% solids and a styrene:butadiene monomer ratio of 24:76. Typical concentration of SBR latex used for modification of asphalt ranges from 1-5 % (w/w).

## 2.5.4 Elvaloy® AM

Elvaloy® AM (DuPont) is a reactive terpolymer with the chemical designation EGA (ethylene/glycidyl/acrylate). It is a random terpolymer of ethylene, n-butylacrylate and glycidyl methacrylate (GMA). The polymer consists of an ethylene backbone modified with two types of functional groups. The glycidyl group acts as the main reaction site while the acrylate functionalities add flexibility and elastomeric properties to the chain. Since the ethylene backbone is saturated, the polymer itself is relatively resistant to oxidation or aging. The GMA portion of the molecule is believed to be responsible for the reaction observed when Elvaloy is mixed and heated with asphalt. The epoxide ring in the glycidal structure is believed to react with various functional groups in the asphaltene molecule. Asphaltenes which have carboxylic acid

*function*

shown ir

ASPHALT

*Figu*

*Elv*

temperature

reaction wi

Typical con

by weight of

## 2.5.5 Crum

The us

mandated by

automobile tir

the recycled

cannot be ac

particle size

particles are

functionalities can open the epoxy ring in an addition reaction to form aromatic esters as shown in the suggested reaction mechanism in Figure 2.4 [31].

$$ASPHALTENE-CO-H \;+\; O\langle\begin{array}{c}CH_2\\CH_2\\CH_2\\CH_2\end{array} \longrightarrow ASPHALTENE-C-O-CH_2$$
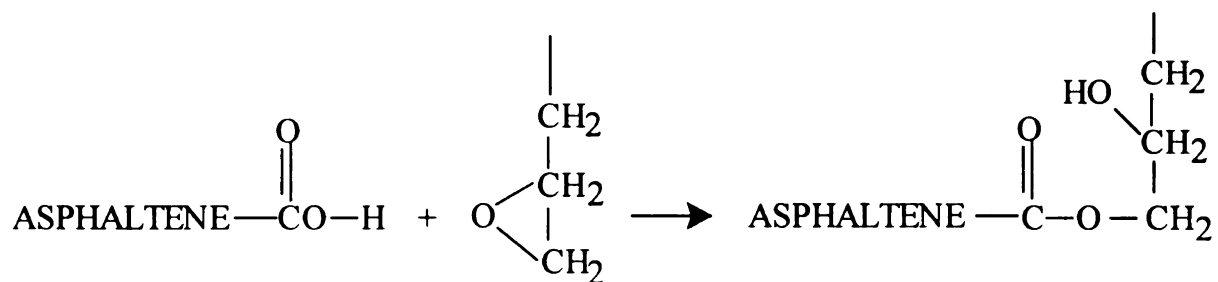
**Figure 2.4 Suggested chemical Reaction of Elvaloy AM with asphaltenes**

Elvaloy AM is obtained in the form of solid pellets. The pellets melt at high temperature and react with asphalt at 380°F to form a stable, homogenous binder. The reaction with asphalt assures a permanent and uniform dispersion within the binder. Typical concentration of Elvaloy AM used for modification of asphalt ranges from 1-3 % by weight of asphalt.

### 2.5.5  Crumb Rubber

The use of recycled crumb rubber as an additive to asphalt concrete pavements is mandated by congressional legislation to address the problem of recycling used automobile tires. The tires are ground to a very fine powder called crumb rubber. Due to the recycled nature of the material, the composition of the rubber particles varies and cannot be accurately determined. The crumb rubber used in the study had an average particle size of 80 μm. Since most rubber used in tires is vulcanized, crumb rubber particles are vulcanized and may have various additives such as anti-oxidants and UV

stabilizers

a large surf

oils from tl

rubber parti

up to  20°

concentratic

surrounding

## 2.5.6  Opti

The l

manufacture

the polymer

lead to exces

oxidation du

mixing condi

the resulting

at which ther

Table 2.5 sho

avoid degrad.

polymers exc

380°F.  Afte

oxidative ag

Experimenta

Engineering. N

stabilizers which make the rubber resistant to oxidative attack. The rubber particles have a large surface area due to the small particle size and can absorb low molecular weight oils from the surroundings. This is an important characteristic to bear in mind since the rubber particles are physically dispersed in the asphalt binder and crumb rubber loadings up to 20% by weight of asphalt binder can be used. The combination of high concentration and high surface area can lead to significant absorption of oils from the surrounding asphalt binder.

### 2.5.6 Optimum Asphalt-Polymer Mixing Conditions[1]

The blending of polymer modifiers with asphalt binder is an important step in the manufacture of modified asphalts. Inadequate mixing can lead to phase segregation of the polymer modifier while very aggressive mixing conditions at high temperatures can lead to excessive oxidation/aging and degradation of the asphalt. To avoid excessive oxidation during processing while achieving good dispersion of the polymer, various mixing conditions were evaluated for each polymer [31]. The rheological properties of the resulting blends were characterized and the optimum conditions defined as the point at which there is no longer a significant increase in properties with additional mixing. Table 2.5 shows the optimum mixing conditions determined for different polymers. To avoid degradation of the polymers, mixing temperatures were limited to 350°F for all polymers except Elvaloy AM which has a supplier recommended mixing temperature of 380°F. After mixing, all binders not used immediately were stored at -10°C to avoid oxidative aging.

---

[1] Experimental work conducted by Hawley M., Shull J., Lee Y. and France L., Dept. of Chemical Engineering, Michigan State University.

**Table 2**

| Polymer |
|---------|
| SBS |
| SEBS |
| SBR Lat |
| Elvaloy |
| CRM |

## 2.6 Comp

Polym

nature of the

materials were

various elasto

prior to incor

addition on the

**Table 2.5 Optimum mixing conditions for different polymer modifiers**

| Polymer Modifier | Mixing Time | Temperature | Conditions |
|---|---|---|---|
| SBS | 2 hours | 350°F | High shear (1600 rpm) |
| SEBS | 2 hours | 350°F | High shear (1600 rpm) |
| SBR Latex | 30 minutes | 350°F | High shear (1600 rpm) |
| Elvaloy AM | 2 hours | 380°F | High shear (1600 rpm) |
| CRM | 30 minutes | 350°F | Low shear (1200 rpm) |

## 2.6    Composition of ASR (Automobile Shredder Residue)

Polymer rich ASR with a maximum particle size of 12 mm was used. Due to the nature of the material, exact compositional analysis was not possible. The following materials were identified in the ASR obtained: HDPE, PVC, PP, ABS, PS, nylon, rubber, various elastomers, wood and fibers. Various surface treatments were applied to the ASR prior to incorporation in cement concrete. Chapter Three describes the effect of ASR addition on the properties of cement concrete in greater detail.

Th

automobile

tensile stre

expected to

strength an

cement mat

and cement

ASR inclusi

some cases.

propagation

**3.1 Surfa**

In or

various surfa

used for ASR

Control : Th

Acid Etchin

dichromate

# CHAPTER THREE

# AUTOMOBILE SHREDDER RESIDUE MODIFIED CEMENT CONCRETE

The addition of ASR to cement concrete is a value added application for automobile shredder residue. The ASR used had a high polymer content and the high tensile strength and toughness of the polymers compared to that of cement concrete are expected to enhance the final properties of the cement concrete. An enhancement in the strength and toughness is possible if the ASR particles have good interaction with the cement matrix, which can be related to the interfacial adhesion between the ASR particle and cement matrix [44]. Strong adhesion between the ASR and the matrix can cause the ASR inclusions to behave as a toughening phase by dissipating fracture energy and in some cases, bridging the cracks in the brittle cement matrix and inhibiting crack propagation [45].

## 3.1 Surface Treatments for ASR

In order to achieve a good interfacial bond between the cement and the ASR, various surface treatments were evaluated. The 7 different types of surface treatments used for ASR are described below.

*Control* : The ASR was used as received.

*Acid Etching* : The ASR is dipped in a Chromerage (sulphuric acid and sodium dichromate solution) for 1 hour at 55°C. After the material is removed from the acid bath,

32

it is rinsed in

material is dri

*Detergent Wa*

air dried at ro

Triton X-100

degradable liq

*Mechanical R*

the dry combi

*Latex Coating*

Repellent, Kop

*Sulphonation*

seconds which

on the surface

exposing it to

it is rinsed in water for 30 minutes to remove any acid residue from the surface. The material is dried in air at room temperature for 24 hours prior to use.

*Detergent Wash* :  The ASR particles were dipped in a detergent solution for 10 sec. and air dried at room temperature for 24 hours. The detergent used was a 0.1% solution of Triton X-100 (iso-octyl phenoxy polyethoxy ethanol and ethylene oxide) which is a bio-degradable liquid with 100% active non-ionic surface-active agent.

*Mechanical Rubbing* :  The ASR was combined with 0.75 inch crushed stone gravel and the dry combination mixed in a concrete mixer for 30 minutes.

*Latex Coating* :  The ASR was dipped in a latex solution (Wolman® Raincoat Water Repellent, Kop-Coat, Inc.) and dried in air at room temperature for 24 hours.

*Sulphonation* :  The ASR was exposed to a stream of sulphur trioxide gas for a few seconds which modifies the surface chemically by adding high energy sulphonate groups on the surface. The surface thus obtained is acidic in nature and it is neutralised by exposing it to calcium carbonate.

mechan

### 3.2.1  C

C

system. V

spreads o

The angle

*the contac*

of the solid

where,

$\gamma_{SV}$     = sur

$\gamma_{SL}$     = int

$\gamma_{LV}$     = sur

$\theta$      = con

The c

and the solid

wet the solid

area of the s

## 3.2 Experimental

Three types of experiments were performed to investigate the surface energy, mechanical properties and fracture morphology of the ASR modified cement concrete.

### 3.2.1 Contact Angle Measurement

Contact angles are a thermodynamic measure of the wettability of a solid-liquid system. When a sessile drop of liquid is placed on a solid surface, the drop of liquid spreads or contracts and eventually the solid-liquid-vapour system reaches equilibrium. The angle the drop makes with the solid at the point of contact at equilibrium is termed the contact angle ($\theta$). The contact angle is related to the surface and interfacial energies of the solid and liquid by Young's Equation (Eq. 3.1) [30]

$$\cos\theta = \frac{\gamma_{SV} - \gamma_{SL}}{\gamma_{LV}}$$

(3.1)

where,

$\gamma_{SV}$ = surface tension of the solid in equilibrium with vapour

$\gamma_{SL}$ = interfacial tension of the solid in equilibrium with liquid

$\gamma_{LV}$ = surface tension of the liquid in equilibrium with vapour

$\theta$ = contact angle in degrees

The quantity ($\gamma_{SV}$-$\gamma_{SL}$) is the difference in energy between the free solid surface and the solid surface wetted by the liquid. This provides the driving force for the liquid to wet the solid surface. The total energy gained by the system when the liquid covers a unit area of the solid surface is then given by the term {$\gamma_{LV}$ + ($\gamma_{SV}$-$\gamma_{SL}$)} which is called the

34

thermodynam

the thermody

Thus

thermodynam

from 0° to 18

This represen

and covers th

the liquid is s

incomplete co

Surfac

surface energy

contact angles

A cont

deionised wat

pure deionised

The goniome

(ASR) partici

and the drop

produces a

calibrated at

the point of

thermodynamic work of adhesion ($W_{SLV}$). Young's equation can be expressed in terms of the thermodynamic work of adhesion to yield the Young-Dupré equation (Eq. 3.2) [30]

$$W_{SLV} = \gamma_{LV}(1 + \cos\theta)$$ (3.2)

Thus it can be seen that contact angles can be used as a measure of the thermodynamic work of adhesion for a given solid-liquid pair. Contact angles can vary from 0° to 180°. For a contact angle equal to 0°, the liquid is said to spread on the solid. This represents the ideal state where a liquid has complete affinity for the solid surface and covers the solid surface spontaneously. For values of contact angles higher than 90°, the liquid is said to be non-wetting and presents practical problems for adhesion due to incomplete contact between the two phases.

Surface treatments for enhancement of adhesion are designed to increase the surface energy of the solid and thus lower the contact angle. By measuring the changes in contact angles, the efficiency of different surface treatments can be compared.

A contact angle goniometer was used to measure the wettability of ASR with pure deionised water. Since the cement matrix is hydrophilic, the contact angles of ASR with pure deionised water can give a measure of the wettability of the ASR with the cement. The goniometer (Rame-Hart Goniometer) has a leveling platform on which the solid (ASR) particles are placed. A small drop (approx. 2μl volume) is placed on the surface and the drop is examined directly through a low power traveling microscope which produces a sharply defined silhouette of the drop. The microscope has a protractor calibrated at 1 degree intervals. The tangential angle the drop makes with the surface at the point of contact is measured as shown in Fig. 3.1. Contact angles were measured for

35

the 6 differ

treatments.

F

**3.2.2 Direct**

Direct

cured cement

or increase in

adhesion betw

the particles

concentration

particulate in

such an inc

particles and

crack tip an

the 6 different surface    treatments and also for combinations of different surface

treatments.
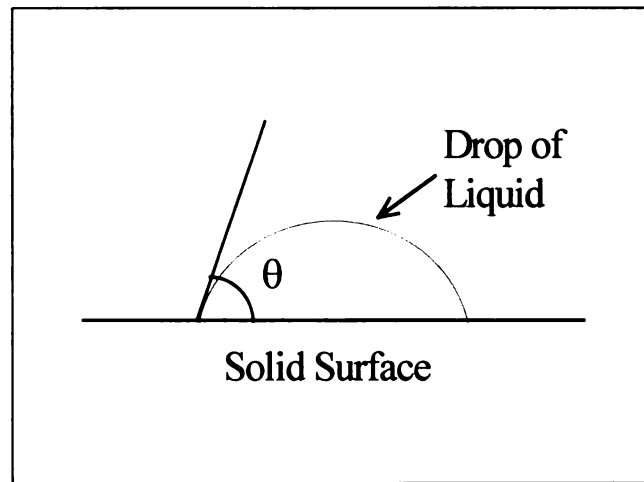


**Figure 3.1  Schematic representation of the contact angle ($\theta$)**

## 3.2.2   Direct Tensile Tests

Direct tensile tests were performed to measure the change in tensile strength of

cured cement concrete after addition of ASR. Particulate inclusions can lead to a decrease

or increase in the tensile strength of a material depending on the amount of interfacial

adhesion between the inclusions and the cement matrix. In case of poor adhesion between

the particles and the matrix, the particles can act as flaws and give rise to sharp stress

concentrations and ultimately nucleate cracks. However, with good interfacial adhesion,

particulate inclusions can act as toughening phases. When a propagating crack reaches

such an inclusion, the fracture energy can be absorbed by the elastomeric polymer

particles and dissipated in different directions. This reduces the stress concentration at the

crack tip and terminates the propagation of the crack.  Thus, tensile tests can provide

some info

Cement co

treatments.

**Tensile Sa**

Fou

(1) Bow-tie

plates. (2)

tapered end

avoid direct

U-shaped en

Co.) Of the

be unsatisfac

stress conce

Figure 3.2 sh

The t

testing machi

conditions. T

linear extens

dogbone wit

the test. the

center of th

crosshead sp

some information about the interfacial strength of the ASR-cement concrete system. Cement concrete samples were prepared with different ASR content and ASR surface treatments.

## Tensile Sample Preparation and Testing

Four different ASR-cement concrete sample configurations were evaluated. (1) Bow-tie tensile specimen clamped by means of wedge action between tapered end-plates, (2) Bow-tie specimen notched at the sides and clamped by wedging between tapered end-plates, (3) Bow-tie specimen with ends epoxied to U-shaped end plates to avoid direct clamping of the concrete samples and (4) Tensile dog-bone specimen with U-shaped end plates glued at the ends with epoxy (MS-907, Miller-Stephenson Chemical Co.) Of the four types of specimen described above, types 1, 2 and 3 were determined to be unsatisfactory due to premature failure near the clamped ends caused by unfavourable stress concentrations. The square dog-bone configuration was thus used for all tests. Figure 3.2 shows the dog-bone sample configuration.

The tensile tests were performed on a UTS mechanical screw driven mechanical testing machine (SFM-20, United Test Systems) at ambient temperature and humidity conditions. The samples were aligned accurately along the tensile axis. A mechanical linear extensometer with 1 inch guage length was attached to the center portion of the dogbone with metal extension strips (Figure 3.3) to measure the strain accurately. After the test, the validity of the data was ensured by noting that the locus of failure was in the center of the sample and not near the clamped ends. The tests were performed with a crosshead speed of 0.04 inch/min. and a preload of 5 lb. to ensure proper alignment.

### 3.2.3 Frac

The

information

material. In

test specimer

examined in

(ESEM). Th

samples by

diamond bla

aluminum fo

coolant used

optically for

marked and f

### 3.2.3 Fracture Surface Morphology

The examination and analysis of the fracture surface morphology can yield information about the nature, locus and mechanism of the failure processes in the material. In the case of ASR modified cement concrete, the fracture surfaces of tensile test specimen were examined to determine the locus of failure. The fracture surfaces were examined in a Philips Electroscan 2020 Environmental Scanning Electron Microscope (ESEM). The fracture surfaces were first isolated from the tested dogbone tensile test samples by cutting approximately 1/4 inch thick sections near the fractured end with a diamond blade saw. Prior to cutting it is important to cover the fracture surface with aluminum foil or plastic film to prevent contamination of the fracture surface with the coolant used by the saw. After isolating the fracture surfaces, they were examined optically for regions of interest. Regions with ASR particles on the fracture surface were marked and further examined in the ESEM at high magnifications.

10"

Figure 3.3
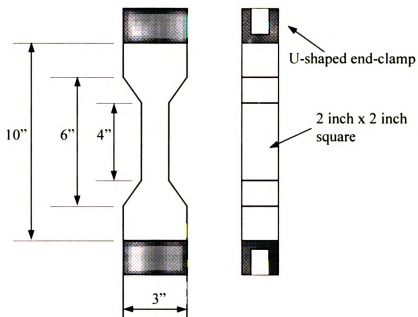
Figure 3.2  Tensile test sample configuration



Figure 3.3  Tensile test specimen showing locus of failure and strain guage fixture

## 3.3    Result

Results

presented belo

### 3.3.1  Conta

The co

It is difficult

mixture of va

process. To

particles (rub

nature of the

be the same

composition a

of rubber wer

various types

can be seen ir

## 3.3 Results

Results for the three types of tests described above for cement concrete are presented below.

### 3.3.1 Contact Angle

The contact angle data was obtained by selecting representative particles of ASR. It is difficult to isolate and analyse the substrate material accurately since ASR is a mixture of various types of plastics and rubbers in different stages of the natural aging process. To maintain some standard for purposes of comparison, elastomeric ASR particles (rubber particles) were selected for contact angle measurements. Due to the nature of the ASR, the various substrates used for contact angle measurements could not be the same and the results should be interpreted with the knowledge that the exact composition and state of the different substrates used could not be ascertained. Flat pieces of rubber were chosen for the tests and care was taken to choose similar particles for the various types of surface treated ASR. The contact angles obtained after surface treatment can be seen in Fig. 3-4.

Control (untre

Detergent Wa

Detergent + Ru

Mechanical Ru

Detergent +

Latex C

Sulpho

Acid E

Detergent

The co

were obtained

Some surface

etching incre

detergent wa

indicate any

matrix for th

3.3.2. Dire

Base
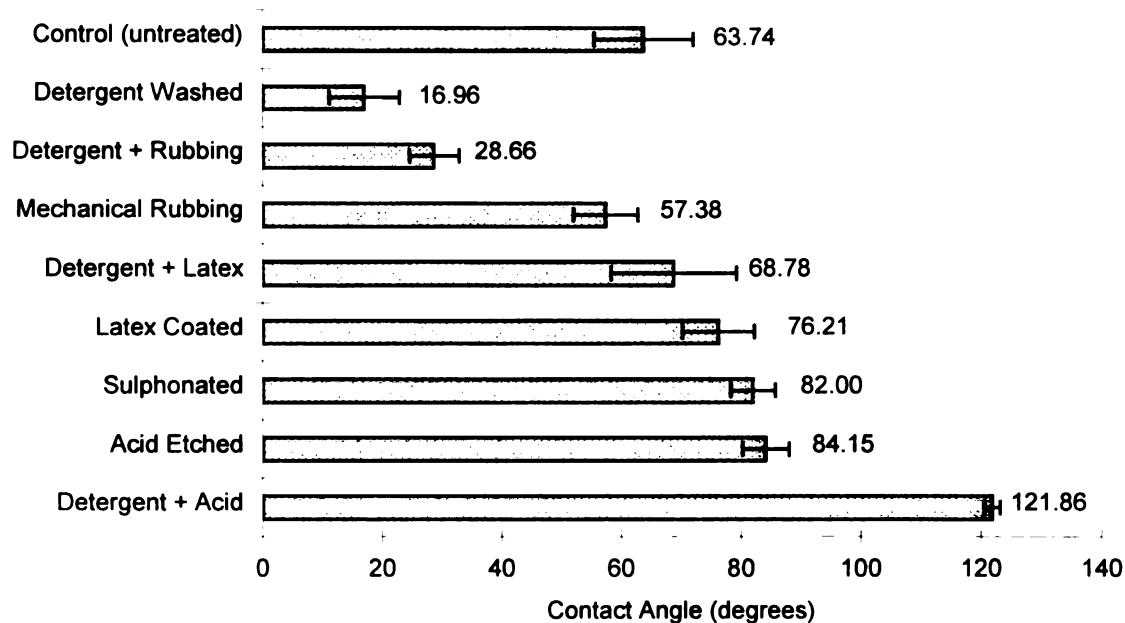
of surface

**Figure 3.4    Contact angles of surface treated ASR**

The contact angles show a wide variation with surface treatment. The best results were obtained with detergent washing. The contact angle decreases to from 64° to 17°. Some surface treatments were seen to increase the contact angle. Sulphonation and Acid etching increased the contact angles to 82° and 85° respectively. Combination of detergent washing with acid etching, latex coating and mechanical rubbing did not indicate any additional benefits. The contact angle results were used to determine the test matrix for the direct tensile tests.

### 3.3.2. Direct Tensile Test

Based on the contact angle results, tensile tests were performed on various types of surface treated ASR-cement concrete compositions as well as combinations of surface

41

treatments. T

by varying th

The p

3.5 shows th

tensile streng

and 4% ASR

Deter

surface treatr

water. Deterg

ASR has a v

tensile streng

contact angle

respectively

show any sta

ASR concer

sulphonation

combinations

types of surf

The

ASR modi:

seen to con

optimum cc

treatments. The effect of ASR content on the cement concrete properties was determined by varying the ASR content from 2% to 4% by volume.

The peak load at failure was determined from the load-displacement curves. Fig. 3.5 shows the effect of ASR addition on the tensile strength of cement concrete. The tensile strength wasn't affected adversely by the inclusion of ASR and addition of 3% and 4% ASR showed a slight improvement in strength.

Detergent wash and sulphonation were selected for comparison from the various surface treatments for ASR due to the wide difference observed in the contact angles with water. Detergent washed ASR has a very low contact angle with water while sulphonated ASR has a very high contact angle. This can result in a large difference in the ultimate tensile strength of the material due to the dependence of interfacial adhesion on the contact angles. Fig. 3.6 and 3.7 show the effects of detergent washing and sulphonation respectively on the tensile strength of the cement concrete. Detergent washing did not show any statistically significant effect on the tensile strength and with higher (3-4%) ASR concentration, the average tensile strength showed a slight increase. With sulphonation, the tensile strength was seen to decrease. Other surface treatments and combinations of these treatments were also tested. The summary of results for all other types of surface treatments can be seen in fig. 3.8.

The various surface treatments for ASR did not affect the tensile strength of the ASR modified cement concrete significantly. However, the concentration of ASR was seen to control the ultimate tensile strength. 3% ASR loading was determined to be the optimum concentration.

42

Maximum Tensile Load (lb)

2500

2000

1500

1000

500

0

Figure

Maximum Tensile Load (lb)

2500

2000

1500

1000

500
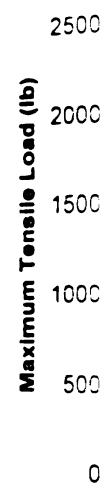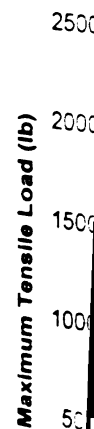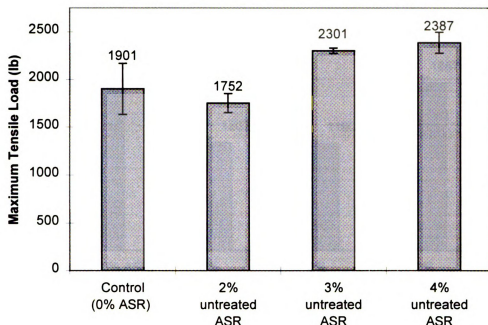
Figure 3.6

**Figure 3.5  Tensile strength of untreated ASR modified cement concrete**
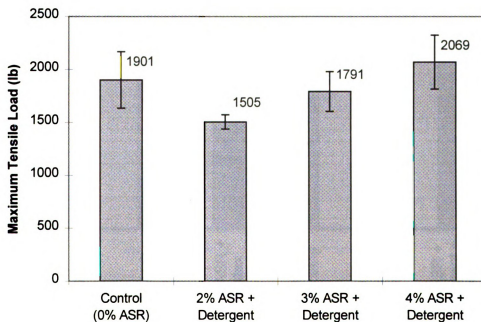


**Figure 3.6  Tensile strength of detergent washed ASR modified cement concrete**
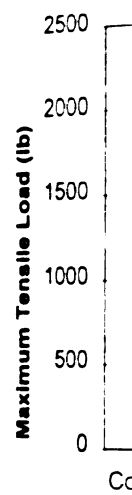
Figure 3.7
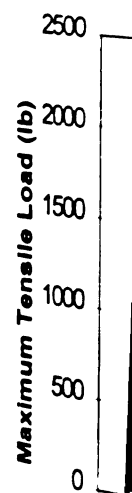


Figure 3.8
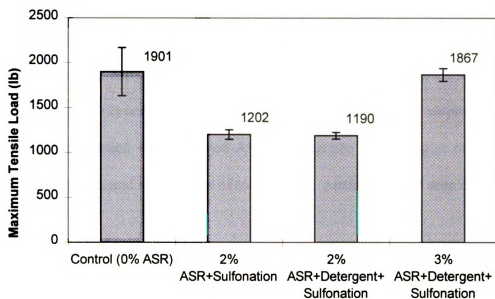
**Figure 3.7    Tensile strength of sulphonated ASR modified cement concrete**
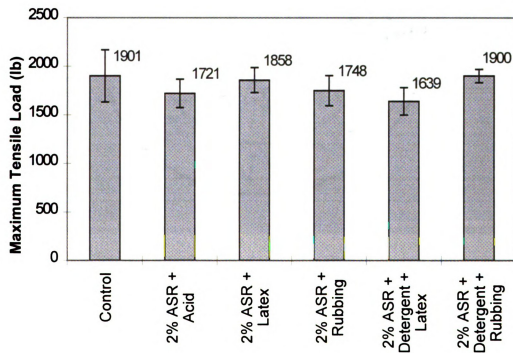


**Figure 3.8    Summary of tensile test results for other ASR surface treatments**

3.3.

and

con

(5)

typ

3-1.

### 3.3.3 Fracture Surface Morphology

In characterizing the surface morphology, the surface of the ASR, cement matrix and the interface between them was the main criterion. The samples tested were : (1) control samples, (2) untreated ASR, (3) detergent washed ASR, (4) sulphonated ASR and (5) detergent washed + sulphonated ASR. The surface morphologies of these different types of concrete, and the surfaces of treated ASR particles can be seen in Figures 3-9 to 3-13.
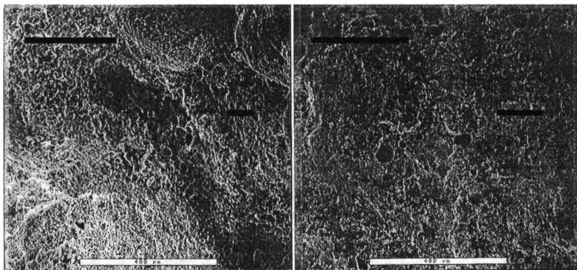


**Figure 3.9 Surface morphology of cement matrix in control cement concrete samples at 100X. (White bar = 400μm)**

Fi

Fig
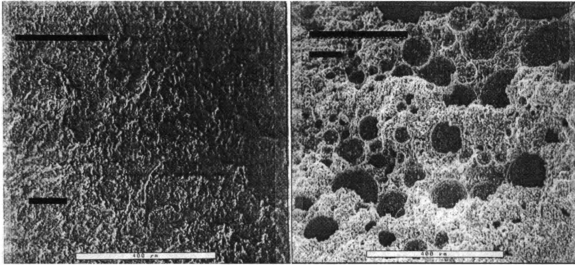
**Figure 3.10  Surface morphology of ASR particle (left) and cement matrix (right) in untreated ASR-concrete samples at 100X. (White bar = 400 μm)**
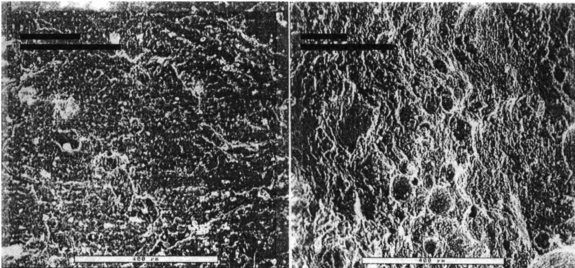


**Figure 3.11  Surface morphology of ASR particle (left) and cement matrix (right) in detergent washed ASR-concrete samples at 100X. (White bar = 400μm)**
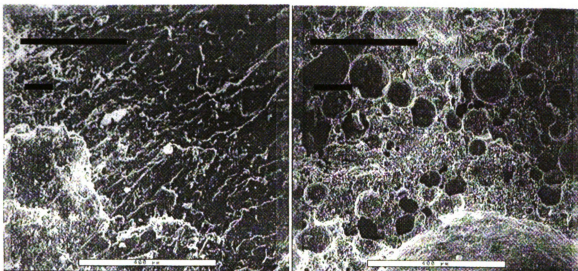
**Figure 3.12 Surface morphology of ASR particle (left) and cement matrix (right) in sulphonated ASR-concrete samples at 100X. (White bar = 400 μm)**
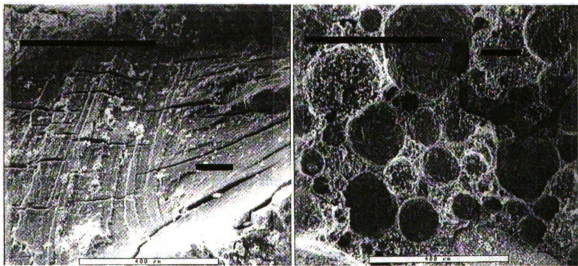


**Figure 3.13 Surface morphology of ASR particle (left) and cement matrix (right) in detergent washed+sulphonated ASR-concrete at 100X. (White bar =400 μm)**

The su

concentration

effective in re

mixing proce

energetics a le

The te

addition of A

with the help

specimen.

The m

mainly pull

cleavage of t

difference in t

however show

Sulphonated

fracture surf

number of

detergent w

morphology

be a contr

concrete. Th

## 3.4 Discussions

The surface treatments for ASR prior to use were found to be less critical than the concentration of ASR used in cement concrete. Surface treatments were seen to be effective in reducing the contact angles of the ASR with water, but in the cement concrete mixing process, the forced contact between the ASR and the cement makes surface energetics a less critical factor.

The tensile strength of the cement concrete was found to be unaffected by the addition of ASR particles except in the case of sulphonated ASR. This can be explained with the help of morphological data obtained from the fracture surfaces of tensile test specimen.

The macroscopic observation of the fracture surfaces show that the ASR particles mainly pull out from the matrix. In the few cases of mechanical interlocking, there is cleavage of the ASR particles. From the morphological analysis, there is no apparent difference in the surface of the ASR inclusions in the different samples. The matrix phase however shows different features. In the 2% Sulphonated and 2% Detergent washed + Sulphonated ASR samples, a large number of voids were observed throughout the fracture surface. This correlates with the low tensile strength of these samples. The number of voids in the matrix were qualitatively smaller and less frequent in the detergent washed, untreated and control samples. Thus from the fracture surface morphology it can be seen that the void content and distribution in the cement phase can be a controlling factor in the ultimate tensile properties of ASR modified cement concrete. The total void content of cement concrete specimen was measured in a related

48

study [46] an

surface treate

10

8

6

AIR CONTENT (%)

4

2

0

**Figure 3.1.**

In the

This surface

acidic surfac

the ASR-ce

content for

findings fro

study [46] and results for the net air void content in cement concrete samples for different surface treated ASR is shown in Figure 3.14.
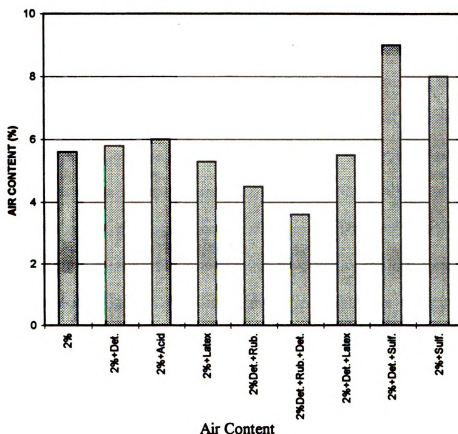


**Figure 3.14    Air void content of surface treated ASR modified cement concrete**

In the case of sulphonation, the surface of the treated particles is acidic in nature. This surface is neutralised by $CaCO_3$, but in the case of incomplete neutralisation this acidic surface can react with the basic cement matrix and cause formation of voids along the ASR-cement interface as seen in the last two columns in Figure 3.14. The air void content for other surface treated ASR were lower than sulphonated ASR and confirms the findings from microstructural observations. The high amount of resultant voids can give

rise to high

tensile stren

### 3.5    Con

The

concrete wa

of the ceme

sufficient to

premature fa

dependent on

evaluated in

improvemen

not improve

received ASF

An ex

the effect of

compressive

shrinkage. im

scaling resis

It wa

has some be

higher abras

like reducti

rise to high stress concentrations and promote the crack growth process leading to low tensile strength.

## 3.5 Conclusions

The objective of the investigation into the suitability of ASR as a filler in cement concrete was to find a value added application for ASR without affecting the properties of the cement concrete adversely. It was shown that 3-4% ASR concentration was sufficient to retain and in some cases improve the tensile properties of concrete. The premature failure of cement concrete modified with sulphonated ASR was found to be dependent on the void morphology in the cement phase. Various surface treatments were evaluated in order to enhance the wettability of the polymer particles, but despite the improvement in wettability seen from contact angle experiments, the tensile strength does not improve significantly and the best performance was obtained from untreated, as received ASR.

An extended study[2] was undertaken at Michigan State University, to investigate the effect of ASR addition on the engineering properties of cement concrete such as compressive strength, flexural strength, water absorption, free and restrained drying shrinkage, impact strength, rapid chloride permeability, freeze-thaw durability, deice salt scaling resistance and abrasion resistance [46].

It was determined from these studies that the addition of ASR to cement concrete has some benefits such as improvement in resistance to shrinkage and water absorption, higher abrasion resistance, tensile and impact strength. However there are adverse effects like reduction in chloride permeability, compressive and flexural strength. After

balancing

volume fr

improved c

: Sorushian P

balancing the improvements and the adverse effects it was determined that the use of 3% volume fraction of ASR as an additive to cement concrete yielded a product with improved overall performance for slab-on-grade pavement applications [46].

[2] Sorushian P., Department of Civil and Environmental Engineering, Michigan State University, USA.

In the

important to st

components a.

and morpholo

properties fro

understanding

modification a

environmental

structural and

toughness mea

With t

characterizatio

- Asphalt bi

- Void Mor

- Fracture t

- Polymer p

- Fracture s

- Lap shear

# CHAPTER FOUR

## ASPHALT CONCRETE

In the study of a complex material like polymer modified asphalt concrete, it is important to study the key morphological and microstructural properties of the individual components as well as their interactions and failure mechanisms [47]. Microstructural and morphological information is extremely important in the prediction of pavement properties from the physical and chemical data for binders and aggregates. An understanding of the morphological changes occurring in asphalt as a result of polymer modification and their effect on the locus and mechanism of failure as a function of environmental conditions is a critical factor in pavement design and optimization. The structural and engineering properties of asphalt concrete can be predicted from fracture toughness measurements and fracture morphology.

With these objectives, experimental methods have been developed for the characterization of the following properties -

- Asphalt binder morphology

- Void Morphology

- Fracture toughness

- Polymer phase morphology

- Fracture surface morphology

- Lap shear adhesion

The

fundamental

a predictive t

## 4.1 Asph

An en

2020, was us

modified and

Electron Mic

of the ESEN

conductive co

the microstruc

and asphalt co

The pressure

typically used

either $CO_2$ or

destructive env

the ESEM fo

accelerating v

All ES

binder thin f

mold in a hot

temperature u

The cumulative information obtained from these experiments will provide a fundamental understanding of the materials and processes in asphalt concrete and provide a predictive tool for pavement performance.

## 4.1    Asphalt Binder Morphology

An environmental scanning electron microscope (ESEM), Phillips ElectroScan 2020, was used to investigate the microstructure and morphology of unmodified, polymer modified and aged asphalt binders. The ESEM (Figure 4.1) is similar to the Scanning Electron Microscope (SEM) in operation, but has a few advantages. The main advantage of the ESEM is the ability to observe non-conductive materials without the use of conductive coatings on the surface. This makes the instrument an ideal choice to observe the microstructure, crack growth mechanisms and fracture morphology of asphalt binders and asphalt concrete; materials which would be susceptible to charging effects in a SEM. The pressure level in the ESEM specimen chamber is significantly higher than that typically used in an SEM and pressure is maintained between 2 to 5 torr by introducing either $CO_2$ or water vapor in the chamber. This provides a relatively benign and non-destructive environment in which sample damage is minimized. The conditions used in the ESEM for all experiments were: 2 to 2.5 torr pressure using water vapor, 20keV accelerating voltage, 55% condenser lens setting and 2.1 second scan time.

All ESEM morphological studies on asphalt binders were performed on asphalt binder thin films of thickness 0.005 inch prepared using a picture frame compression mold in a hot press. The thickness of the picture frame used was 0.005 inch. The molding temperature used was 15°C below the softening temperature of the asphalt system which

was measured

of 50°C (unm

asphalt binder

post-cured sil

binder for 5-

asphalt binde

preparation, t

aluminum fo

Th

extensive

surface, e

that asph

5 minute

was measured by thermal-mechanical analysis (TMA). Typical values were in the range of 50°C (unmodified AC-10) and 60°C (AC-10-5%SBS). After preheating the plates, the asphalt binder was placed in the open mold between paper release liners treated with a post-cured silicone based release coating. Contact pressure was applied to preheat the binder for 5-10 minutes and the press closed at a rate of 2kips/min. All the prepared asphalt binder films were stored in a refrigerator till used. For final ESEM sample preparation, the release paper was removed and the asphalt binder thin film placed on an aluminum foil substrate.



**Figure 4.1  Philips Electroscan 2020, Environmental Scanning Electron Microscope**

The prepared samples were mounted in the ESEM and the surface observed extensively for any features. Because of the absence of a conductive layer on the sample surface, evaporation of oils from the surface region is believed to occur and it was found that asphalt binder thin films exposed to the electron beam, for times ranging from 0.5 to 5 minutes depending on the type of binder, showed a network structure [47, 48] in the

bind

the

cont

tensi

perfc

aspha

chara

detail

binder as seen in Figure 4.2. This network structure was found to be a characteristic of the binder and showed changes in structure with polymer addition, aging and asphaltene content of the binder. Tests were performed on binder films strained in the ESEM using a tensile loading stage to observe the deformation of the network structure. Tests were also performed on pre-strained asphalt binder films and asphalt binders having different asphaltene contents to verify the deformation behavior of the asphalt network and it's characterize it's dependence on the asphaltene content. These results are discussed in detail in Chapter 5.
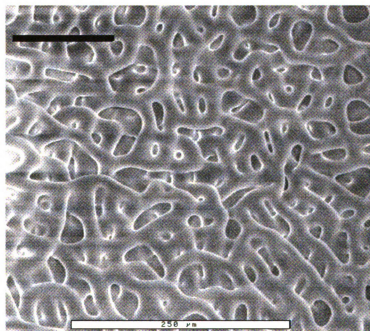


**Figure 4.2  Typical network structure seen in asphalt binder thin films after exposure to the electron beam in the ESEM (White bar = 250 μm)**

Las

fluo

freq

is ex

filter

in th

by u

can l

distri

can t

condi

when

the p

featur

fluore

appro

captu

invert

invers

used

## 4.2 Polymer Phase Morphology

The polymer phase morphology in PMA was studied [47, 48] using the Confocal Laser Scanning Microscope (LSM, Zeiss 10) which works on the principle of fluorescence. Unsaturated bonds in materials can fluoresce when exciting light at specific frequencies is incident upon that material. When a polymer containing unsaturated bonds is excited with a laser , the emitted fluorescence can be observed with the help of suitable filters. This is useful in determining the shape, size and distribution of the polymer phase in the asphalt binder matrix. The confocal LSM differs from other microscopic methods by utilizing an intense laser source which collects light only from the focal plane, which can be below the material surface. This allows the observation of the polymer phase distribution in the bulk of the asphalt binder instead of the surface where the morphology can be affected by any number of factors including the processing methods, storage conditions, etc. Polymers like SBS, SEBS and SBR were observed to fluoresce strongly when illuminated with blue light (488 nm) thereby revealing the size and distribution of the polymer constituent phase. Under reflected light, the modified asphalt binder appears featureless. However, when examined under blue laser excitation (488 nm wavelength), fluorescence was obtained in the red region (590-620 nm wavelength). Using the appropriate band pass filter (590-620 nm) the polymer phase is seen clearly. The image is captured by a computer and is saved in gray scale in PIC format. The gray scale is then inverted using an image processing software (Corel Photopaint) for better clarity. After inversion, the polymer phase can be seen as a dark area over a light background.

The ESEM technique used for determining asphalt binder morphology was also used to determine the polymer phase morphology of the particulate Crumb Rubber

56

(CRM) and

excitation b

unsaturation

low temper

morphology

## 4.3   Voi

Two

analysis, vi

experiment

their distrib

### 4.3.1   San

The

asphalt cor

preparation

aid cutting

in the saw

absence of

binder nea

process an

mm were

cleaner fo

(CRM) and Elvaloy AM (Elvaloy) since these polymers did not show fluorescence under excitation by blue, green or red laser. This could be due to the very low amount of unsaturation in these polymers. ESEM imaging of SBR modified asphalt binder films at low temperatures (5°C) using the same technique employed for observing asphalt binder morphology showed the morphology of the SBR phase.

## 4.3 Void Morphology

Two experimental methods were evaluated for void morphology and void analysis, viz. Thin Section Image Analysis [25] and Void Casting. The aim of the experiments was to identify the different types of air-voids present in asphalt concrete, their distribution and microstructure.

### 4.3.1 Sample Preparation

The void analysis samples were prepared from 15mm thick sections cut from asphalt concrete Marshall samples using a Felker 41-AR diamond blade saw. Section preparation followed the method of Kirsten Ericksen [49-51] and Edward Scott [25]. To aid cutting, the samples were refrigerated for 24 hours prior to cutting and the water bath in the saw was filled with ice to keep the sample and blade temperature low. In the absence of such precautions there can be a large amount of local softening of the asphalt binder near the cutting edge. This is caused by frictional heat generated during the cutting process and can damage the blade and the sample. Sections of dimensions 70 x 50 x 15 mm were cut in this manner. These sections were cleaned in a Bransonic ultrasonic cleaner for 2 minutes using de-ionized water and then dried at room temperature for 24

hours. Aft...

asphalt co...

fluorescent...

with fluore...

light and b...

at 530 nm...

filter. The...

sections in...

The section...

immediatel...

reduced to...

held at this...

as the air e...

from the s...

process he...

subsides. u...

impregnat...

temperatur...

Leco wate...

polishing ...

carbide ab...

each grit ...

dried sect...

hours. After air-drying, the samples were placed in a desiccator for 24 hours. The cleaned asphalt concrete sections were vacuum impregnated with a two part epoxy resin and a fluorescent dye (Struers Epofix/Epodye resin impregnation system) to fill the air-voids with fluorescent epoxy. The Epodye (Hudson Yellow) fluoresces at 440nm in visible light and between 256 nm and 285 nm in ultraviolet light. Fluorescence emission occurs at 530 nm making the impregnated voids detectable through an appropriate band pass filter. The impregnated samples were prepared by immersing the dry asphalt concrete sections in the mixed Epofix resin with 5 grams Epodye added to 1 liter of Epofix resin. The sections were immersed in an aluminum tray containing the fluorescent resin and immediately placed in a vacuum chamber (VWR 1410, General Electric) and the pressure reduced to -0.97 bar. It takes 2 to 2.5 minutes to reach this pressure and the samples are held at this pressure for 3 minutes. Outgassing occurs within the asphalt concrete samples as the air entrapped in the voids is removed. The epoxy foams till all the air is removed from the samples. Partially releasing the vacuum 2 to 3 times during the outgassing process helps to get thorough impregnation of the samples. When the outgassing subsides, the chamber is vented to the atmosphere slowly over 2 to 3 minutes. The impregnated samples are removed and placed on a flat surface for curing at room temperature for 7 days. After cure, the impregnated sections were rough polished on a Leco water cooled belt grinder (BG-20) to remove excess epoxy from the surface. Final polishing was done on a Struers Abramin Automated polisher progressively using silicon carbide abrasive paper of grits 120, 240, 320, 600, 1000, 2400 and 4000, polishing at each grit for 2 minutes. The samples were then rinsed and dried at room temperature. The dried sections were glued to flat glass petrographic slides (dimensions 51x75 mm) using

EPON 8

Petro-Th

mm thic

impregna

are hence

### 4.3.2  T

Th

observed

An excite

second ba

source use

were captu

CUE-2 im

impregnate

the fluores

in the 2-di

1.67X pho

The

by the car

images wo

histogram

scales gre

EPON 828 epoxy and V-40 curing agent (Shell Oil Co.) A thin sectioning saw (Buehler Petro-Thin) was used to cut and polish the asphalt section on each slide to about 1-1.5 mm thickness. Final polishing was done in small increments till the thickness of the impregnated asphalt concrete section was 30 microns. Sections prepared in this manner are henceforth referred to as thin sections and used for image analysis of voids.

### 4.3.2  Thin Section Image Analysis

The void microstructure and morphology of thin asphalt concrete sections was observed under a BH-2 Olympus microscope using reflected light and a set of two filters. An exciter filter was used to cut off the source light above 515 nm wavelength and a second band pass filter at 530 nm was used in the path of the reflected light. The light source used was a 100W TH3 Olympus power source with a halogen bulb. The images were captured by a CCD video camera and the output directed to a computer running CUE-2 image analysis software (Olympus). The thin sections, as explained earlier, are impregnated with fluorescent epoxy that fills the air-voids in the asphalt concrete, thus the fluorescent areas observed are directly related to the shape and size of the voids seen in the 2-dimensional section. A 2.5X objective lens was used in the microscope and a 1.67X photo relay lens was used in the CCD camera giving a net magnification of 38X.

The CUE-2 system analyses images in 256 color gray scale. The images captured by the camera were digitized and converted to gray scale. To achieve better contrast, the images were converted to black and white by selecting a dividing value on the gray scale histogram. All the gray scales below the dividing value were converted to black and the scales greater than the dividing value were converted to white. A dividing value of 40

was seen

dependent

conversion

areas on a

the image

The

identifiable

specific le

the object

the object.

ratio is the

factor is a

circle and

length of tl

analyzed. 7

is the dist

starting fro

The

sample are

a minimu

was found

section. T

and 2-4 th

was seen to give the best results. The selection of the dividing value is operator dependent and care should be taken to remain consistent over multiple samples. After conversion of the 256 gray scale image to bi-level, the fluorescing areas are seen as white areas on a black background. Since the software is designed to analyze the black areas, the image is inverted so that voids appear as black areas on a white background.

The analysis was performed by the software and the parameters recorded for each identifiable void were: area, perimeter, Ferret's diameter, aspect ratio, shape factor, specific length, areafract and average radius. The Ferret's diameter is the projection of the object measured at predetermined angles through the center of gravity to the edges of the object. This was measured at four different angles; $0°$, $45°$, $90°$ and $135°$. The aspect ratio is the ratio of the minimum Ferret diameter to the maximum Ferret diameter. Shape factor is a measurement of the sharpness of an object. A shape factor of 1 refers to a circle and a shape factor of 0 refers to a straight line. The specific length is the total length of the object. Areafract is the ratio of the area of the object to the total frame area analyzed. The average radius is the mean of the eight Martin radii, where a Martin radius is the distance from the center of gravity to the object edge measured at $45°$ intervals starting from $0°$.

The area analyzed for each sample should be at least 500 mm$^2$ spread over a total sample area of 7,000 mm$^2$ [25,50]. The thin sections have an area of 3,500 mm$^2$ and thus a minimum of two sections were analyzed for each sample. The field image area at 38X was found to be 17.5 mm$^2$. Thus a minimum of 29 samplings have to be taken from every section. To enhance accuracy, an average of 70 samplings were done on each thin section and 2-4 thin sections were analyzed for each composition.

The

was further

area (A*): E

Form factor

Dur

sample was

software as

void sizes

eliminating

The raw data was saved by the CUE-2 software in spreadsheet format. This data was further processed to obtain the following parameters: Air void content (Pa); Average area (A*); Equivalent circle diameter (Da); Average equivalent circle diameter (Da*) and Form factor (F). The equations used for these calculations are shown in Table 4.1 [25].

During image analysis, irregularities in the lighting and refraction from the sample was seen to give rise to electrical noise which is interpreted by the image analysis software as voids. Previous studies have shown that noise is prevalent in the analyzed void sizes smaller than 50 microns [25, 50]. Most of this noise was rejected by eliminating void sizes smaller than 50 microns during the pre-processing step.

| Total Air V |
|---|

| Average ar |
|---|

| Equivalent |
|---|

| Average<br>diameter. I |
|---|

| Form Fact |
|---|

*Note: A*

**Table 4.1 Equations Used in Image Analysis [25]**

| Total Air Void Content, Pa | $P_a = \dfrac{\sum A}{Number \cdot of \cdot fields \times field \cdot area}$ | (4-1) |
|---|---|---|
| Average area of air-voids, A* | $A* = \dfrac{\sum A}{Number \cdot of \cdot air \cdot voids}$ | (4-2) |
| Equivalent circle diameter, Da | $D_a = 2\sqrt{\dfrac{A}{\Pi}}$ | (4-3) |
| Average equivalent circle diameter, Da* | $D_a^* = \dfrac{\sum D_a}{Number \cdot of \cdot air \cdot voids}$ | (4-4) |
| Form Factor, F* | $F = \dfrac{(Da)^2}{F_e^2}*100$ | (4-5) |

*Note:* $A$ = *Area of void*

62

4.3.3 Void

An

quantitative

main probl

analysis of

The values

25% of the

4-5%. Th

representat

accuracy o

concrete a

asphalt car

for analysi

Th

sections us

from aspha

cut section

with fluor

room temp

impregnat

only the a

it assume

measurem

### 4.3.3 Void Casting Method

An alternate method for void analysis was developed to achieve better quantitative results than those obtained from the thin section image analysis method. The main problem encountered in the thin section image analysis was the two-dimensional analysis of the irregularly shaped three-dimensional air-voids found in asphalt concrete. The values for total air-void content obtained by the image analysis were generally about 25% of the expected air void content based on the Marshall sample design expectation of 4-5%. The void casting method provides a way to obtain three-dimensional representations of the air-voids from the bulk of the asphalt concrete; thus increasing the accuracy of the data obtained. The concept involves visualizing the air-voids in asphalt concrete as 'molds'. These 'molds' can be impregnated with epoxy and after cure the asphalt can be extracted with solvents to provide 3-dimensional castings of the air-voids for analysis.

The initial sample preparation for this method was similar to that used for thin sections used in image analysis. Asphalt concrete sections 15 mm in thickness were cut from asphalt concrete Marshall samples using a diamond blade saw (Felker 41-AR). The cut sections were dried in air at room temperature for 24 hours and vacuum impregnated with fluorescent epoxy. The impregnated sections were allowed to cure for 7 days at room temperature. After full cure was achieved, the excess epoxy from the surface of the impregnated sections was removed using a water cooled belt grinder (Leco, BG-20) till only the asphalt concrete surface was visible. The sections were polished on all sides till it assumed a rectangular shape with even thickness. This was done to ease the measurement of the total volume of the section. The impregnated samples were heated in

63

an oven at

apart into

taken to av

structure ir

excess of

binder and

chloroethy

removed.

retained p

fluorescen

Figure 4.3

epoxy part

gm. and th

D792-86 [

each epox

cumulativ

void cont

distributio

an oven at 100°C for 10 minutes to soften the asphalt. The softened samples were broken apart into 4 to 5 smaller parts by gently applying pressure with a glass rod. Care was taken to avoid using excessive force during this step in order to keep the epoxy filled void structure intact. The samples (approx. 35 x 50 x 15 mm) were immersed for 10 minutes in excess of tri-chloroethylene (100 to 200 ml) which is a very good solvent for asphalt binder and does not affect the epoxy when exposed for short times. The mixture of tri-chloroethylene and asphalt concrete was put in a centrifuge and all the solvent was removed. This process was repeated till all the binder in the sample was extracted. The retained portion in the centrifuge consists of clean aggregates and the voids cast in fluorescent epoxy. The epoxy particles were separated from the aggregates manually. Figure 4.3 shows the voids typically obtained from a section of asphalt concrete. The epoxy particles were weighed individually using a Sartorus balance accurate to 0.0001 gm. and the weights recorded. The density of the epoxy used was calculated using ASTM D792-86 [52] and found to be 1.1144 gm/cc at 23°C. Using the density and the weight of each epoxy particle, the volume of each air-void in the sample was calculated. The cumulative void volume and the net volume of the sample was used to calculate the air-void content of the sample. Since the volume of each void is known, the void size distribution can be plotted accurately.

**4.4 In**

Th

and the fa

were load

magnifica

**4.4.1 Sa**

of aspha

samples

water to

gross sur
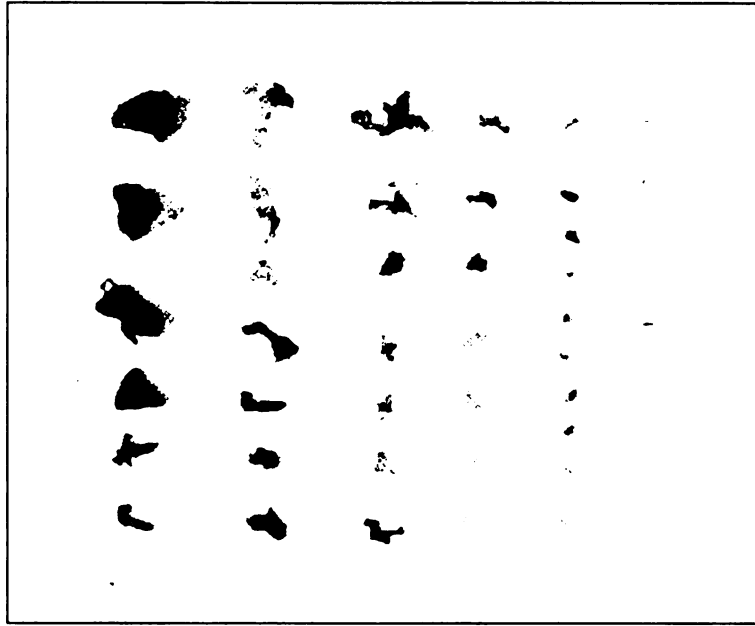
**Figure 4.3 Three-dimensional voids in asphalt concrete**

## 4.4 In-situ ESEM Tensile Tests

The ESEM tensile test was used to study the fracture morphology, locus of failure and the failure mechanisms in asphalt concrete [19, 48]. Thin asphalt concrete sections were loaded in a tensile stage in the ESEM and the failure process was observed at high magnifications.

### 4.4.1 Sample Preparation and Testing

The samples used for the ESEM tensile test were 30 x 15 x 1 mm sections of asphalt concrete cut from 63.5 x 101.6 mm diameter asphalt concrete Marshall samples using a Felker 41-AR diamond blade saw. The cut sections were washed in water to remove debris and polished lightly using 120 grit abrasive paper to remove any gross surface imperfections. The polished sections were dried at room temperature for 24

hours in

Stephens

8010) wi

stage. Th

The poly

section to

backing v

stage. The

by a swit

entire sur

crack init

process. b

that the s

observe a

load-displ

observed.

mechanis

2.5 torr p

setting a:

temperatu

T

was also

used for d

hours in a desiccator. The dried sections were adhesively bonded with epoxy (Miller Stephenson Chemical Co., MS907) to strips of 0.01 inch thick polycarbonate film (Lexan 8010) with dimensions 40 x 20 mm. to facilitate loading and clamping in the tensile stage. The sample configuration for *in-situ* ESEM tensile tests can be seen in figure 4.4. The polycarbonate backing film was notched under the center of the asphalt concrete section to keep the locus of failure in that physical region. The edges of the polycarbonate backing were drilled to accommodate the mounting screws on the ESEM tensile loading stage. The tensile stage is mounted in the ESEM and the strain rate is manually controlled by a switch. This is necessary since the samples are strained in small increments, the entire surface of the sample scanned for initiation of cracks, and then strained again till crack initiation is observed. This method allows for careful observation of the failure process, but does not allow the monitoring of sustained load on the sample. It was found that the samples relaxed and the applied load decreased during the time it takes to observe and record the features on the sample surface, thus preventing any quantitative load-displacement correlations to be made with the fracture surface morphology observed. When a crack is located, the sample is strained further and the crack growth mechanism is observed and recorded. The operating conditions in the ESEM were : 2 to 2.5 torr pressure using water vapor, 20keV accelerating voltage, 55% condenser lens setting and 2.1 second scan time. In addition, some tests were performed at -20°C temperature, to observe the low temperature adhesive failure processes.

The fracture surface images were saved as graphic files and the fracture process was also saved on video for future analysis and reference. Samples of fresh PMAC were used for characterizing fracture morphology
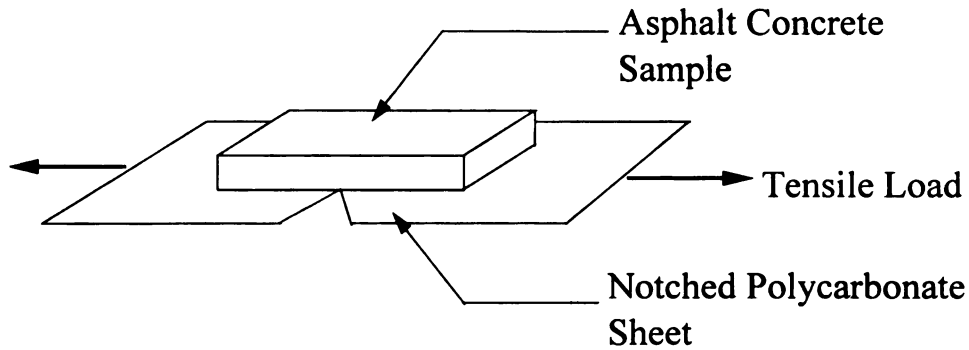
Sample Dimensions : 30 mm x 15 mm x 1mm

**Figure 4.4  Sample configuration for in-situ ESEM tensile test**

## 4.5     Fracture Toughness

Fracture toughness is the energy required per unit area to create a new crack

surface [53 ]. The value of the fracture toughness relates to the resistance of the material

to crack propagation.  This property is thus important to characterize the performance of

asphalt concrete.  At temperatures below $0^{o}C$, the fracture in asphalt concrete was

observed to be adhesive. Adhesive failure is defined as fracture surface propagation via

the asphalt binder-aggregate interface. Thus at low temperatures, the fracture toughness

can be used to characterize the interfacial strength or adhesive strength of the asphalt

concrete.

There are several different methods and definitions of the fracture toughness [54].

For elastic materials fracture toughness can be measured in terms of the critical stress

intensity factor ($K_{IC}$) or the critical strain energy release rate ($G_{IC}$). These parameters are

defined by the principles of Linear Elastic Fracture Mechanics (LEFM) and describe

linearly elastic materials very well. However, non-homogenous, viscoelastic materials

like asphalt concrete are not linearly elastic and have a large amounts of plastic

deformat

Thus it

Fracture

thus giv

paramete

T

crack pr

fracture t

55]. Exp

testing a

B

thickness

and failur

maximun

energy to

where,

$J_{IC}$ =

b =

U =

a =

deformation, especially at the crack tip, which is not accounted for in the LEFM theories. Thus it is necessary to devise experiments based on the principles of Elastic Plastic Fracture Mechanics (EPFM) which account for plastic deformation at the crack tip and thus give a better representation of the fracture toughness of the material. One such parameter used to determine the fracture toughness is the J-contour integral [54-55].

The J-contour integral is a path independent measure of the energy required for crack propagation at a notch tip. The critical value of the J-contour integral gives the fracture toughness of an elastic-plastic material with a large plastic deformation zone [54-55]. Experimentally, the critical J-integral fracture toughness ($J_{IC}$) is determined by testing a series of notched beams in a 3-point bending beam configuration.

Beams notched to different lengths ranging from 40% to 60% of the beam thickness were tested. A load vs. midpoint deflection curve was recorded for each sample and failure (crack propagation) was defined as the point at which the load on the beam is maximum. The energy under the curve till the 'failure point' is termed as the 'total strain energy to failure'. The critical value of the J-integral, $J_{IC}$, is given by Equation 4-6 [56]:

$$J_{IC} = -\frac{1}{b}\left(\frac{dU}{da}\right) \tag{4-6}$$

where,

$J_{IC}$  = critical value of J-integral in plane strain, Pa-m (lb-in/in$^2$)

b  = beam width, mm (in.)

U  = total strain energy to failure in the notched beam, J (lb-in)

a  = notch length, mm (in.)

### 4.5.1 Sample Preparation and Testing

At the present time, ASTM standard tests do not exist specifically for the testing of notched asphalt concrete beams. Hence the following sample preparation and test procedures were used. Asphalt concrete beams of dimensions 50.8 x 50.8 x 203.2 mm (2 x 2 x 8 in.) were used for testing. These beams were cut from a larger beam of dimensions 101.6 x 101.6 x 406.4 mm (4 x 4 x 16 in.) compacted using the California Kneading Compactor in the Soils Testing Laboratory of the Michigan Department of Transportation, Materials Research Lab, Lansing, Michigan.

The beam mixes were prepared in the Dept. of Civil & Environmental Engineering at Michigan State University as described in previous chapters. Each beam was made from 10 kg. asphalt concrete mix divided into three equal parts of 3334 gm. each. The beam mixes were heated at 175°C (350°F) for 2 hours and allowed to equilibrate prior to compaction. The number of blows used for each specimen was modified to achieve an expected air void content between 3 and 5 percent. Each compacted beam was cut into four identical beams of dimensions 50.8 x 50.8 x 203.2 mm (2 x 2 x 8 in.) using a diamond blade saw. All surface irregularities were polished and a notch was cut in the center along the beam width to the required depth ( 40% to 60% of the beam width) with a diamond blade saw.

A minimum of 4 different notch lengths were used for each composition. The notched beams were allowed to dry for 24 hours at room temperature and then equilibrated at -10°C (14°F) for 2 hours in a temperature controlled chamber using liquid nitrogen as cooling agent. The 3-point bending beam test was performed in the UTS using a LVDT to measure the mid-point deflection. The tests were performed at a constant loading rate of 1.27 mm/min. (0.05 in./min.) and 117.8 mm (7 in.) span. A schematic of the sample configuration is shown in Figure 4.5.
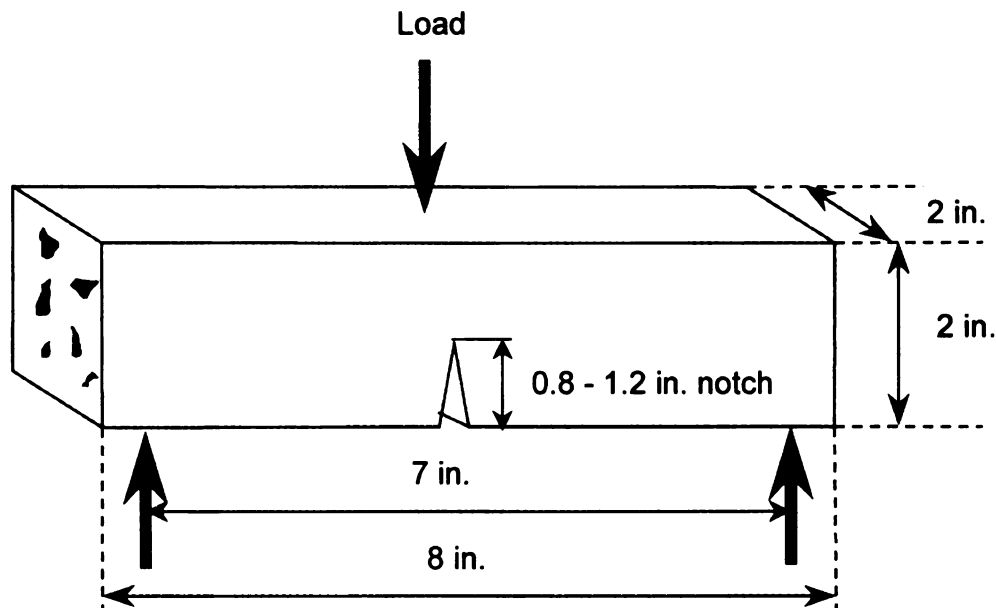


**Figure 4.5  Three-point bending beam sample configuration
for low temperature fracture toughness tests**

Load - deflection curves were plotted and the point of failure determined. The total strain energy per unit width (U/b) was plotted against the notch length and a linear fit to these points was obtained through regression. The slope of this line gives the rate of change of strain energy per unit width with respect to the notch length at failure, or the critical value of the J-contour integral fracture toughness ($J_{1C}$).

### 4.5.2    Effect of Aggregate Gradation

Aggregate gradation is an important factor to be considered in fracture toughness measurement. The repeatability of the data obtained improves significantly with a reduction in the aggregate size compared to the G7 gradation used for Marshall samples. When the aggregate size is large compared to the beam width, the aggregate size distribution at the notch tip can be very non-uniform. Since the fracture toughness measures the energy required for crack initiation at the notch tip, the presence of a large aggregates at the notch-tip can lead to scattered results due to the difference in modulus between the aggregate and asphalt binder. The repeatability increases as the ratio of aggregate size and beam width decreases. It was found that by using an aggregate gradation where 99% of the maximum aggregate size was 25% or smaller than the minimum beam dimension, the repeatability increased significantly. In repeatability tests performed on notched beam samples, the percent standard deviation was found to be greater than 10% for beams made with the G7 gradation. Beams made with the Fine Mix have higher repeatability and standard deviations were found to be below 10%. Representative repeatability test data is given in Table 4.2.

71

### 4.5.3 Selection of Fine Aggregate Gradation

The asphalt concrete beam width used for fracture toughness measurement was limited to 2 inches due to limitations of available material and equipment. Thus the G7 gradation could not be used for the fracture toughness samples. Due to the necessity of maintaining the maximum aggregate size in the asphalt concrete to 25% of the beam width, it was considered necessary to use a finer aggregate gradation. The fine mix gradation (FMG) used for fracture toughness tests is shown in Table 4.3. The rationale for selecting this gradation is given in the following section.

**Table 4.2  Effect of aggregate size on peak load of notched three-point bending beam test samples**

| Asphalt Binder | AC10 | AC10 | AC5 |
|---|---|---|---|
| Notch Length | 50% of width | 60% of width | 50% of width |
| Gradation | G7 | G7 | Fine Mix |
| Sample 1, peak load (lb) | 136 | 108 | 113 |
| Sample 2, peak load (lb) | 198 | 136 | 113 |
| Sample 3, peak load (lb) | 196 | 133 | 123 |
| Sample 4, peak load (lb) | 244 | 110 | 126 |
| Average | 193.5 | 121.8 | 118.8 |
| Std. Deviation | 22.9 % | 12.2% | 5.7% |

**Table 4.3 Fine Mix Gradation (FMG) used for Fracture Toughness Tests**

| Size (mm) | FINE MIX GRADATION | | | |
| --- | --- | --- | --- | --- |
| | Passing % | Retained % | Weight (gm) | Cumulative weight (gm) |
| 19 | 100 | 0 | 0 | 0 |
| 12.5 | 100 | 0 | 0 | 0 |
| 9.5 | 100 | 0 | 0 | 0 |
| 7.7 | 99 | 1 | 32.5 | 32.5 |
| 4.75 | 68 | 31 | 1007.5 | 1040 |
| 2.37 | 38 | 30 | 975 | 2015 |
| 1.18 | 26 | 12 | 390 | 2405 |
| 0.6 | 14 | 12 | 390 | 2795 |
| 0.3 | 10 | 4 | 130 | 2925 |
| 0.15 | 7 | 3 | 97.5 | 3022.5 |
| 0.075 | 4 | 3 | 97.5 | 3120 |
| Fly ash | 0 | 4 | 130 | 3250 |

### 4.5.4 Binder Film Thickness in Asphalt Concrete

The bulk modulus of asphalt concrete is dependant on the aggregate gradation used. Due to the change in gradation between the Marshall samples and the fracture toughness samples, a difference in the bulk modulus between the two types of mixes is expected. The fracture toughness, however, is a material property and thus does not depend on the sample geometry or the bulk modulus. It is a microscopic property and not a macroscopic property. Asphalt concrete is a composite material and it may be visualized as comprising of three major regions: aggregate, asphalt binder and the asphalt binder-aggregate interface. The fracture toughness is strongly dependant on the average thickness of the asphalt film between aggregates. The film thickness is also related to the durability of the asphalt concrete as thin films are more susceptible to aging by oxidation. In order to maintain a good basis of comparison between two mix gradations, it is deemed more important by the author to have similar asphalt binder film thickness than to have similar values of bulk modulus. For a given composition of asphalt concrete (94.3% aggregate, 5.7% asphalt binder) the asphalt film thickness is inversely dependant on the surface area of the aggregates. As the aggregate size reduces, the surface area increases leading to a decrease in the average binder film thickness.

The selection of the fine mix gradation was guided by a need to minimize the change in surface area while reducing the maximum aggregate size. This was accomplished by increasing the percent composition of the aggregates for the larger sizes and keeping the composition unchanged for the finer sizes. This can be seen more clearly in Figure 4.6.

The film thickness of the asphalt binder was calculated for the G7 and Fine Mix

Gradation. The methods used for these calculations are empirical in nature due to the

non-uniformity of aggregates. The equations used for calculation of the aggregate surface

area [57] and asphalt film thickness [58] are shown below.
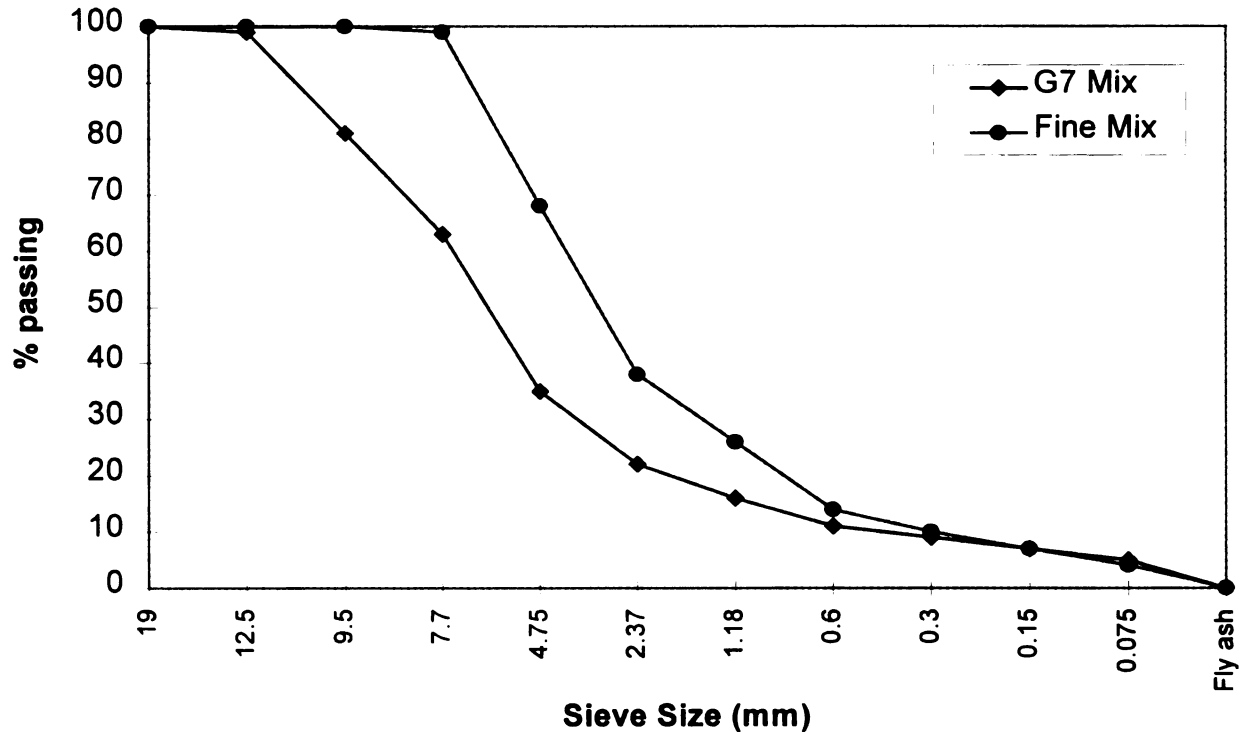


**Figure 4.6  Comparison between Fine Mix Gradation used for fracture
toughness samples and G7 Gradation used for Marshall samples.**

## Aggregate Surface Area Calculations

The surface area of aggregates was calculated according to the following equation [57].

$$SA = \Sigma \, ( \, SAF_i * P_i \, )$$ (4-7)

where

SA $\quad = $ Surface area of aggregate (sq.ft. / lb.)

$SAF_i \quad = $ Surface area factor for $i^{th}$ sieve

$P_i \quad = $ Fraction of total aggregate passing the $i^{th}$ sieve

The surface area factors for sieve sizes are empirical values calculated to approximate the surface area of the irregular aggregates. Table 4.4 shows the surface area factors used in calculations.

### Table 4.4 Surface area factors for aggregate [57].

| Sieve Size | Surface Area Factors |
|---|---|
| Percent Passing Maximum Sieve Size | 2 |
| Percent Passing No. 4 | 2 |
| Percent Passing No. 8 | 4 |
| Percent Passing No. 16 | 8 |
| Percent Passing No. 30 | 14 |
| Percent Passing No. 50 | 30 |
| Percent Passing No. 100 | 60 |
| Percent Passing No. 200 | 160 |

### Asphalt Film Thickness Calculation

The film thickness of the asphalt binder in the mix is not only a function of binder content and surface area. It is found that the asphalt binder penetrates the porous aggregate surfaces and thus the total amount of binder available for forming a film between two aggregate particles is reduced. The average asphalt binder film thickness in the mix taking into account the absorbed binder volume is given by [58] :

$$T_f = \frac{V_{asp} * (304,800)}{SA * W} \tag{4.8}$$

where

$T_f$      = Average film thickness (microns)

$V_{asp}$      = Effective Volume of asphalt cement (cu. ft.)

SA      = Surface area of aggregate (sq. ft./lb aggregate)

W      = Weight of aggregate (lb)

The Effective Volume of asphalt binder ($V_{asp}$) is the amount of material available for coating the aggregates and is the difference between the total asphalt binder added to the mix and the amount of asphalt binder absorbed by the aggregates. The average asphalt absorption capacity of the aggregates used was found to be 1.1% [40].

The asphalt binder film thickness calculated for the G7 and FMG mix (5.7% asphalt binder content) is shown in Table 4.5. The binder film thickness was found to be 11.1 μm for the G7 mix and 10.5 μm for the FMG.

**Table 4.5 Asphalt Binder Film Thickness for G7 and Fine Mix Gradations**

| Aggregate Gradation | G7 | Fine Mix | |
|---|---|---|---|
| Aggregate Surface Area | 21.3 | 22.5 | sq.ft./lb. |
| Weight of Aggregates | 11.9 | 11.9 | lb |
| Weight of Asphalt Binder | 0.7 | 0.7 | lb |
| Density of Asphalt Binder | 63.6 | 63.6 | lb/cu.ft |
| Aggregate Absorption Capacity | 1.1% | 1.1% | |
| Effective Volume of Asphalt Binder | 0.01 | 0.01 | cu.ft. |
| **Asphalt Binder Film Thickness** | **11.1** | **10.5** | **microns** |

## 4.6 Lap-Shear Adhesion

The Lap-shear test gives a measurement of the adhesive bond strength between two flat parallel plates having an overlap adhesive joint, when pulled apart under tensile loads. The test samples were prepared with aggregate sections and asphalt binder thin films similar to those used for characterization of asphalt binder morphology .

The substrate sections were made from 5mm thick slabs cut out from large aggregates. These were cut into sections 1"x1" in area, using a diamond saw. The cut sections were polished with a 200 grit abrasive paper for 20 minutes until no saw marks were visible on the surface. They were cleaned with alcohol and preheated in an air oven to the same temperature used for compression molding of the asphalt film. The asphalt film was cut into 7/8"x7/8" squares and sandwiched between two preheated rock sections. A 1 kg load was applied to the specimen assembly and the compression load

increased to 10 kg after the specimen cooled down to room temperature in an hour. The prepared specimen were tested in lap-shear mode[3]. Lap-shear tests were performed at five test temperatures (20°C, 10°C, 0°C, -10°C, -20°C) for polymer modified AC5 and AC10 binders with polymer content ranging from 0% to 6%. Fracture surfaces of the tested lap-shear samples were examined to characterize the failure modes using optical microscopy. The failure modes were broadly classified into three categories : adhesive, cohesive and mixed mode failure.

## 4.7    Summary

The experimental plan used for characterization of polymer modified asphalt concrete was structured to provide systematic information about the binder-aggregate interface, the microstructure and morphology of the binder and the mechanics of the failure processes in asphalt concrete. The information obtained from these experiments provides insight into the complex processes occurring within the asphalt concrete which lead to pavement distress under service conditions. The changes in properties of asphalt concrete due to polymer modification of the binder can be characterized using this information. With a database of these fundamental properties available, these tests can serve as tools for the prediction of asphalt concrete behaviour from the properties of the component materials. The results obtained from these tests are presented in Chapter 5.

---

[3] Lap-shear tests were performed by Dr. E. Eugene Shin, Research Specialist, Advanced Materials Engineering Experiment Station (AMEES), Michigan State University, USA.

# CHAPTER FIVE

# RESULTS

## 5.1 Asphalt Binder Morphology

The morphology of asphalt binder can be revealed in the Environmental Scanning Electron Microscope (ESEM) after exposure to the electron beam (e-beam). When the asphalt binder film is initially viewed, the surface appears to be featureless. However, after the e-beam has been allowed to raster across the surface of the film for 2-3 minutes, a network structure appears. The proposed mechanism for this is based upon the three phase structure of asphalt binder. Asphalt consists of three phases: high molecular weight asphaltenes, medium molecular weight resins and low molecular weight oils. The asphaltenes create a continuous networked phase and are surrounded by a sheath of resin [25,36,48]. The oils make up the rest of the volume and plasticize the asphaltene network. When the asphalt binder is exposed to the electron beam, the oils are believed to evaporate from the surface due to local heating and the underlying network is revealed in the area exposed to the electron beam as seen in Figure 5.1. On removal of the electron beam, the network structure disappears and the surface becomes featureless in 2-3 minutes as the oils from the surrounding asphalt diffuse back into the region. This process can be repeated several times on the same area to reproduce the network structure. The network is capable of deformation under applied loads. Figure 5.2 shows a series of micrographs of the asphalt network subjected to tensile load. The network gradually deforms and aligns itself in the direction of the load.
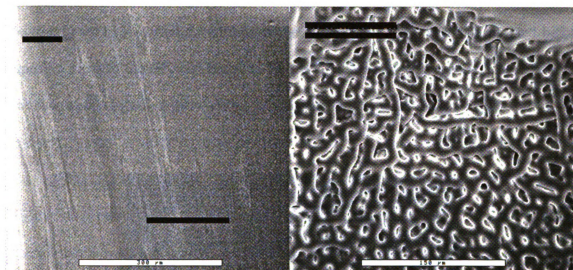
Figure 5.1  Network morphology of asphalt binder.  Left : Featureless surface of asphalt film immediately after exposure to the electron beam (150X, white bar = 300μm). Right : The randomly oriented network structure seen after exposure to the electron beam for 2-3 minutes (300X, white bar = 150 μm).
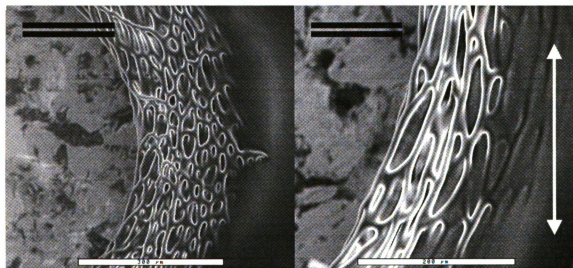


Figure 5.2   Network structure in asphalt binder film under progressive tensile loading (150X). The network aligns itself in the direction of loading (indicated by arrow.) Left: White bar = 300μm. Right: White bar = 200μm.

In order to determine if the network structure is real or an artifact induced by the electron beam as it rasters the surface of the binder, thin films were pre-strained before exposing them to the electron beam in the ESEM. The network structure in these films was seen to be aligned in the direction of the strain as shown in Figure 5.3.
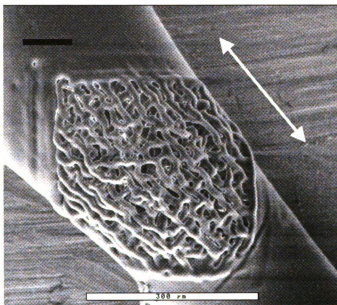


**Figure 5.3  Pre-strained AC10 asphalt binder thin film, exposed to the electron beam shows network structure aligned in the direction of applied strain (indicated by arrow) at 155X. White bar = 300 μm.**

Since the films were strained prior to e-beam exposure and the network in unstretched films does not show any alignment, it is evident that the network structure is real and exists within the asphalt and that the deformation causes alignment of the network in the direction of the applied strain.

### 5.1.1 Morphology of Aged Asphalt Binders

Aged asphalt binders have a significantly different morphology than fresh binders. During the aging process, asphalt undergoes extensive oxidation and there is an increase in the molecular weight of the constituents [31-32]. Low molecular weight fractions, i.e. oils, decrease and the fraction of high molecular weight constituents (resins and asphaltenes) increase. This leads to an increase in the viscosity and modulus of the binder, but adversely affects the toughness and the fracture properties of asphalt concrete. Aging of asphalt binder was simulated using the Thin Film Oven Test (TFOT, AASHTO T179 or ASTM D1754-87) followed by the Pressure Aging Vessel (PAV, AASHTO PP1) Test. Details of the aged sample preparation are discussed in more detail by Shull [31]. One of the prominent features of aged asphalt is the appearance of the network structure. The smooth network fibrils seen in fresh binders appear very coarse and thickened after aging as seen in Figure 5.4.
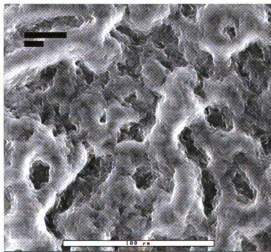


**Figure 5.4 Typical morphology of aged asphalt binders. The network fibrils appear coarse and the network can only be seen after substantially long (5-10 minutes) exposure to the electron beam (500X). White bar = 100 μm.**

### 5.1.2   Effect of Polymer Addition on the Morphology of Aged Asphalt Binders

Polymer modified asphalt binders have an enhanced resistance to aging which can be measured in terms of retention of properties in aged polymer modified asphalt binder and concrete. These differences are also seen in the morphology of the binder. The network morphology of polymer modified asphalt is similar to that of fresh asphalt and the network fibrils do not appear coarse. Figure 5.5 shows the morphology of aged AC10-0% Elvaloy AM and AC10-3% Elvaloy AM. In the unmodified binder which is severely aged due to the combined effect of the high temperature used for blending Elvaloy AM into the asphalt and accelerated aging in the Thin Film Oven Test-Pressure Aging Vessel (TFOT-PAV) tests, the network structure is barely visible after an exposure of 7 minutes while the polymer modified binder with an identical history has a network structure similar to a fresh binder.
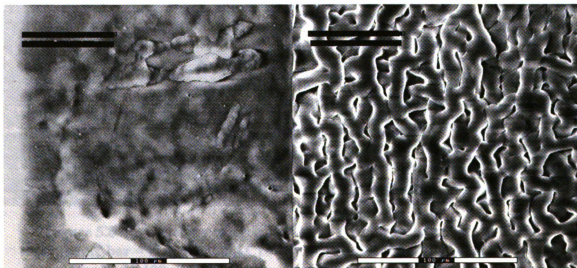


**Figure 5.5  Morphology of aged AC10-0% Elvaloy AM (left) and AC10-3% Elvaloy AM (right) after 7 minutes of exposure to the electron beam (500X, white bar = 100 μm.)**

Similar behaviour is observed in the case of SBS, SEBS and SBR latex modified AC5 and AC10 asphalt binders. However, the behaviour of crumb rubber is contrary to this. The morphology of crumb rubber modified asphalt binders appears very coarse, while that of binder with 0% crumb rubber is similar to fresh binders as seen in Figure 5-6. This may be explained by the fact that the mixing conditions for crumb rubber modified binders are mild (350F, 30 minutes) and consequently the binders do not undergo significant oxidation during mixing. Binders with 0% crumb rubber, when aged further by TFO-PAV, retain most of their original properties. However, in the case of binders with added crumb rubber, the rubber particles are believed to absorb the oils and thus give the binders the characteristic coarse appearance of aged binders.
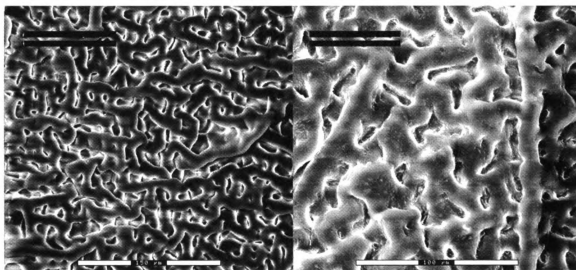


**Figure 5.6 Morphology of aged AC10-0% Crumb Rubber (left) at 300X (white bar = 150μm) and AC10-10% Crumb Rubber (right) at 500X (white bar = 100μm) after 2 minutes of exposure to the electron beam.**

This characteristic of the crumb rubber modified binders may be worthy of further study, especially in the context of durability of asphalt concrete. The rubber particles may act as reservoirs for the low molecular weight fractions of asphalt during the life-span of the road; effectively preventing the oxidation of oils early in the life span of the pavement and maintaining a steady supply of these absorbed oils to the asphalt binder as the pavement ages naturally and the concentration of oils outside the rubber particles decreases.

### 5.1.3 Effect of Asphaltene Content on the Morphology of Asphalt Binders

Asphalt binders from different sources having different asphaltene content were obtained from MDoT to study the effect of asphaltene content on binder morphology. Three asphalt binders were obtained -

| Source | Asphaltene Content |
| --- | --- |
| Koch Matls. Co., IL | 8.8% |
| Amoco Oil Co., IN | 15.5% |
| T-M Oil Co., MI | 20.4% |

The network structure was observed in all three binders, but the rate at which the asphalt network becomes visible was found to be dependent on the asphaltene content of the binder. The differences observed in the three binders are discussed below.

*8.8% Asphaltene Content*

The 8.8% asphaltene content binders form the network structure rapidly (approx. 15 sec.) at 300X magnification. On removal of the e-beam, the oils diffuse back into the area rapidly and the surface returns to its original featureless state in approximately 30 seconds. The fibril density is low and fibrils have a larger diameter. Figure 5-7 shows the network formation of an asphalt binder with 8.8% asphaltene content at different times and stages of formation.
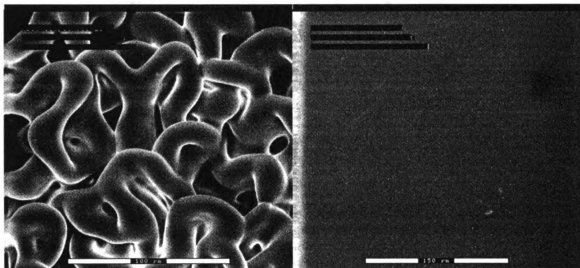


**Figure 5.7  Morphology of 8.8% asphaltene content binder. Left: the network is visible in 15 seconds (white bar = 100 μm). Right: surface returns to original state 30 seconds after beam removal (white bar = 150 μm).**

*15.5% Asphaltene Content*

The 15.5% asphaltene content binder network resembles the AC5 and AC10 binders used in the study. The network density is higher than the 8.8% asphaltene binders and the network fibril diameters are smaller. Network formation is slower ( approximately 30 seconds) and on removal of the e-beam the oil diffusion process takes longer ( approximately 1 min). Figure 5-8 shows the network formation seen in binder with 15.5% asphaltene content at different times and stages of formation.
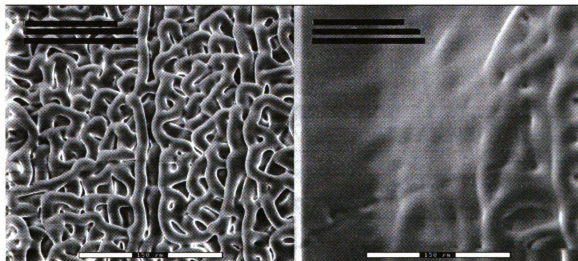


**Figure 5.8 Morphology of 15.5% asphaltene content binder. Left: the network is visible in 30 seconds (white bar = 150 μm). Right: surface returns to original state 1 minute after beam removal (white bar = 150 μm).**

*20.4% Asphaltene Content*

The 20.4% asphaltene content binders have the highest network density. Fibril diameters are smallest among the three binders. The kinetics are slow and it takes 1-2 minutes to form the network and after the e-beam is removed, the oils take 3-4 minutes to diffuse back into the region. Figure 5-9 shows the network formation seen in binder with 20.4% asphaltene content at different times and stages of formation.
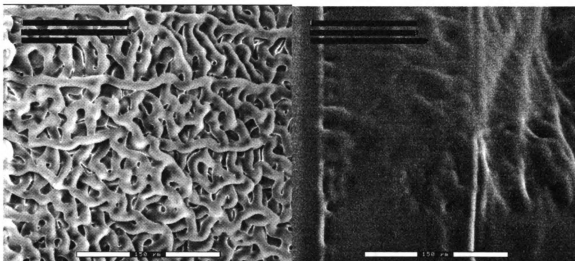


**Figure 5.9  Morphology of 20.4% asphaltene content binder. Left: the network is visible in 1 minute (white bar = 150 μm). Right: surface returns to original state 4 minutes after beam removal (white bar = 150 μm).**

From these results it can be suggested that the process involved in the revelation of the network structure by e-beam exposure and the disappearance of the structure on e-beam removal is diffusion controlled and directly related to the asphaltene content and rheological characteristics of the binder.

## 5.2    Polymer Phase Morphology

Laser scanning confocal microscopy was used to determine morphology of the SBS, SEBS and SBR polymer phase in AC10 asphalts. As described previously, blue laser (488 nm) was used for excitation and the fluorescence was measured using a red band pass filter (590-620 nm). The images obtained were inverted for clarity and thus the polymer phase appears as a dark region over a light background which represents asphalt. Figure 5-10 shows a LSM micrograph of unmodified asphalt at a magnification of 200X. The surface is featureless and a small amount of background fluorescence from the unsaturation in the asphalt binder is observed.
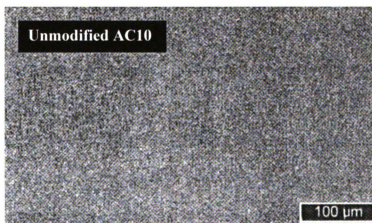


**Figure 5.10  LSM micrograph of unmodified AC10 binder in fluorescent mode.**

In polymer modified asphalt, the LSM was able to detect the distribution of the polymer in the binder. AC10 binder modified with 5% polymer was used to compare the morphology of SBS, SEBS and SBR. Figure 5.11 shows LSM micrographs of SBS and SEBS modified AC-10 asphalt binder. It is seen that SBS and SEBS form discrete phases at a concentration of 5% by weight. The size of the SBS and SEBS phases ranges from 1 to 20 μm and appears to consist of spherical or slightly elongated microscopic domains.

Such morphology for SBS has been reported by Adedeji et. al. [59] where the SBS network is not formed below 10 wt.% SBS and discrete SBS rich microdomains are observed which undergo transformation from short cylinders to lamellae and finally to spheres. Similarly, Ho et al. [60] report an elongated hexagonal cylinder-like microstructure in SEBS modified asphalt. This is consistent with the morphology of SBS and SEBS observed in the LSM.

The LSM was also used to investigate AC10 modified with 5wt% SBR. SBR latex fluoresces strongly and forms a networked phase in the asphalt as shown in Figure 5.12. The SBR network is made up of fine, well aligned strands approximately 0.5 μm in diameter.

It is interesting to compare the LSM images of the SBR modified asphalt to ESEM images of these same samples. As in previous ESEM experiments with asphalt binder thin films, the electron beam was allowed to raster over an unmodified AC10 asphalt film and an AC10-5%SBR film. Initially, the control AC10 asphalt is featureless but a network structure is visible after 3 minutes of exposure and the fibrils in the network are randomly oriented and have a diameter of ~10 μm, which is similar to that observed in SBS and SEBS modified asphalts. However, the network structure of the SBR modified asphalt is significantly different. After exposure to the electron beam, the fibrils in the SBR modified asphalt were seen to be strongly aligned compared to the control sample as seen in Figure 5.13.
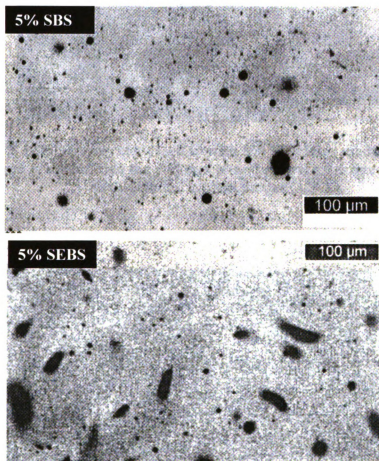
**Figure 5.11  LSM micrograph of AC10 with 5% SBS and SEBS modifier in
fluorescent mode (dark areas indicate the polymer phase) showing discrete polymer
phase in the asphalt binder (200X).**
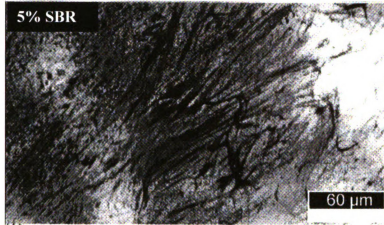
**Figure 5.12  LSM micrograph of AC10 with 5% SBR latex modifier in fluorescent mode (dark areas indicate the polymer phase) showing the fine network of SBR strands in the asphalt binder (333 X).**
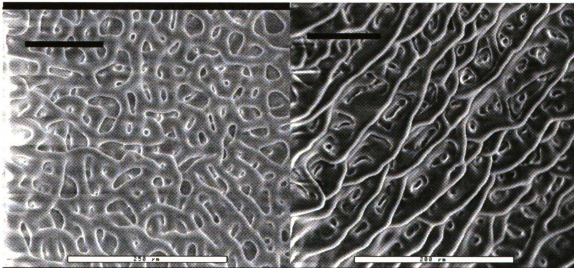


**Figure 5.13  ESEM micrographs of AC10 asphalt binder with 0% SBR (left, white bar = 250 μm) and 5% SBR (right, white bar = 200 μm). The network fibrils in the control sample are random while the SBR modified sample shows an alignment of the network fibrils.**

The binder morphology seen in the ESEM qualitatively agrees with results using fluorescence microscopy. The ESEM investigations show that the network structure in the SBR modified asphalt is well aligned - this is anticipated since the SBR is strongly textured according to the LSM results. However, there is a discrepancy in that the diameter of the fibrils observed with the ESEM and LSM are quite different. The SBR strands shown in Figure 5.11 are ~0.5-1.0 μm in diameter, which is smaller than the fibrils shown in Figure 5.12 (~5.0 μm diameter). This is attributed to the fact that the fluorescent images show only the SBR phase, while the ESEM images rely on the removal of the low molecular weight oils to reveal the network structure and therefore the fibrils seen in the ESEM micrographs contain asphaltene, resin and polymer constituents.

## 5.3    Void Morphology

### 5.3.1   Thin Section Image Analysis

Void analysis provides an understanding of the different types of voids found in asphalt concrete, viz. interfacial voids, binder phase voids and isolated voids [25]. Binder phase voids are small in size and are completely surrounded by the asphalt binder. Interfacial voids are large irregular shaped air-voids found near the surface of the aggregates. Isolated voids are air-voids trapped between aggregates where the binder does not penetrate. The image analysis system used statistical mean circle diameters and aspect ratios of voids in a thin plane section to calculate the net air-void content. This method, however, did not give an accurate measure of the actual net air-void content in the asphalt concrete since the void distribution and void shapes in asphalt concrete samples are non-uniform. A quantitative two-dimensional analysis of such voids thus

does not yield good results for the sampling size used. Table 5-1 shows the results of the thin section void analysis performed on SBS and SEBS modified asphalt concrete (AC5 and AC10).

**Table 5.1  Air void content of SBS and SEBS modified asphalt concrete by image analysis.**

| Image Analysis | AC5 | AC5-5%SBS | AC10 | AC10-5%SBS | AC10-5%SEBS |
|---|---|---|---|---|---|
| Air Void Content (vol. %) | 1.28 | 0.97 | 1.58 | 1.56 | 0.70 |
| Number of Air Voids | 547 | 107 | 118 | 124 | 396 |
| Avg. Equivalent Circle Dia. (mm) | 0.09 | 0.16 | 0.39 | 0.32 | 0.10 |
| Avg. Form Factor | 37 | 39 | 40 | 41 | 38 |
| Total Area of Section (cm$^2$) | 30 | 30 | 32 | 32 | 32 |
| Total Scan Area (cm$^2$) | 21 | 21 | 24 | 24 | 24 |

The approximate void content of the asphalt concrete used in the above tests was 4-5% according to the mix design and bulk measurement of the sample density. Thus the thin section void analysis was found to be unrepresentative of the true air void content of asphalt under the test conditions used. The main reason for this is the difficulty in representing irregular three-dimensional voids by a two-dimensional technique. This is acknowledged by Scott [25] and Rouge et al. [61-63] have shown that it is possible to obtain relationships between the observed surface porosity from 2-dimensional image analysis and the 3-dimensional void volume obtained by a bulk technique such as mercury porosimetry in materials with regular, open pores such as brake pads. At the current time, it is the opinion of the author that the 2-dimensional image analysis technique for analysis of air-voids in asphalt concrete needs further refinement and study before it can be applied quantitatively with confidence.

### 5.3.2 Void Casting Method

The void casting method gives a more accurate measure of the net air-void content in asphalt concrete. It also allows the visualization of air voids (interfacial and binder phase voids) in three dimensions. This is a better method to characterize void shapes and sizes than the image analysis which only characterizes the uneven voids in two dimensions and extrapolates the results.

The void content and distribution in asphalt concrete was characterized for SBR and Elvaloy AM modified binders using this method. Table 5-2 shows the net air void content of the modified asphalt concrete samples. The distribution of voids in the asphalt concrete can be characterized by considering the distribution of void volume. Two major types of voids, binder phase voids and interfacial voids were characterized. Binder phase voids are generally small in size and experimental observations suggest they have void volumes smaller than approximately 10 cu.mm. Binder phase voids are beneficial to the properties of asphalt concrete as they allow for expansion of the binder at high temperatures preventing bleeding of the binder from the concrete. For the purposes of semi-quantitative analysis of the change in void distribution due to polymer modification, all voids smaller than 10 cu.mm. were considered as binder phase voids and all voids greater than 10 cu.mm. were considered as interfacial voids. Interfacial voids are large, irregular and not beneficial since they provide starting points for adhesive fracture in asphalt concrete. Environmental freeze-thaw cycling during winter can lead to adhesive failure if a large number of interfacial voids are present by providing initiation points for cracks.

**Table 5.2  Air void content of SBR and Elvaloy AM modified
asphalt concrete calculated by void casting**

| Material | Volume Sampled (cu. mm) | Air Void Content (volume %) |
|---|---|---|
| AC5-0%SBR | 27104 | 4.04 |
| AC5-5%SBR | 38280 | 4.66 |
| AC5-0%Elvaloy AM | 27825 | 6.95 |
| AC5-2%Elvaloy AM | 28224 | 4.97 |

The normalized distribution of void volume in SBR and Elvaloy modified AC5 is shown in Figures 5.14 and 5.15 respectively. In unmodified AC5 asphalt concrete, the void distribution shows approximately 80% interfacial voids while the content increases to approximately 86% with SBR modification. Elvaloy AM modified asphalt, which has a higher binder processing temperature than SBR modified binder, was found to have approx. 89% interfacial voids without any polymer added and approx. 95% interfacial voids for 2% Elvaloy AM content. The change in void volume distribution between unmodified and modified asphalt for both types of polymer shows that a significant amount of the void volume is contributed by interfacial voids (voids larger than 10 cu.mm.) and polymer modification increases the proportion of interfacial voids by a small fraction. The consistent increase in the interfacial void volume may be a result of the processing conditions of the asphalt concrete samples. All Marshall samples used in the study were mixed at the same temperature. Polymer modified asphalt binders generally have a higher viscosity than unmodified asphalt binders and when processed at the same temperature, binders with different viscosities are likely to have different flow and wetting behaviour. Interfacial voids are formed due to incomplete wetting of the aggregate by the binder during mixing and a binder with higher viscosity may be expected to have more interfacial voids as seen in these results. The total change in void

volume distribution for the four types of samples, the melt temperature of the binder and the viscosity of the binders at 275°F is shown in Table 5.3.

**Table 5.3  Distribution of void volume in SBR and Elvaloy AM modified AC5**

| Material | Binder Phase Voids ($<10mm^3$) | Interfacial Voids ($>10mm^3$) | Melting Temperature (°C) | Viscosity at 275°F (cp) |
|---|---|---|---|---|
| AC5-0%SBR | 20 % | 80 % | 38 | 260 |
| AC5-5%SBR | 14 % | 86 % | 46 | 2337 |
| AC5-0%Elvaloy AM | 11 % | 89 % | 52 | 988 |
| AC5-2%Elvaloy AM | 5 % | 95 % | 57 | 3715 |

The increase in net interfacial void volume correlates with the increase in binder viscosity as a result of polymer addition and this may be a key factor that should be taken into account. The proper selection of processing temperatures is important in the case of polymer modified asphalts and care should be taken to maintain the binder viscosity at a level at which good wetting of the aggregate is achieved.
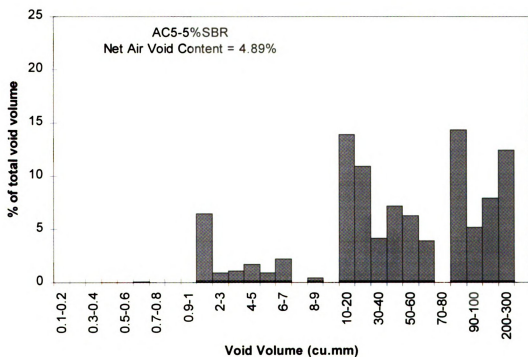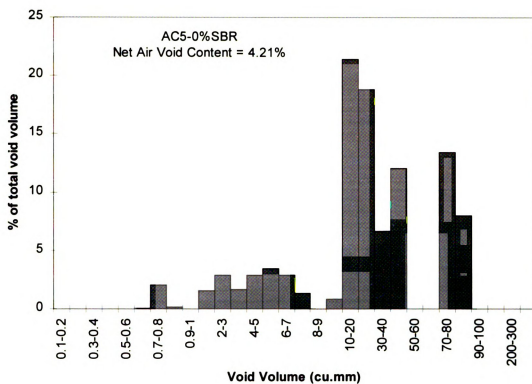
**Figure 5.14    Void volume distribution in AC5 with 0% and 5% SBR**
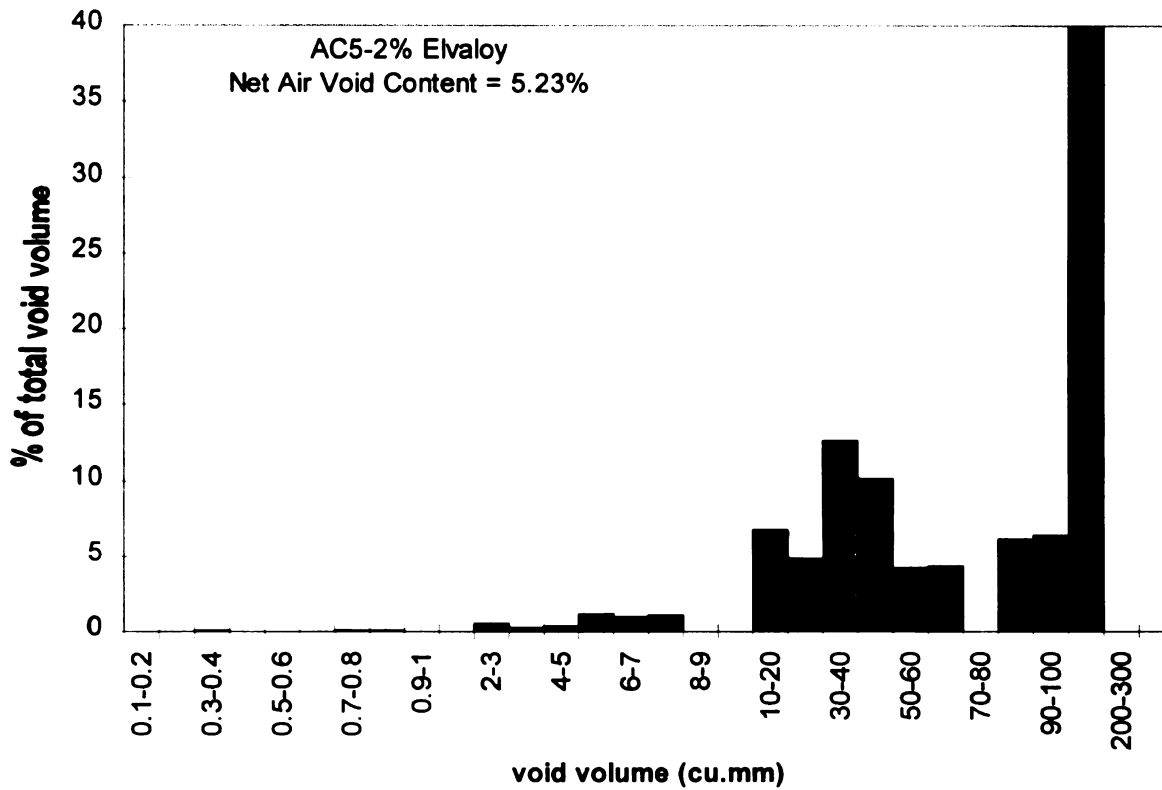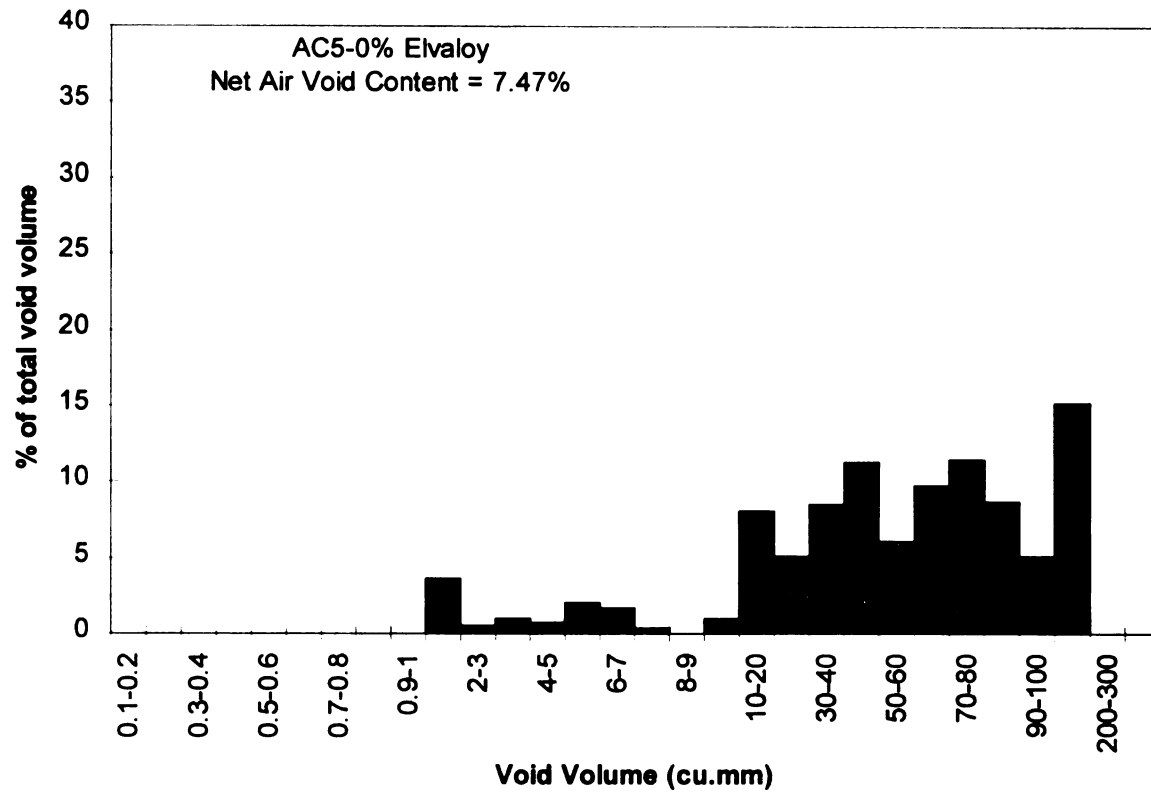
**Figure 5.15**   Void volume distribution in AC5 with 0% and 2% Elvaloy AM

## 5.4    In-situ ESEM Tensile Tests

The in-situ tensile test performed on asphalt concrete sections is an excellent method to identify the fracture mechanisms and fracture morphology in asphalt concrete. The network structure seen in asphalt binder thin films is also seen in asphalt concrete specimen during the tensile fracture tests. The network strands in the binder play an important role during the fracture process of asphalt concrete. Polymer modified asphalt concrete shows a vastly different fracture morphology than unmodified asphalt concrete due to the changes in binder morphology. These changes include a reduction in adhesive (interfacial) failure, a corresponding increase in cohesive (binder phase) failure and the appearance of crack bridging mechanisms. The fracture process is seen to progress in three stages: void formation, void growth and crack propagation [19,25]. When the asphalt concrete specimen is strained, isolated voids develop in the binder phase. After sustained deformation the voids increase in size and finally interconnect giving rise to a continuous crack. As the voids grow in size, the binder between voids necks and forms long asphalt bridges (fibrils) across the growing crack. In order for the crack to grow, these fibrils have to be fractured and this process absorbs a part of the fracture energy, thus providing a mechanism for energy dissipation which improves the resistance offered by the material to fracture processes.

The ESEM tensile test results show differences in the fracture morphology of the different types of polymer modified asphalt concretes. Adhesive and cohesive failure modes were observed. Adhesive failure is defined as failure where crack propagation occurs at the asphalt binder-aggregate interface and is generally seen at low temperatures due to the increase in the binder modulus. Cohesive failure is defined as

failure where the crack propagates through the asphalt binder phase only. This type of failure is seen at higher temperatures (above 0°C) where the asphalt binder modulus is very low. Figure 5-16 shows micrographs of typical adhesive and cohesive failure in asphalt concrete.
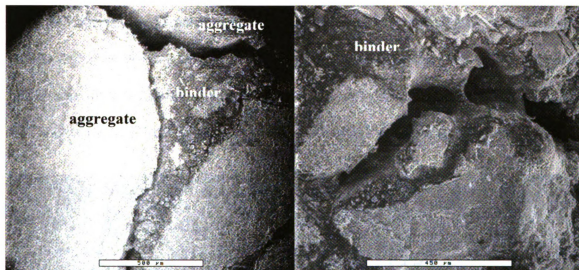


**Figure 5.16 ESEM micrographs showing adhesive failure in asphalt concrete at 0°C at 65X (left, white bar = 500 μm) and cohesive failure at 25°C at 100X (right, white bar = 450 μm)**

Cohesive failure is the preferred type of fracture mechanism since it is associated with fibril formation, an energy dissipating process. Adhesive failure is a more serious problem at low temperatures, leading to extensive cracking and stripping. The locations at which fibrils are formed can be considered to be areas with very good asphalt-aggregate adhesion.

*Unmodified AC5*

Unmodified AC5 shows a tendency for the fracture to proceed along the aggregate boundaries. The failure was observed to be both adhesive and cohesive. The mechanism of cohesive failure starts with void formation in the binder phase. These voids grow and interconnect, leaving a few fibrils which act as crack bridges. The fibrils are about 6-7 microns in diameter and begin to neck after being sufficiently strained. Fibril rupture occurs at about 2 micron neck diameter and 50-100 micron length. Only a few fibrils were observed across the fracture surface in unmodified concrete samples. Figure 5.17 shows a typical fracture in unmodified AC5 asphalt concrete at 370X and 100X.
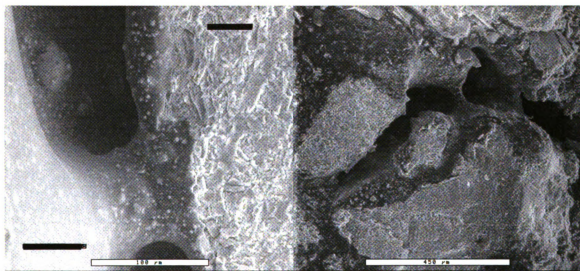


**Figure 5.17 Typical fracture in unmodified AC5 asphalt concrete.**
**Left: 370X (white bar = 100 μm),  Right: 100X (white bar =450 μm).**

*AC5-SBS*

The fracture morphology is strongly affected by the addition of SBS. Figure 5.18 shows a large number of fibrils across a crack in AC5-5%SBS at 400X and 100X. The most noticeable feature is an increase in the number of fibrils formed and their deformation behavior. The fibrils are thinner, longer and appear to be interconnected. They are more elastic and have higher elongation at break. Most fibrils are stable up to elongations of 130 microns. The number of fibrils forming across the crack increase in direct proportion to the concentration of the polymer added. There do not seem to be any apparent morphological changes in the fibrils due to increasing polymer concentration.
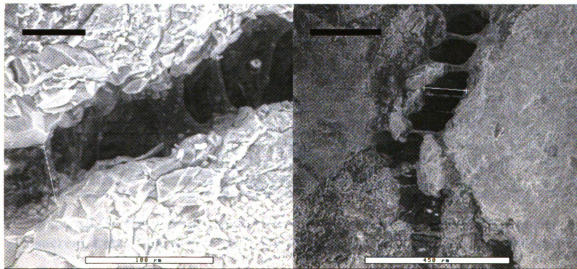


**Figure 5.18    Micrographs showing cohesive failure and increased fibril formation in AC5-5%SBS asphalt concrete. Left: 400X (white bar = 100 μm),  Right: 100X (white bar = 450 μm).**

The morphology seen in SEBS modified AC5 samples is similar to that of SBS modified AC5. Figure 5.19 shows the failure process in AC5-2%SEBS asphalt concrete at 100X and 415X. The fibril formation is not as dense as that seen in SBS. The elongation at break is approximately 70-130 microns. Failures were mostly cohesive and gross adhesive failure was only seen in a few instances. Compared to unmodified AC5, SEBS modified AC5 shows higher fibril formation and elongation.
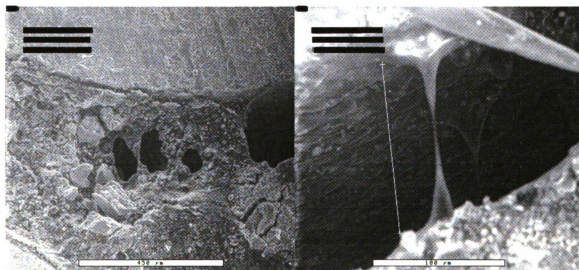


**Figure 5.19 Micrographs showing failure process in AC5-2%SEBS asphalt concrete. Left: 100X (white bar = 450 μm), Right: 415X (white bar = 100 μm.)**

*AC5-ELVALOY AM®*

Elvaloy modified AC5 binders appear to have a much higher stiffness compared to other previously studied polymer modified systems. Figure 5-20 shows a typical fracture in AC5-2%Elvaloy, exhibiting an extremely low fibril density (150X). Fracture was observed to predominantly occur near the binder-aggregate interface rather than in the binder phase. The modified binder forms coarse bridges across the crack face, but very low fibril densities

were observed. The number of fibrils formed were fewer than seen in the unmodified material and decreased rapidly with increasing polymer concentration. The individual binder fibrils are about 7-8 microns in diameter at the base and about 2 microns at the neck at the point of failure. Elvaloy concentration does not visibly affect the morphology at this level. From the change in fibril density and fracture morphology, Elvaloy modified binders appear to have reduced viscoelastic behavior.
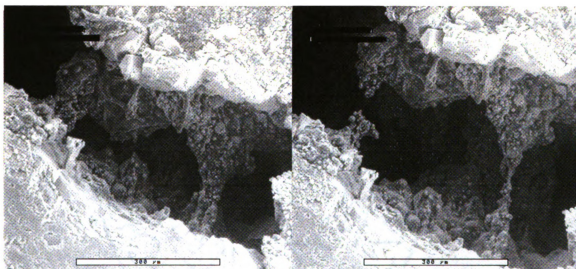


**Figure 5.20 Typical fracture surface in AC5-2%Elvaloy showing low fibril density.**
**Left: 150X, Right: 150X. White bar = 300 μm.**

*AC5-SBR*

With the addition of SBR latex, binder morphology undergoes a vast change. Figure 5.21 shows a typical fracture in AC5-5%SBR at 300X and 1000X. The micrographs show a high density of tough fibrils at large crack widths. The binder remains soft and can sustain high plastic deformation. The aspect ratio and appearance of the binder fibrils changes with longer, thinner strands connecting the two fracture surfaces. The fibril density obtained with SBR is the highest amongst all the polymer modified binders studied. The deformation

behavior is also different in that the entire fibril elongates instead of necking. SBS, SEBS, Elvaloy and unmodified binders normally show fibril rupture at a crack width of 50 μm to 300 μm. SBR fibrils remain stable even when the crack width is on the order of millimeters, and macroscopic observations indicate that some fibrils extend to approximately 25-50 mm before rupture. The fibril density is seen to be directly proportional to the concentration of SBR latex in the binder. Most fibrils have an extremely high aspect ratio, remaining stable even up to diameters of 700 nm. Fibrils are also seen to be clearly attached to the aggregates at their ends. This type of morphology is likely to prove beneficial in terms of crack inhibition and crack healing in asphalt concrete.
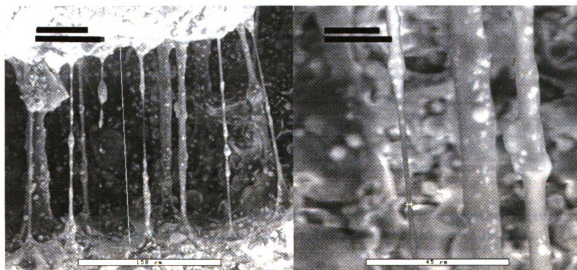


**Figure 5.21  Micrographs showing cohesive failure and increased fibril formation in AC5-5%SBR asphalt concrete. Left: 300X (white bar = 150 μm),  Right: 1000X (white bar = 45 μm.)**

*AC5 - Crumb Rubber*

With the addition of crumb rubber, the asphalt binder fibrils were observed to have much higher elongation at break (~600 microns) and the fibril density shows a slight

increase as compared to unmodified AC5. The fracture surfaces appear to be covered with asphalt and no bare aggregate surfaces were observed. Figure 5.22 shows the failure surface of AC5-10% Crumb Rubber with long fibrils bridging the fracture. The network structure seen in asphalt binder thin films can also be seen in the tensile tests. The asphalt binder network fibril seen in the figure has a diameter of ~8μm which correlates with the network dimensions observed in the ESEM studies of asphalt binder.
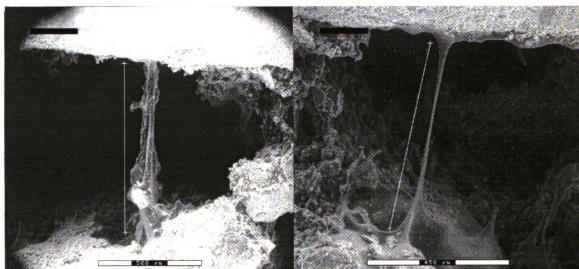


**Figure 5.22    Micrographs showing aligned network fibrils across the fracture surface in AC5-10% Crumb Rubber. Left: 65X (white bar = 500 μm), Right: 100X (white bar = 450 μm.)**

### 5.4.1 Role of Binder Morphology in Fracture Process

The observation of the asphalt binder network in tensile fracture tests further validates the physical nature of the network. The network fibrils are believed to be responsible for the strength of the asphalt binder. As has been noted before, asphalt bridges form across the fracture surfaces as the crack progresses. Closer observation of these fibrils shows that the binder morphology in asphalt concrete remains similar to that seen in pure binder films. As the fracture process in asphalt concrete progresses, the binder fibrils deform in a manner similar to that seen in pure binder films. Figure 5.23 shows the systematic deformation of binder network fibrils. The asphalt bridges initially consist of a group of binder network fibrils which align themselves in the direction of strain and slowly deform and rupture as the strain increases over a critical value. This process of deformation dissipates fracture energy and increases the overall fracture resistance of asphalt concrete. The overall changes seen in the fracture morphology of asphalt are semi-quantitatively summarized for all types of polymer modifiers in Table 5.4.
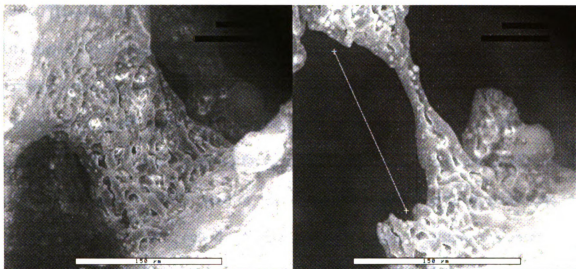
**Figure 5.23 Micrographs showing details of the network structure seen in asphalt concrete and its deformation as the sample is subjected to a tensile load. Left: 305X, Right: 350X. White bar = 150 μm.**

**Table 5.4 Summary of changes in fracture morphology of asphalt due to polymer modification.**

| Material | Average Fibril Length | Average Fibril Diameter at Break | Fibril Density Relative to Unmodified Asphalt |
|---|---|---|---|
| AC5 | 50-100 μm | 2 μm | |
| AC5 - SBS | 70-130 μm | 2 μm | + |
| AC5 - SEBS | 70-130 μm | 2 μm | + |
| AC5 - SBR | 1 - 2 mm | 700 nm | +++ |
| AC5 - Elvaloy AM® | 70-100 μm | 2 μm | - |
| AC5 - Crumb Rubber | 600 μm | 2 μm | + |

(+) indicates increase in fibril density
(-) indicates decrease in fibril density

## 5.5    Fracture Toughness Test Results

The J-contour integral fracture toughness is an estimate of the fracture toughness of a material near the initiation of slow stable crack growth. The low temperature fracture toughness of asphalt concrete was determined by 3-point bending beam tests using beams notched to different depths. Notch lengths corresponding to 40%, 45%, 50%, 55% and 60% of the sample width were used for each composition at a temperature of -10°C. The test temperature was chosen based on the failure modes observed in lap-shear tests. At temperatures above -10°C, cohesive failure in the asphalt-binder system was observed in lap shear test specimens while at temperatures below -10°C the failure was observed to be interfacial adhesive failure. The primary failure process in asphalt concrete is low temperature fracture caused by freeze-thaw cycling and thus the effect of adhesion on the fracture toughness can be determined by low temperature fracture tests.

Asphalt concrete is a composite material consisting of three components: aggregate reinforcement, asphalt binder matrix and the aggregate-binder interface. The properties of the concrete are affected by the properties of the individual constituents. A change in the quality of aggregate, gradation, angularity, porosity or any other property can change the ultimate properties of the concrete. Similarly, the quality of the asphalt binder, film thickness and viscosity change the properties of the concrete. For this reason it is important to realise that the absolute values obtained in fracture tests are not of much consequence by themselves, but must be used for purposes of comparison and identification of trends. Since the various binders used have different processing conditions and final properties, comparisons will be made only within each type of modified binder system.  It should be noted that SBS and Crumb Rubber samples used in

fracture toughness tests were made using AC5 binder obtained from a different batch from that used in all the other tests described previously. Since the properties of asphalt binder may differ from batch to batch, direct comparisons between two systems can be lead to erroneous conclusions. Fracture toughness test results are shown in the following sections. In all fracture toughness results, error bars represent the standard error in calculation of $J_{IC}$. The load-displacement curves for all compositions tested are provided in Appendix A.

*AC5 – SEBS*

Polymer modified AC5 concrete beams were tested at concentrations of 0%, 3% and 5% SEBS. These concentrations were chosen based on the optimum concentrations of SEBS modifier determined from rheological studies. The fracture toughness improves with the addition of 3%SEBS but with an increase in the concentration to 5%SEBS, the toughness decreases below that of 3% SEBS, but still shows an improvement over unmodified AC5. Figure 5.24 shows the change in fracture toughness due to SEBS modification.

*AC5 - Elvaloy AM*

Elvaloy AM modified AC5 samples were made at 0%, 1% and 2% concentration. The addition of Elvaloy AM does not seem to have any effect on the low temperature fracture toughness of AC5 asphalt concrete. The fracture toughness is almost constant for 0% and 1% concentration and decreases slightly at 2% Elvaloy concentration as seen in Figure 5.25.
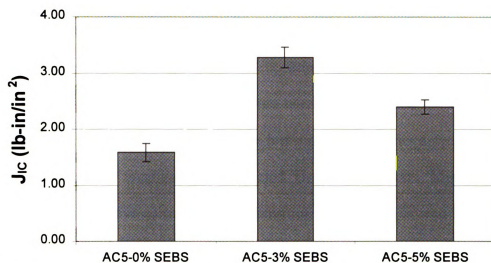
**Figure 5.24  Fracture toughness of SEBS modified AC5 asphalt concrete at -10°C**
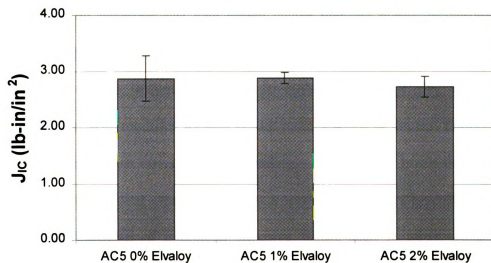


**Figure 5.25  Fracture toughness of Elvaloy modified AC5 asphalt concrete at -10°C**

*AC5 – SBR*

The addition of SBR latex to AC5 at 3% and 5% concentration causes a decrease in the fracture toughness of asphalt concrete at -10°C as seen in Figure 5.26. The decrease in toughness is incremental and contrary to the conclusion suggested by the ESEM fracture tests where an extremely high amount of fibril formation is observed. The presence of asphalt fibrils is expected to absorb fracture energy and increase the toughness at low temperatures. SBR modified binders have low stiffness and thus a decrease in the low temperature fracture toughness is unexpected. However, the term "low-temperature" is relative to the cohesive-adhesive failure transition temperature as seen in the Lap-Shear tests. For the other polymer modified systems studied, this temperature is found to be in the 0°C to -10°C region. SBR, having a lower Tg than the other polymers studied (SBS and SEBS), could cause a depression in this failure mode transition temperature. This is supported by the lap-shear test data which shows that the binder properties decrease linearly in the high temperature region. The fracture toughness is dependent on a variety of material properties, including the yield strength of the binder. The low Tg of SBR latex makes the SBR modified asphalt binder more viscous at the test temperature than other binders and failure occurs at correspondingly lower energy levels than expected. In effect, the SBR modified asphalt may have a tendency to fail cohesively in the binder phase at -10°C instead of interfacial adhesive failure seen in other binders. This is supported by the failure modes seen in lap shear tests where mixed adhesive and cohesive failure was observed in SBR modified AC5 at -10°C.

This suggests that the direct comparison of the effect of polymer modification on the fracture toughness must take into account the failure mode and the    difference

between the test temperature and Tg of the polymer modifier. Various polymer modified asphalts tested at a common test temperature may not provide meaningful direct comparisons regarding the intrinsic properties of the asphalt concrete. Different standards based on the rheological properties of the polymer modifiers would be more suitable for evaluation of properties of polymer modified asphalt concrete.
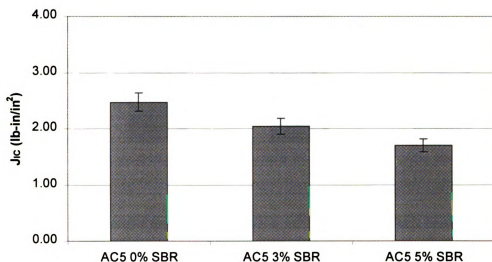


**Figure 5.26     Fracture toughness of SBR modified AC5 asphalt concrete at -10°C**

*AC5 - SBS*

Polymer modified AC5 concrete beams were tested at concentrations of 0%, 3% and 5% SBS. Due to unforeseen high usage of the asphalt binder obtained at the start of the program, a shortage of AC5 binder was experienced. Thus it was necessary to use AC5 binder from a different batch for making SBS modified fracture toughness samples. These results thus should not be assumed to correlate with other data presented. The SBS concentrations were chosen based on the optimum concentrations of SBS in AC5

determined from rheological studies. The fracture toughness of SBS modified AC5 was seen to decrease compared to that of unmodified asphalt concrete. Figure 5.27 shows the change in fracture toughness with SBS modification.
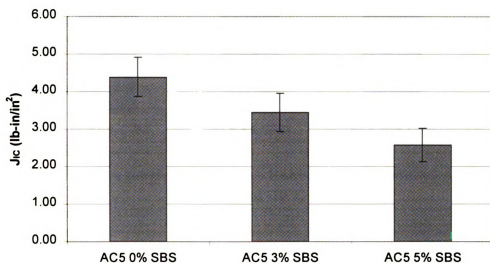


**Figure 5.27    Fracture toughness of SBS modified AC5 asphalt concrete at -10°C**

*AC5 – CRM*

Crumb Rubber modified AC5 concrete was tested at concentrations of 0%, 5% and 10% CRM concentration. The AC5 asphalt binder used for these samples was not from the same batch used for all other testing described in this thesis. The fracture toughness shows an initial decrease in toughness but increases at higher concentrations. The changes, however are not statistically significant as seen in Figure 5.28.  Table 5.5 gives a summary of all fracture toughness test results.
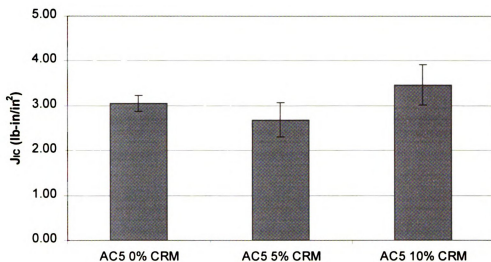
**Figure 5.28    Fracture toughness of Crumb Rubber (CRM) modified AC5 asphalt concrete at -10°C**

**Table 5.5    Summary of fracture toughness test results**

| Composition | $J_{IC}$ Fracture Toughness (lb-in/in$^2$) | Remarks |
|---|---|---|
| AC5 - 0% SEBS | 1.6 ± 0.16 | Original AC5 binder |
| AC5 - 3% SEBS | 3.3 ± 0.19 | |
| AC5 - 5% SEBS | 2.4 ± 0.13 | |
| AC5 - 0% SBR | 2.5 ± 0.16 | Original AC5 binder |
| AC5 - 3% SBR | 2.0 ± 0.14 | |
| AC5 - 5% SBR | 1.7 ± 0.11 | |
| AC5 - 0% Elvaloy | 2.9 ± 0.40 | Original AC5 binder |
| AC5 - 1% Elvaloy | 2.9 ± 0.10 | |
| AC5 - 2% Elvaloy | 2.7 ± 0.19 | |
| AC5 - 0% Crumb Rubber | 3.0 ± 0.18 | New AC5 binder |
| AC5 - 5% Crumb Rubber | 2.7 ± 0.38 | |
| AC5 - 10% Crumb Rubber | 3.5 ± 0.45 | |
| AC5 - 0% SBS | 4.3 ± 0.52 | New AC5 binder |
| AC5 - 3% SBS | 3.4 ± 0.50 | |
| AC5 - 5% SBS | 2.6 ± 0.44 | |

## 5.6    Lap-Shear Adhesion

Lap shear tests give a measurement of the bond strength between two flat parallel plates having an overlap adhesive joint in shear (Mode II) when pulled apart under tensile loads.  The test results show that the lap shear tests can identify the effects of polymer modification, temperature and failure modes on the asphalt binder-aggregate bond strength. Tests were performed on Granite, the prominent type of aggregate found in the aggregate mix [40]. Fracture surface analysis was used to identify the failure modes as a function of polymer content and temperature using optical microscopy. The failure surfaces were classified into six types - Type I to Type VI. The gradual change in appearance of the failure surfaces can be seen in Figure 5.29. Type I, II, II, IV and V are cohesive failures in the asphalt binder and the appearance of asphalt ligaments gets progressively finer from Type I to Type V. The Type VI failure is an interfacial adhesive failure where the fracture progresses along the asphalt binder-aggregate interface. This failure is seen exclusively at low temperatures where the asphalt binder modulus increases above that of the interface. This is the most important region for the study of low temperature adhesive fracture processes since at high temperatures the cohesive failure measures the properties of the asphalt binder and not the interface. The change in failure modes was characterized for each polymer modifier as a function of temperature. It can be seen that as the temperature decreases, the shear strength of the bond increases. The cohesive-adhesive transition temperature for most materials was found to be -10°C.
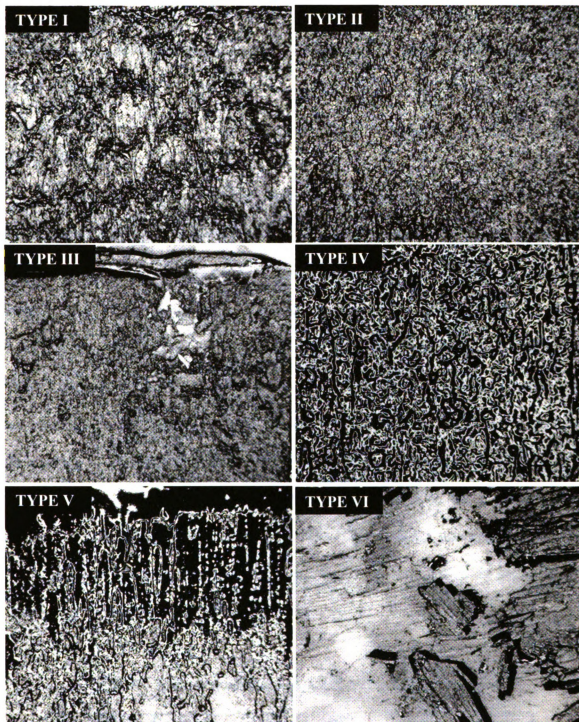
**Figure 5.29     Failure modes in lap shear test specimen. Type I-V show cohesive failure in the binder at high temperatures. Type VI shows binder-aggregate interfacial (adhesive) failure at low temperatures (11X).**

A summary of illustrative lap-shear test results for fresh polymer modified asphalt binders is given in the following sections. Complete tables of lap shear results can be found in Appendix B.

*AC5 - SBS*

In SBS modified binders, there is a minor change in the lap shear bond strength at temperatures above 0°C. It is also seen that at high temperatures the lap shear strength decreases slightly at polymer loadings above 3%. At temperatures below 0°C, the positive effect of polymer modification can be clearly seen. The transition in failure mode from cohesive to adhesive occurs between 0°C and -10°C for SBS modified binders. Table 5.6 shows the change in failure mode as a function of polymer concentration and temperature. It should be noted that the onset of adhesive failure is depressed by 10°C by the addition of SBS modifier. The variation of lap shear strength of SBS modified AC5 with polymer content and temperature is seen in Figure 5.30. In the adhesive failure region (-10°C to -20°C) SBS modified AC5 shows improvement over unmodified AC5. Since the failure is interfacial, this increase can be directly correlated to the improvement in adhesion due to polymer modification.

**Table 5.6  Failure modes in SBS modified AC5 lap shear tests**

| AC5 SBS | 20°C | 10°C | 0°C | -10°C | -20°C |
|---------|------|------|-----|-------|-------|
| 0% | Cohesive | Cohesive | Adhesive | Adhesive | Adhesive |
| 2% | Cohesive | Cohesive | Cohesive | Adhesive | Adhesive |
| 3% | Cohesive | Cohesive | Cohesive | Adhesive | Adhesive |
| 4% | Cohesive | Cohesive | Cohesive | Adhesive | Adhesive |
| 5% | Cohesive | Cohesive | Cohesive | Adhesive | Adhesive |
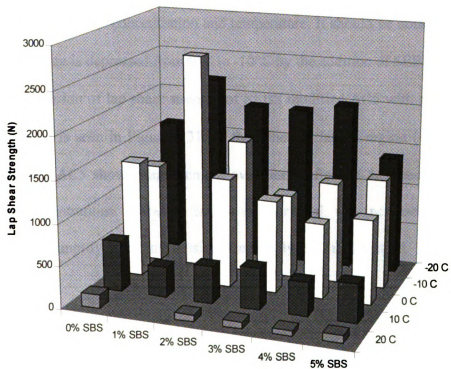
**Figure 5.30  Lap shear strength of SBS modified AC5 as a function of polymer concentration and temperature.**

*AC5 - SEBS*

In SEBS modified binders, there is no significant change in the lap shear bond strength at temperatures above 0°C. At temperatures below 0°C, addition of SEBS leads to an improvement in the lap shear strength. The transition in failure mode from cohesive to adhesive occurs between 0°C and -10°C. Table 5-7 shows the change in failure mode as a function of polymer concentration and temperature. It should be noted that the onset of adhesive failure is depressed from 0°C to -10°C by the addition of SEBS modifier.

The variation of lap shear strength of SEBS modified AC5 with polymer content and temperature is seen in Figure 5.31. In the adhesive failure region (-10°C to -20°C) SEBS modified AC5 shows improvement over unmodified AC5, especially at 1% and 2% SEBS concentrations. Since the failure is interfacial, this increase can be directly correlated to the improvement in adhesion due to polymer modification.

**Table 5.7  Failure modes in SEBS modified AC5 lap shear tests**

| AC5 SEBS | 20°C | 10°C | 0°C | -10°C | -20°C |
|----------|------|------|-----|-------|-------|
| 0% | Cohesive | Cohesive | Adhesive | Adhesive | Adhesive |
| 2% | Cohesive | Cohesive | Cohesive | Adhesive | Adhesive |
| 3% | Cohesive | Cohesive | Cohesive | Adhesive | Adhesive |
| 4% | Cohesive | Cohesive | Cohesive | Adhesive | Adhesive |
| 5% | Cohesive | Cohesive | Cohesive | Adhesive | Adhesive |
| 6% | Cohesive | Cohesive | Cohesive | Adhesive | Adhesive |
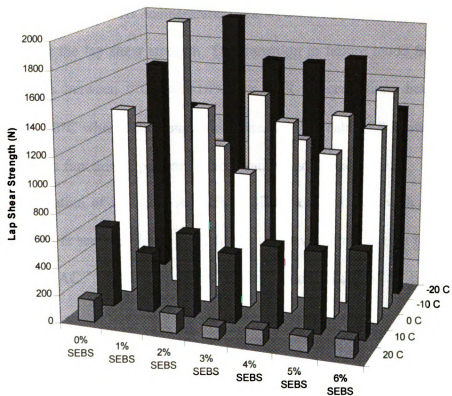
**Figure 5.31  Lap shear strength of SEBS modified AC5 as a function of polymer concentration and temperature.**

The addition of SBR causes no significant change in the lap shear bond strength at low polymer concentrations above 0°C. As the amount of SBR latex in the binder is increased, the cohesive strength of the binder decreases due to the increasing viscous modulus of the binder. At temperatures below 0°C, addition of SBR leads to an improvement in the lap shear strength. The transition in failure mode from cohesive to adhesive occurs between 0°C and -10°C for SBR concentrations below 3% and is depressed to –20°C when SBR content increases to 5%. Table 5.8 shows the change in failure mode as a function of polymer concentration and temperature.

The variation of lap shear strength of SBR modified AC5 with polymer content and temperature is seen in Figure 5.32. In the adhesive failure region (-10°C to -20°C) SBR modified AC5 shows improvement over unmodified AC5, especially at 5% concentration.

**Table 5.8  Failure modes in SBR modified AC5 lap shear tests**

| AC5 SBR | 10°C | 0°C | -10°C | -20°C |
|---|---|---|---|---|
| 0% | Cohesive | Cohesive | Adhesive | Adhesive |
| 1% | Cohesive | Cohesive | Adhesive | Adhesive |
| 3% | Cohesive | Cohesive | Mixed | Adhesive |
| 5% | Cohesive | Cohesive | Cohesive | Adhesive |
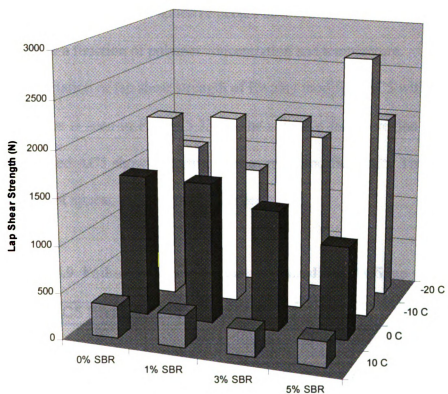
**Figure 5.32    Lap shear strength of SBR modified AC5 as a function of polymer concentration and temperature.**

*AC5 - Elvaloy AM*

Similar to other polymer modifiers studied, the addition of Elvaloy does not affect the lap
shear strength significantly at temperatures above 0°C. At temperatures below 0°C,
addition of Elvaloy leads to an improvement in the lap shear strength. The transition in
failure mode from cohesive to adhesive occurs near -10°C. Table 5.9 shows the change in
failure mode as a function of polymer concentration and temperature.

The variation of lap shear strength of Elvaloy modified AC5 with polymer content
and temperature is seen in Figure 5.33. In the adhesive failure region (-10°C to -20°C)
Elvaloy modified AC5 shows improvement over unmodified AC5. The concentration of
Elvaloy does not appear to affect the properties.

**Table 5.9  Failure modes in Elvaloy AM modified AC5 lap shear tests**

| AC5 Elvaloy | 10°C | 0°C | -10°C | -20°C |
|---|---|---|---|---|
| 0% | Cohesive | Cohesive | Adhesive | Adhesive |
| 1% | Cohesive | Cohesive | Mixed | Adhesive |
| 2% | Cohesive | Cohesive | Adhesive | Adhesive |
| 3% | Cohesive | Cohesive | Mixed | Adhesive |
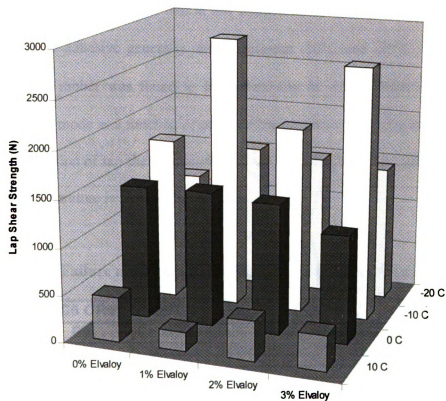
**Figure 5.33  Lap shear strength of Elvaloy modified AC5 as a function of polymer concentration and temperature.**

*AC5 - Crumb Rubber*

The addition of Crumb Rubber at a low concentration of 5% causes a decrease in the lap shear strength. At higher concentrations, the lap shear properties recover and increase above those of unmodified asphalt. Of the various concentrations used, 15% Crumb Rubber was found to perform the best at low temperatures. The transition in failure mode from cohesive to adhesive generally occurs between -10°C and -20°C. However, AC5 with 5% crumb rubber was found to fail cohesively at -10°C. Table 5.10 shows the change in failure mode as a function of polymer concentration and temperature.

The variation of lap shear strength of Crumb Rubber modified AC5 with polymer content and temperature is seen in Figure 5.34.

**Table 5.10  Failure modes in Crumb Rubber modified AC5 lap shear tests**

| AC5 CRM | 20°C | 0°C | -10°C | -20°C |
|---------|------|-----|-------|-------|
| 0% | Cohesive | Cohesive | Cohesive | Adhesive |
| 5% | Cohesive | Cohesive | Adhesive | Adhesive |
| 10% | Cohesive | Cohesive | Cohesive | Adhesive |
| 15% | Cohesive | Cohesive | Cohesive | Adhesive |
| 20% | Cohesive | Cohesive | Cohesive | Adhesive |
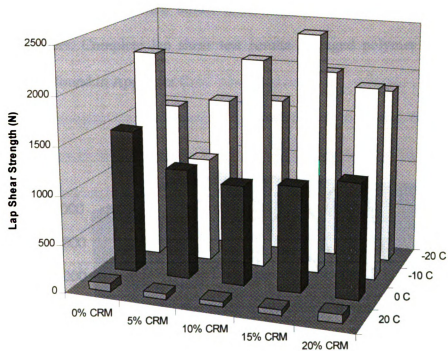
**Figure 5.34** Lap shear strength of Crumb Rubber modified AC5 as a function of polymer concentration and temperature.

*Lap shear testing of aged asphalt*

Lap shear tests on aged asphalt binders indicate that polymer modification retards the aging processes and improve the residual properties of the asphalt binder. Figure 5.35 shows the lap shear strength of aged SBR binders. At high temperatures, the lap shear strength of aged SBR modified binder follows the same trends as fresh asphalt SBR modified binders. Complete lap shear test results for aged polymer modified asphalt binders can be found in Appendix C.
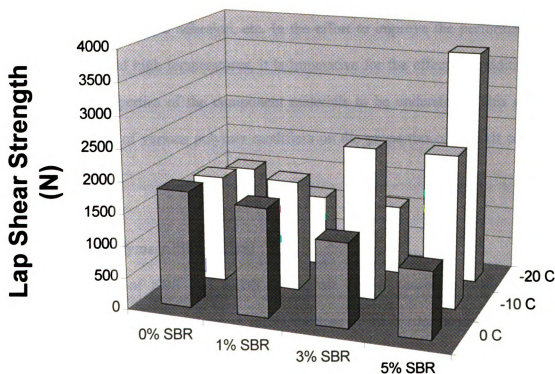


Figure 5.35    Lap shear strength of aged SBR modified AC5 binders at various temperatures

# CHAPTER SIX

# DISCUSSIONS

The results obtained from the morphological and microstructural characterization of asphalt concrete present new understanding of the mechanisms of failure in pavements. Proper analysis and implementation of these results can be beneficial in developing new performance based specifications for polymer modified asphalt concretes. Specifically, the benefits of polymer modification need to be viewed in terms of improvements in key properties, e.g. resistance to aging, low temperature fracture toughness, asphalt-aggregate adhesion, etc. In the effort to improve the performance of pavements at low and high temperatures, it is imperative for the effects of additives on the fundamental properties of the component materials to be understood. This chapter discusses the effects of various polymer modifiers on the properties of asphalt concrete and asphalt binder.

## 6.1    Dispersed Polymers (SBS/SEBS)

The addition of SBS and SEBS to asphalt binder causes a change in the morphology of the binder. The network microstructure of the binder does not appear to change visibly, yet room temperature fracture morphology shows a significant increase in fracture energy dissipating mechanisms like crack bridging by asphalt fibrils. This is an effect of the decrease in the glass transition of the asphalt binder due to the addition of SBS/SEBS. There is also an increase in the number of fibrils formed during fracture and this may be due to an overall increase in asphalt-aggregate adhesion with the locations of

fibril formation representing areas with increased adhesion and acting as anchor points for the fibrils during the process of crack widening and deformation. Using the mixing procedures outlined earlier, SBS and SEBS form discrete, well-dispersed spherical phases about 1-20 μm in diameter. Even at polymer concentrations of 5 wt.%, no continuous polymer networks are observed in the binder. Continuous networks of SBS and SEBS (phase inversion) in asphalt are expected only at concentrations approaching 10 wt% [59,60].

Asphalt-aggregate adhesion increases with the addition of SBS/SEBS as seen in lap shear test results. In the adhesive failure region (-10°C and below) the modified asphalt binder has higher ultimate lap shear strength. The quantitative lap shear test data must be taken in conjunction with the qualitative analysis of various failure modes observed. The failure mode is seen to change from cohesive to adhesive around 0°C for unmodified AC5 and -10°C for SBS/SEBS modified AC5. Direct comparison of lap shear strength of unmodified and modified AC5 at 0°C is misleading since the measured quantity indicates the adhesive strength of unmodified AC5 and cohesive strength of SBS/SEBS modified AC5. The depression of this failure transition by 10°C is a significant step towards improving low temperature pavement performance where the predominant failure is adhesive.

At low temperatures (-10°C) the fracture toughness of the SEBS modified asphalt concrete increases, whereas the fracture toughness of SBS modified asphalt concrete decreases. The binders used to make the SBS fracture toughness samples was from a different batch and thus the precise reason for the decrease in fracture toughness cannot be determined at this time.

## 6.2 Network Polymers (SBR Latex)

SBR latex is a network forming polymer and after addition to asphalt, it forms an independent network of SBR strands of ~10μm diameter. The asphalt fibrils formed during fracture of asphalt concrete are longer than those seen in SBS and SEBS. The SBR modified binder is softer than the SBS and SEBS modified binders, which is evident by the lower softening and melting points. There are two reasons for this : (1) The binder is mixed at 350°F for 30 minutes which reduces the amount of oxidative aging during the blending process and (2) The Tg of the SBR latex is lower than that of SBS and SEBS.

The lap shear strength data for SBR modified asphalt shows an improvement in strength as well as depressing the cohesive-adhesive failure transition from 0°C to -10°C. Moreover, the amount of fibril formation during fracture is very high compared to the other polymers studied and fibrils across the growing crack were observed to remain intact even at crack widths on the order of inches. The factors responsible for this behaviour are the formation of the SBR network inside the asphalt as well as the improvement in interfacial adhesion. To further validate the theory of improvement in interfacial adhesion, experiments were performed where the SBR was localised at the interface by independently coating the aggregates with SBR latex. Latex coatings of 5μm and 10μm thickness were applied on the aggregates and the lap-shear strength and toughness were measured. Figure 6.1 shows the typical load-displacement response of SBR coated aggregate-binder systems at -10°C and -20°C. It can be seen that the strain to failure increases by 400 to 500% when SBR is concentrated at the asphalt-aggregate interface with no significant change in the ultimate lap-shear strength. The effect of the interfacial coating decreases as the coating thickness increases. The binder also has an

133

effect on the lap shear properties. Unmodified AC5 and AC5-5 wt.% SBR were used along with SBR coated aggregate to make lap-shear specimen. It was observed that at high temperatures there is no significant change in properties due to addition of SBR but at lower temperatures (-10°C and -20°C) the addition of SBR to the binder further enhances the ultimate lap shear strength as well as the strain to failure.

The enhancement in properties due to the presence of SBR at the interface indicates the importance of the interface in the final properties of asphalt concrete. It is believed that polymer modification of the binder also leads to the modification of the binder-aggregate interface in asphalt concrete. The cumulative effect of interfacial and matrix modification ultimately leads to enhanced low temperature properties and the interfacial/adhesive failure transition in asphalt concrete occurs at a lower temperature, effectively extending the low temperature performance envelope. Williams et al. [64] have recently shown that SBR coating on aggregates improved the resistance to moisture damage (improved interfacial adhesion).

Although excellent low temperature properties are observed after applying SBR coatings directly to the aggregates, it is estimated that the amount of polymer utilized in this study is too high to be of commercial importance. The average asphalt binder film thickness in Marshall samples is approximately 11μm based on design calculations shown earlier. By applying 5 and 10μm SBR coatings on the aggregate surface, the net polymer to asphalt binder ratio ranges from approximately 50 to 100% making such modification schemes unrealistic in terms of commercial application. However, the effect of the interface and interfacial adhesion on the low temperature performance of asphalt concrete can be understood by such experiments. SBR latex coatings for aggregate as

anti-stripping additives have recently been made available commercially (Ultracote UP-5000, Goodyear/Ultrapave) [65] with SBR particle sizes on the order of 0.5μm. Provided sufficiently thin coatings can be applied to the aggregates, this approach may prove to be beneficial especially for low temperature applications.

Direct coating of aggregates with polymer was only possible with SBR latex as the other polymers studied, SBS, SEBS, Elvaloy and Crumb Rubber were not available in a physically convenient form for coating purposes.
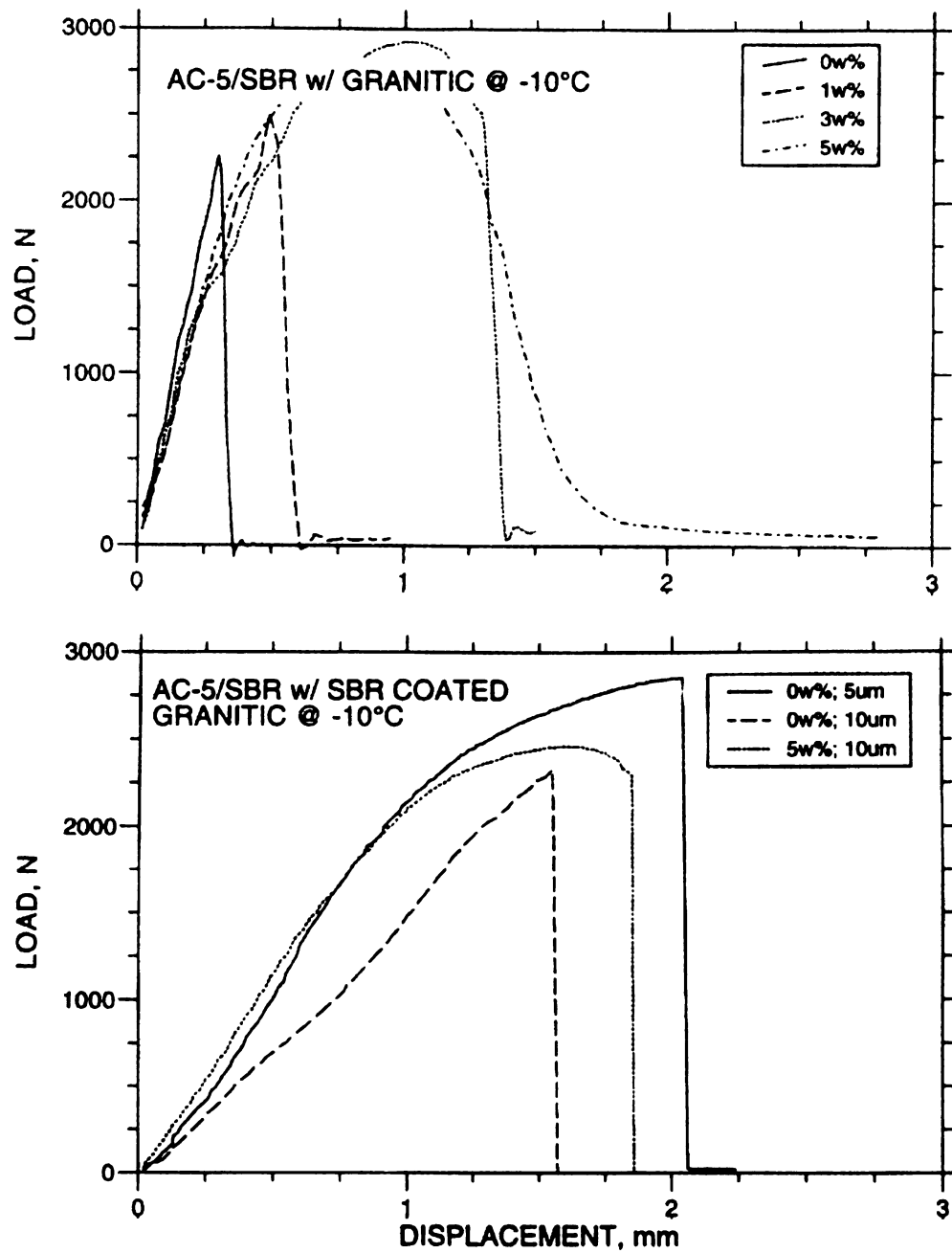
**Figure 6.1** Lap shear load-displacement curves for AC5-SBR and Granitic aggregate at -10°C. SBR coated aggregate systems have a higher displacement at failure due to toughening of the asphalt-binder interface.

136

## 6.3    Reactive Polymers (Elvaloy AM)

Reactive polymers react chemically with the asphalt binder and effectively cross-link the asphalt. This leads to a binder with very high modulus. Although there is no significant change in the binder morphology after addition of Elvaloy AM, the binder microstructure appears similar to aged asphalt with coarse network features and the binder has very high stiffness. This was found to be due to the high mixing temperatures (380°F) used to blend Elvaloy and asphalt in ambient environment. The mixing of Elvaloy in the presence of air causes oxidation to occur in the binder. The lap-shear properties are comparable to other polymer modifiers studied but there is no change in the failure transition from cohesive to adhesive, which occurs at 0°C for unmodified asphalt. After Elvaloy addition the failure mode at -10°C is mixed adhesive and cohesive with an increase in the ultimate lap-shear strength indicating an increase in the binder properties while the pure adhesive failure at this temperature occurs at a lower load indicating that the interfacial adhesion remains unaffected by addition of Elvaloy. This is also seen in the fracture toughness tests where no change is observed after addition of Elvaloy.

To avoid the problem of binder oxidation during initial processing (mixing) the mixing should be done in a closed container with a nitrogen purge. This procedure was found to be effective and the resulting Elvaloy modified binder did not appear to have the coarse network structure typical of aged asphalt. Future tests with Elvaloy modified asphalts should be performed with binders mixed under Nitrogen atmosphere.

## 6.4    Particulate Polymers (Crumb Rubber)

Crumb rubber particles added to asphalt also cause a slight coarsening of the binder network microstructure. This is expected to be due to the rubber particles absorbing the low molecular weight oils in the asphalt. This is similar to the loss of low molecular weight fractions due to oxidation, but since this loss of oils is not permanent, the long term properties of the addition of crumb rubber remain to be evaluated. One theory is that the oils absorbed by the rubber particles are stored and can diffuse back into the asphalt binder as the binder ages naturally and maintain a steady concentration of oils in the asphalt.

The interaction of the rubber particles and asphalt binder is shown in Figure 6.2. The asphalt network fibrils are seen in the ESEM micrograph to have a very good interaction with the rubber particles. The fracture surface of crumb rubber modified asphalt concrete shows no signs of adhesive failure along the asphalt-rubber interface.

The lap shear properties of crumb rubber modified asphalt show an increase in the ultimate strength with the addition of rubber and the change in transition from cohesive to adhesive failure is seen to occur between -10°C and -20°C.  The AC5 asphalt binder used for Crumb Rubber fracture toughness tests was from a different batch than the binder used for other tests and this should be taken into account when comparing results. There is no significant change in the fracture toughness at -10°C due to addition of crumb rubber.
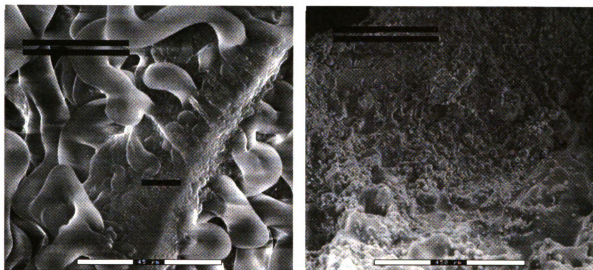
**Figure 6.2** **ESEM micrographs of (a) Interaction of asphalt binder network with crumb rubber particles (left, white bar = 45 μm) and (b) Fracture surface of crumb rubber modified AC10 showing significant amount of asphalt binder residue on the rubber particle surface (right, white bar = 450 μm).**

## 6.5    Lap Shear Tests as Indicators of Interfacial Adhesion

The use of lap shear tests to indicate changes in the interfacial adhesion between asphalt binder and aggregates, although useful in evaluating the interaction between the binder and aggregate as materials, cannot be used as a direct indicator of the true interfacial adhesion in real asphalt concrete. The reason for this is that the aggregate samples used in lap shear tests are necessarily cut and polished aggregate surfaces while aggregates used in actual pavement construction are angular and have a high degree of roughness. Although the roughness of the aggregates does not affect the energetic interactions between the materials, interfacial adhesion generally improves with increasing roughness due to the contribution from mechanical interlocking. This is termed as mechanical adhesion. The absence of significant mechanical adhesion in the lap shear tests thus makes quantitative application of the lap shear test results to

pavement design impractical. Instead, the lap shear tests provide a useful method to evaluate the changes in the interface caused by the addition of polymers. Assuming that final mix processing is carried out at equivalent binder viscosity such that the physical interaction between the asphalt binder and aggregates is similar, the lap shear properties of various polymer modified asphalts determined in the laboratory can be scaled to the real properties expected to be seen in the field. With all other factors being equal, the lap shear test provides a reliable method to compare different modifiers and asphalt binders.

## 6.6    Summary

The use of polymer modification of asphalt to improve pavement properties has been shown to be effective by enhancing the bulk and the interfacial properties of asphalt concrete. Of the four types of polymer modifiers, dispersed thermoplastics and network forming polymers like SBS, SEBS and SBR show the highest potential for improving properties at low temperatures by strengthening the binder-aggregate interface while reacting polymers and particulate reinforcements like Elvaloy and Crumb Rubber respectively work by enhancing the properties of the bulk binder. Since the binder properties become less important at low temperatures where distress is primarily located at the interface, reacting polymers and rubber particle reinforcement has a lower potential of enhancing the low temperature properties.

At high temperatures (above 0°C) polymer modification does not significantly affect the properties of asphalt concrete as detected by lap shear tests. With the exception of SBR, lap shear properties at high temperatures remain constant as polymer is added to the binder. However, lap shear tests are not useful in detecting the potential for high

temperature distresses such as rutting and further experimentation and field tests are necessary to evaluate the high temperature performance of polymer modified asphalt concrete.

The characterization of asphalt binders by ESEM microscopy has provided a new understanding of the nature and structure of asphalts. The changes seen in the network structure of asphalt can be used as a qualitative tool to determine aging in asphalt binders as well as serve as a tool to develop other polymer modifiers which will exploit the microstructure and morphology of the binders. For example, combinations of polymer modifiers like SBR and Elvaloy might lead to interesting changes in the binder microstructure with the reacting polymers enhancing binder properties by crosslinking and reducing the number of sites available for oxidative attack in the binder and the network forming polymers providing high interfacial interaction between the asphalt binder network and the aggregates.

The fracture morphology of asphalt concrete can also be used to design pavement repair schemes. The formation of asphalt fibrils across growing cracks can be a useful property to exploit in pavement healing. The heating of cracks in the pavement caused at low temperatures can close the cracks due to the re-distribution of the binder and a higher amount of fibril formation in the binder can assist this process, even after the cracking has occurred.

In summary, polymer modification has been shown to positively affect the low temperature properties of asphalt concrete. Additional research has been performed to test the bulk properties of asphalt concrete which shows that polymer modification also enhances the high temperature tensile and fatigue strength of asphalt concrete [33, 66].

# CHAPTER SEVEN

# CONCLUSIONS AND RECOMMENDATIONS

The main objective of this study was to characterize the microstructure and morphology of straight and polymer modified asphalt (PMA) binder-aggregate mixtures and their failure mechanisms. Microstructural and morphological information is important in predicting pavement performance based on the physical and chemical properties of binders and aggregates. The identification of morphological changes in asphalt and their effect on the locus of failure and failure mode under a combination of stress and environmental factors is a critical element necessary to evaluate pavement performance

## 7.1    Microstructure and Morphology

Asphalt binder morphology was characterized successfully using an ESEM and a well defined 3-dimensional entangled network was observed in asphalt binder films and asphalt concrete sections.   The network structure is seen in unmodified as well as polymer modified asphalt binders and changes with the asphaltene content.  Comparison of the morphology of three different asphalts shows that the density of the network is proportional to the asphaltene content.  It is suggested that the segments in the network are mainly composed of associations of asphaltene particles and resins, the interstices filled with plasticizing oils.  The oxidative aging of asphalt leads to changes in the network morphology. The smooth network segments in fresh asphalt have a mottled and coarse texture after aging.  This can be used as a qualitative test to determine the extent of

aging in asphalt. Whereas classification of asphalt binders strictly by rheological analysis may show no difference between a high viscosity asphalt and blown (oxidised) asphalt, the changes in morphology are easily detectable and should be taken into account to predict long term performance.

The morphology the polymer phase in modified asphalt is important to develop new specifications and understanding of the precise mechanisms by which improvements in pavement performance are realised. Polymer morphology can be characterized easily with a Confocal Laser Scanning Microscope (LSM) for polymers like SBS, SEBS and SBR which exhibit strong fluorescence. The current industrial standard to confirm homogeneous mixing of polymers and asphalt is visual observation. The ability of the LSM to map depth profiles of the polymer distribution in asphalt is an analytical tool that can be used to determine the homogeneity of PMA. A limitation of this technique is the inability to determine the morphology of polymers that do not exhibit fluorescence. Crumb rubber and Elvaloy AM could not be detected by the LSM and the distribution of these two modifiers could not be characterized. In the case of non-homogeneous polymer modified asphalts such as crumb rubber, it is possible to look at individual particles and their interaction with asphalt binder using microscopic techniques.

SBS and SEBS were found to form a dispersed phase in asphalt at concentrations up to 5%(w/w) while SBR forms a strand-like continuous network at concentrations of 3%(w/w) and higher. Crumb rubber particles were well dispersed in the asphalt and have good interaction with the asphalt network.

## 7.2 Void Morphology and Fracture in Asphalt Concrete

The presence of voids in asphalt concrete is essential to allow expansion of the asphalt binder at high temperatures without bleeding and for water drainage. The size, location and abundance of air voids play a critical role in fracture processes. The voids in asphalt can be characterized into two main categories from the morphological perspective: binder phase voids and interfacial voids. Binder phase voids are typically small spherical voids while interfacial voids tend to be large and irregular voids encircling the aggregate. The analysis of air-voids in polymer modified asphalt concrete suggests adaptation of asphalt concrete mixing procedures based on the rheological properties of the binder. Due to the increase in viscosity of asphalt binders after polymer modification, the wetting and penetration of the aggregate with binder may be different than that in unmodified asphalt. A direct comparison between polymer modified and unmodified asphalt concrete mixed using identical conditions (temperature and time) may not provide an accurate representation of the effect of polymer modification on the void morphology in different systems.

The fracture process in asphalt concrete was studied using an ESEM and the fracture mechanism was determined to progress in three main stages: void formation, void growth and void interconnection. As the asphalt concrete sections were strained, at temperatures above 0°C, voids begin to form in the binder phase. These voids grow in size with increasing strain and finally interconnect as the crack propagates. The propagation of the crack is slow and inhibited by the formation of asphalt ligaments or fibrils across the crack face. The fibrils elongate and rupture, thus dissipating some of the fracture energy. The addition of polymer to asphalt, with the exception of Elvaloy

AM, leads to an increase in the density of fibrils formed during fracture. This is expected to enhance the resistance to crack growth exhibited by asphalt concrete.

The fracture process at low temperatures (below 0°C) is different than that at high temperatures and fracture occurs mainly along the binder-aggregate interface due to adhesive failure. The presence of interfacial air-voids can accelerate the fracture process and crack growth can be qualitatively characterized as rapid. Low temperature fracture is one of the prevalent pavement failures in cold climes like Michigan and thus the presence of interfacial voids is considered to be detrimental to low temperature pavement performance.

## 7.3 Fracture Toughness and Lap Shear Tests

Fracture toughness and lap shear tests were used to determine the changes in asphalt binder-aggregate adhesion due to polymer modification. Lap shear tests indicate that the failure mode in asphalt concrete is determined by a transition temperature above which failure is mainly cohesive in the binder phase. At temperatures below the transition adhesive, interfacial failure is observed. Lap shear tests were performed at various temperatures in 10°C increments from 20°C to -20°C. The addition of polymers has shown that the cohesive to adhesive failure transition temperature decreases from approximately 0°C for unmodified asphalt to atleast -10°C for polymer modified asphalt along with an improvement in the ultimate lap-shear strength. This is an important indication of the improvement in binder-aggregate adhesion due to polymer modification. Table 7.1 shows the adhesive and cohesive failure transition temperatures for different polymer modified AC5 asphalt binders. Lap shear tests also show a higher retention of

145

properties in aged polymer modified asphalt. Along with supporting evidence from the binder morphology, it can be claimed that polymer modification retards the aging of asphalt binders.

**Table 7.1  Lap shear cohesive-adhesive failure transition temperatures for polymer modified AC5 asphalt concrete**

| Composition | Cohesive Failure | Adhesive Failure |
|---|---|---|
| Unmodified AC5 | 10°C | 0°C |
| AC5-3% SBS | 0°C | -10°C |
| AC5-2% SEBS | 0°C | -10°C |
| AC5-5% SBR | -10°C | -20°C |
| AC5-1% Elvaloy® AM | 0°C | -10°C |
| AC5-5% Crumb Rubber | 0°C | -10°C |

Fracture toughness tests were performed for various polymer modified asphalt compositions at -10°C, as a measure of the resistance of the material to adhesive fracture. Polymer modification improves the J-integral fracture toughness for SEBS, but a decrease in fracture toughness was observed in the case of SBS and SBR latex modified systems. This may be due to the choice of testing temperatures as the SBR modified binder-aggregate fails adhesively at a lower temperature (-20°C) in lap shear tests. This can be attributed to the fact that SBR is a random copolymer with a Tg of -50°C, which is much is lower than that of SBS and SEBS which have discrete polystyrene domains with a Tg of 100°C. In order to compare the effect of polymer modification on the adhesion in different systems, it may be more appropriate to conduct fracture toughness tests at

146

temperatures relative to the Tg of the modified asphalt binders instead of a single temperature for all systems.

Another factor that must be taken into account is that the cohesive and adhesive failures reported in Table 7.1 were observed in lap shear test samples which are made from smooth aggregate sections cut with a diamond blade. This renders an aggregate surface that is smooth while aggregate used in pavement construction has a high degree of surface roughness and porosity. Thus the effects of mechanical adhesion due to the absorption of asphalt into the aggregate are minimised in lap shear tests leading to a slight underestimation of the temperature at which adhesive failure occurs in the binder-aggregate interface.

## 7.4    Optimum Polymer Concentration

The recommendation of an optimum concentration of a polymer for modification of asphalt binders is a process that must take into account the chemical, rheological, interfacial and the engineering properties of the asphalt concrete [67]. Research under the direction of Prof. Hawley and Baladi has evaluated the rheological properties [31,32] and the engineering properties of the systems [33] studied here.[4] The recommended optimum concentrations of different polymers for modification of AC5 asphalt from the perspective of : (i) chemical, physical and thermodynamic properties, (ii) microstructural and morphological properties and (iii) structural and engineering properties are shown in Table 7.2 and should only be used as guidelines since a change in the source and

---

[4] Hawley M., Department of Chemical Engineeering, Michigan State University, USA and
   Baladi G., Department of Civil and Environmental Engineering, Michigan State University, USA

composition of asphalt binder, quality and composition of the aggregate and mixing conditions can yield different results.

The SHRP performance grades for the different types of polymer modified asphalt binders are shown in Table 7.3 for reference. It can be seen that as polymer is added to the asphalt binder, the high temperature SHRP performance grade (PG) increases while the low temperature SHRP PG remains almost constant at low concentrations. This suggests enhanced binder rheological properties at high temperatures. Since the SHRP PG only represents binder properties and not those of asphalt concrete, it can be concluded that polymer modified asphalt binders show an *improvement in the high temperature performance without deteriorating the low temperature performance of the binder*. The results from lap-shear and fracture toughness tests on the other hand represent the low temperature properties of the *asphalt concrete* and show clearly that the *low temperature performance of asphalt concrete is enhanced* in most cases.

Since most high temperature failures are dependent on binder properties and low temperature failures on the interfacial properties, polymer modification presents itself as a very attractive modification process.

**Table 7.2 Optimum polymer concentrations suggested for AC5 (PG 58-28) asphalt binder [31-33, 67]**

| | Suggested optimum concentration (wt.%) | | |
|---|---|---|---|
| | Chemical, Physical and Thermodynamic Properties | Microstructural and Morphological Properties | Structural and Engineering Properties |
| SBS | 3 or 5 % | 1-3 % | 5 % |
| SEBS | 2 or 5 % | 1-3 % | 5 % |
| SBR | 3 % | 5 % | 2 % |
| Elvaloy® AM | 1.5 % | 1 % | 1 % |
| Crumb Rubber | 10 % | 10-15 % | 10 % |

**Table 7.3 SHRP performance grades for polymer modified AC5 (PG 58-28) asphalt binder [31-32,67]**

| SBS | | SBR | | Elvaloy®AM | | Crumb Rubber | |
|---|---|---|---|---|---|---|---|
| 0 % | PG 58-22 | 0 % | PG 58-28 | 0 % | PG 76-16 | 0 % | PG 58-18 |
| 1 % | PG 64-22 | 1 % | PG 58-28 | 1 % | PG 76-16 | 5 % | PG 64-N/A |
| 2 % | PG 70-22 | 2 % | PG 64-28 | 2 % | PG 82-16 | 10 % | PG 70-N/A |
| 3 % | PG 70-22 | 3 % | PG 64-28 | 3 % | PG 82-16 | 15 % | PG 82-18 |
| 4 % | PG 70-22 | 4 % | PG 64-28 | 4 % | PG 82-16 | 20 % | PG 82-N/A |
| 5 % | PG 76-16 | 5 % | PG 70-28 | | | | |

*Note: SHRP PG grades (PG XX-XX) represent the high and low temperature ratings. The first number is the high temperature and the second number is the low temperature. PG 58-22 represents 'Performance grade 58 °C high temperature SHRP grade and -22 °C low temperature SHRP grade.'*

## 7.5    Recommendations for Future Work

Based on the results from this study and the information available, there is a need for further research into polymer modification of asphalt. Various areas worthy of further exploration are described below.

*Effect of asphalt source.* Asphalt is obtained from the last remaining fractions of crude oil and with changes in the raw material, the quality of asphalt also changes. In order to generalize the results obtained here, polymer modifiers need to be tested with asphalts from different sources. The use of multiple asphalt sources can facilitate the generalization and application of the results already obtained. Asphalts with different known asphaltene contents should be studied in order to find the relationship between the binder microstructure and the rheological and engineering properties of asphalt binder and concrete.

*Effect of aggregate.* Aggregate used in pavement construction is usually obtained from local quarries and the quality of the aggregate varies widely. While it is assumed that different types of aggregate will exhibit similar behaviour with polymer modified asphalt binders, the evaluation of aggregate from different parts of the country may yield different results. In this study the aggregate used comprised mainly of granite, greenstone, basalt, quartzite, sandstone and limestone. Out of these, granite was chosen as a representative model surface. However, interfacial properties are highly dependent on the nature of the aggregate surface and the varying degrees of crystallinity and grain structure found in different types of aggregates may have an impact on these properties.

*Polymer-asphalt interaction.* Although asphalt binder and polymer phase morphology has been characterized individually, there is a need to develop new experimental techniques that can determine the interaction between the two materials on the microstructural scale. The presence of a network structure in asphalt opens up new avenues for investigation: Do thermoplastic polymer modifiers like SBS, SEBS and SBR associate with the asphaltene network? Do polymer modifiers blend into the asphalt network segments or segregate to the surface, effectively forming a polymer rich sheath around the asphaltenes? These are issues that are of deep importance in understanding the process of polymer modification of asphalt. It has been shown that binder-aggregate failure is characterized by the formation of fibrillar structures that bridge the growing cracks and polymer modification is capable of making changes in these structures. The ability to control the size and strength of these fibrils through polymer modification opens new doors for establishing direct relationships between asphalt binder morphology and pavement performance. Efforts must also be made to pinpoint the failure mode transition temperatures in terms of different polymer modifier types and concentrations.

*Combination of Polymer Modifiers.* The results obtained in this study consistently show that none of the polymers studied perform very effectively at both high and low temperatures. Whereas from the point of view of interfacial failures, low temperature performance is more relevant than high temperature performance, in reality, high temperature distresses are as common as low temperature distresses. The solution to this may lie in using a combination of polymer modifiers which individually enhance performance at extremes of temperatures. One such suggested example is the use of SBR

latex as a coating for aggregate to enhance low temperature properties with an Elvaloy modified asphalt binder.

*Road tests.* It is vital for the results obtained in the laboratory to be validated in the field. This can be accomplished by undertaking road tests using the same materials used in this work to evaluate the performance of various systems. Properties such as rutting, fatigue and thermal cracking behaviour of the pavement subjected to traffic and environmental forces can make these results more valuable as there is no equivalent laboratory technique to a real pavement test section.

This work has sought to identify the various materials and factors that play a key role in pavement performance. With better understanding of the materials and mechanisms involved on a fundamental level, pavement design can be refined and tailored to overcome the various challenges encountered during service.

# APPENDIX A

# FRACTURE TOUGHNESS LOAD-DISPLACEMENT PLOTS

**Figure A.1 Load-deflection curves for AC5 0% SBS beam samples
for various notch lengths at -10°C**
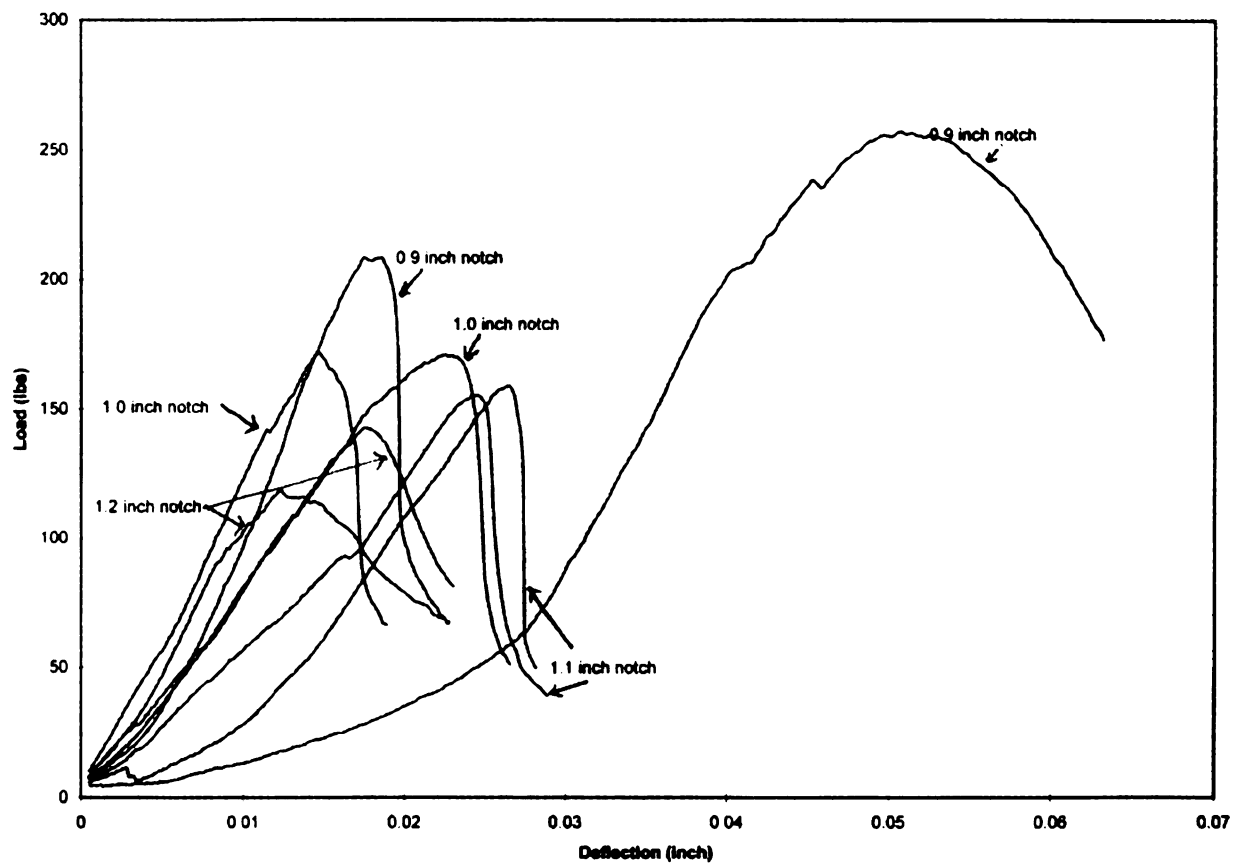
**Figure A.2 Load-deflection curves for AC5 3% SBS beam samples for various notch lengths at -10°C**

155

**Figure A.3  Load-deflection curves for AC5 5% SBS beam samples
for various notch lengths at -10°C**

**Figure A.4 Load-deflection curves for AC5 0% SEBS beam samples for various notch lengths at -10°C**

**Figure A.5  Load-deflection curves for AC5 3% SEBS beam samples
for various notch lengths at -10°C**

**Figure A.6 Load-deflection curves for AC5 5% SEBS beam samples for various notch lengths at -10°C**

**Figure A.7 Load-deflection curves for AC5 0% SBR beam samples for various notch lengths at -10°C**

**Figure A.8  Load-deflection curves for AC5 3% SBR beam samples for various notch lengths at -10°C**
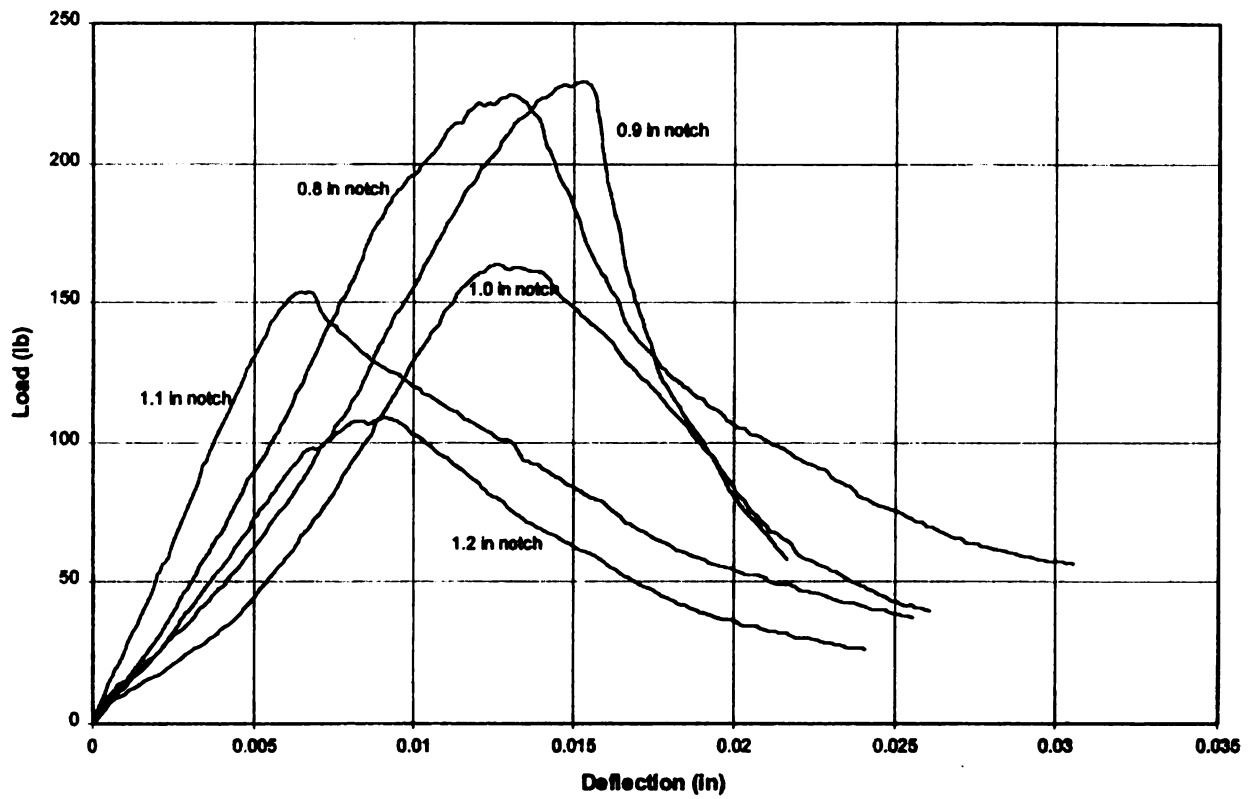
**Figure A.9  Load-deflection curves for AC5 5% SBR beam samples
for various notch lengths at -10°C**
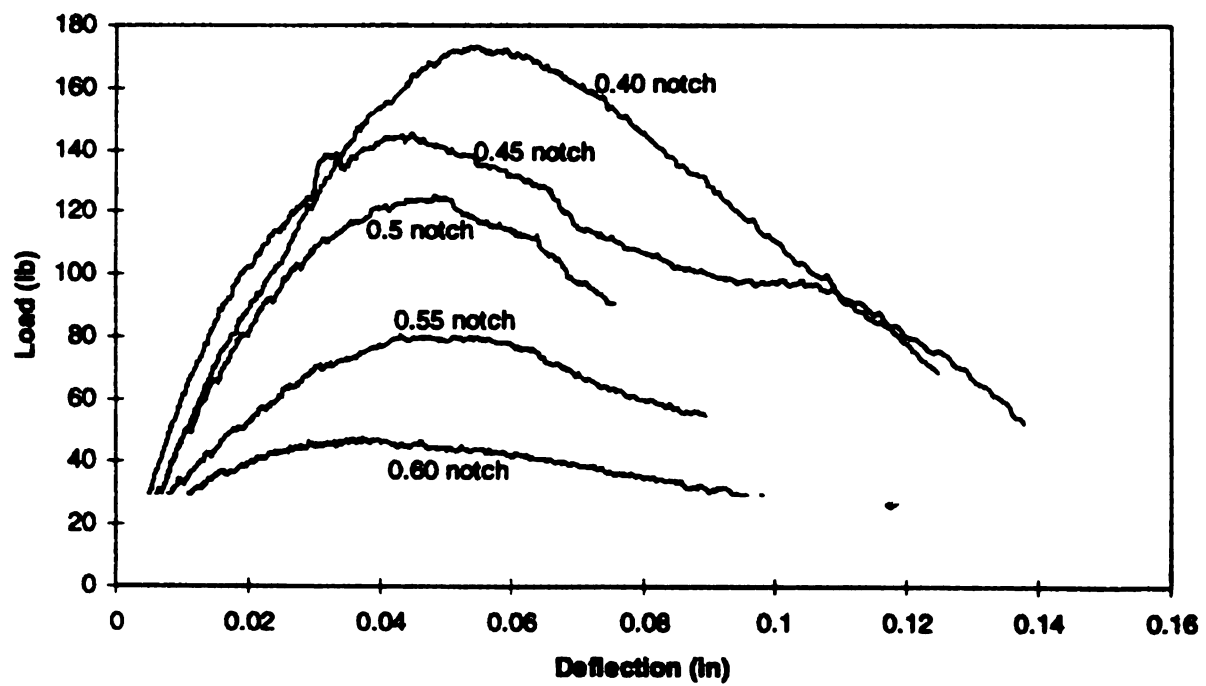
Figure A.10  Load-deflection curves for AC5 0% Elvaloy AM
beam samples for various notch lengths at -10°C
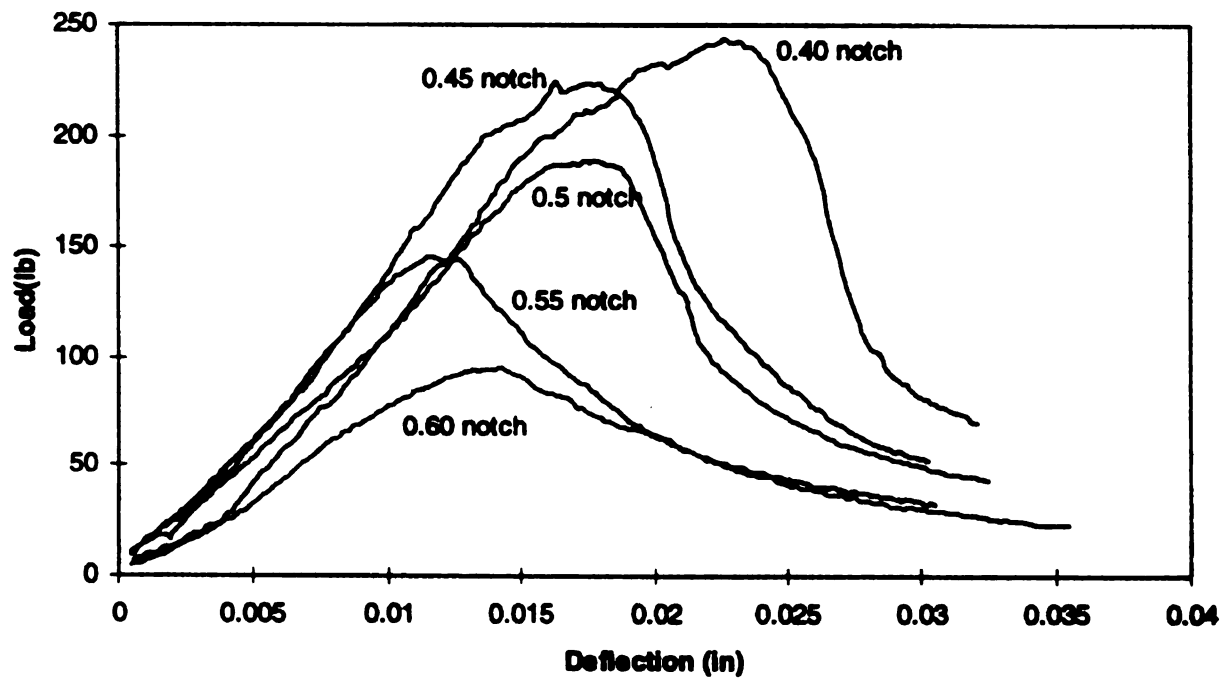
**Figure A.11 Load-deflection curves for AC5 1% Elvaloy AM beam samples for various notch lengths at -10°C**
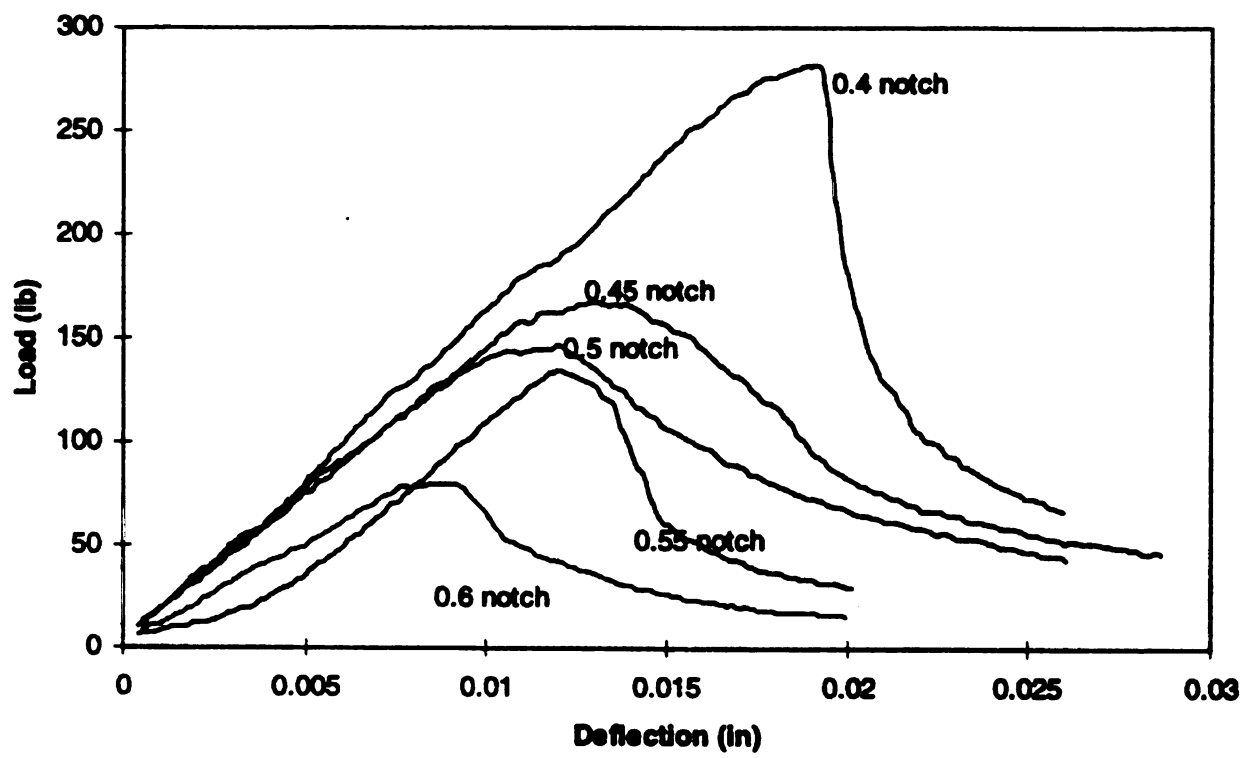
**Figure A.12  Load-deflection curves for AC5 2% Elvaloy AM beam samples for various notch lengths at -10°C**
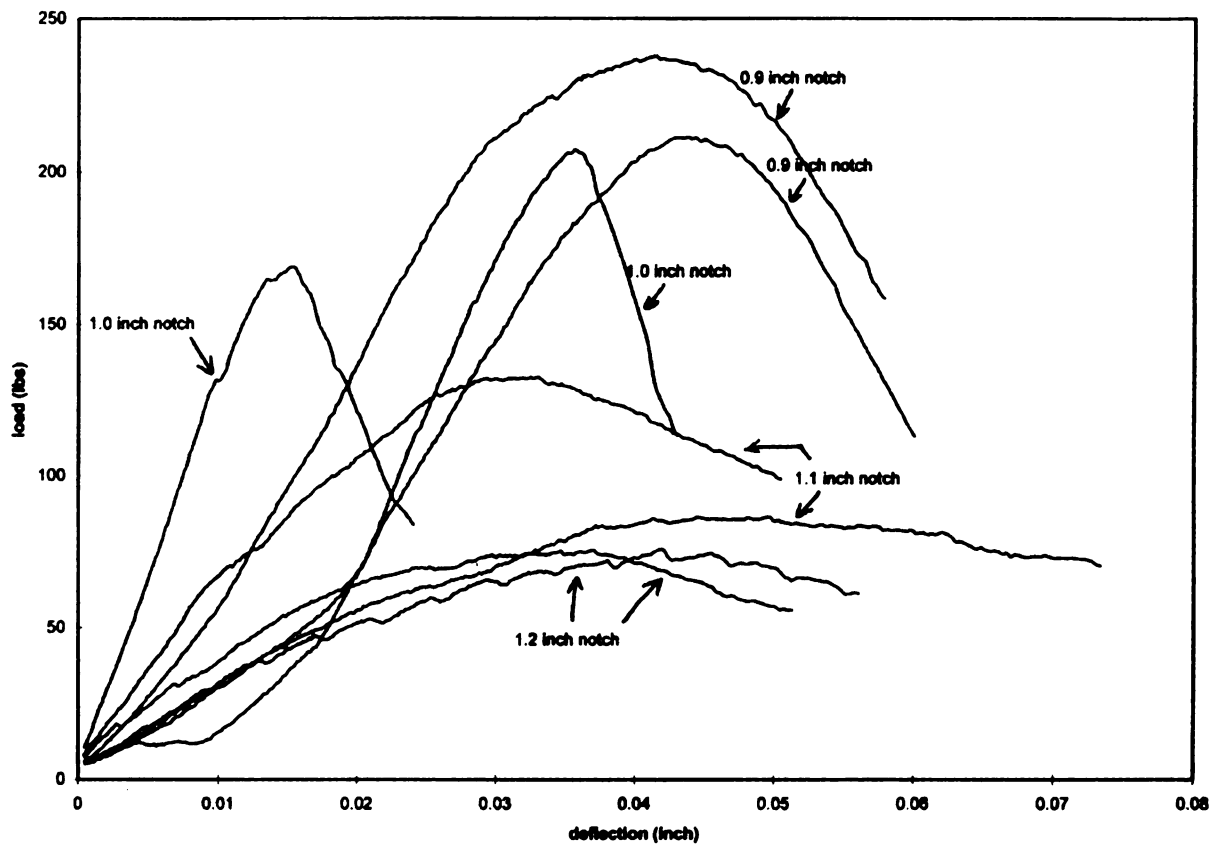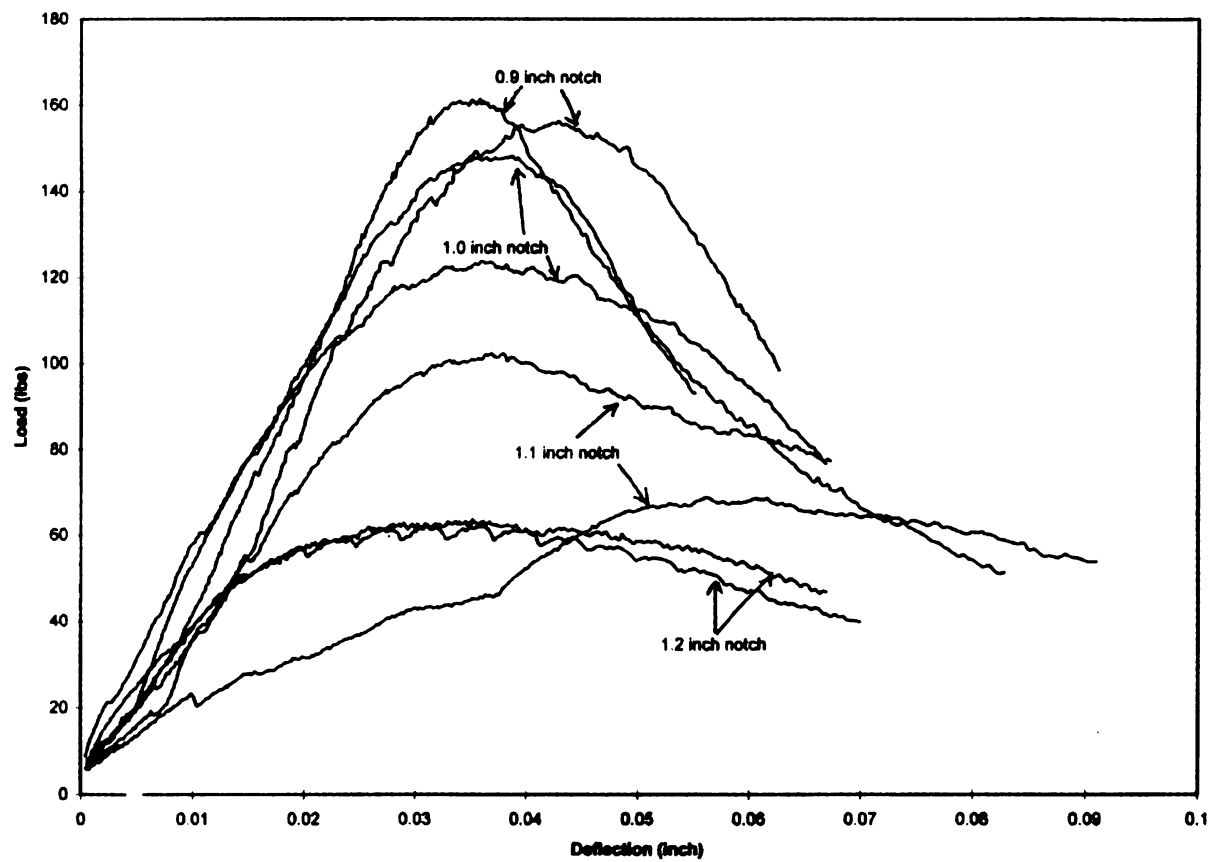
**Figure A.13  Load-deflection curves for AC5 0% Crumb Rubber beam samples for various notch lengths at -10°C**
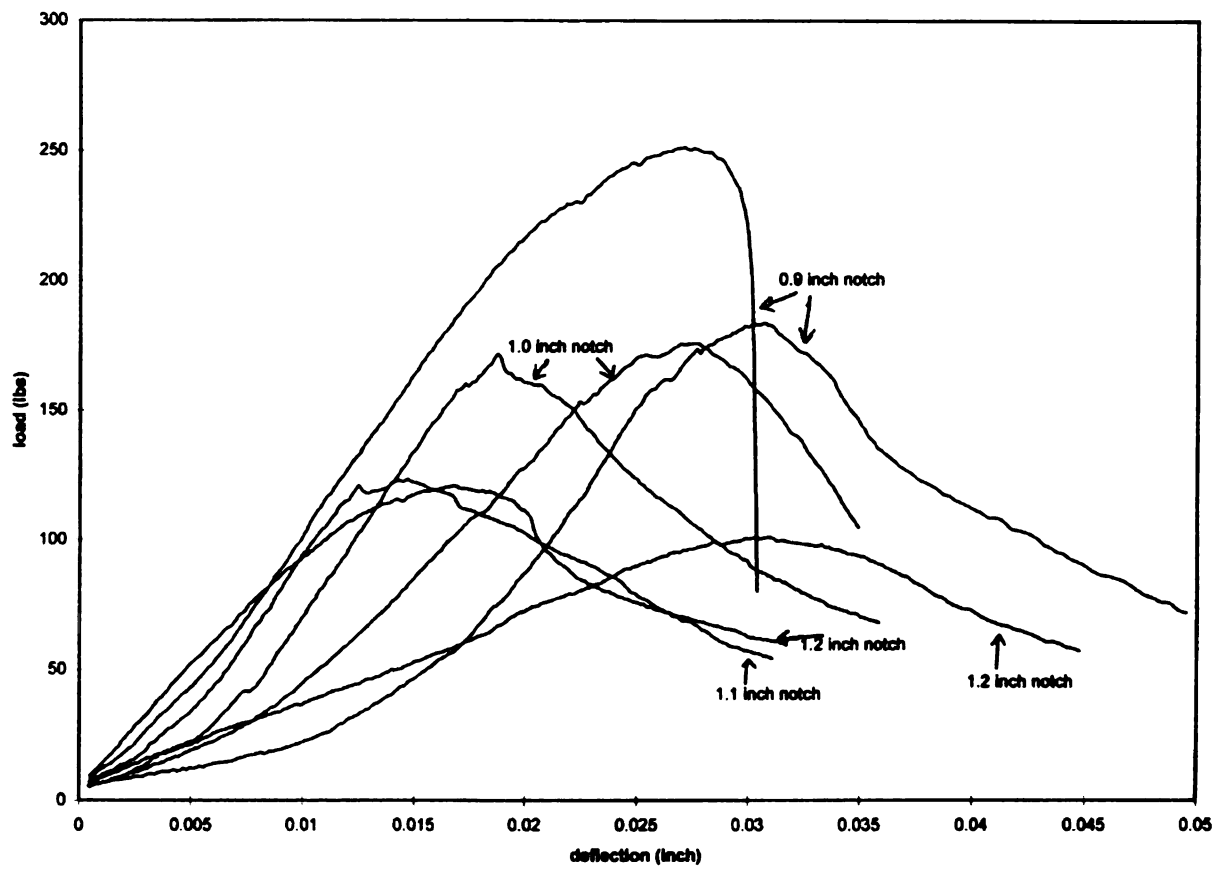
**Figure A.14  Load-deflection curves for AC5 5% Crumb Rubber beam samples for various notch lengths at -10°C**
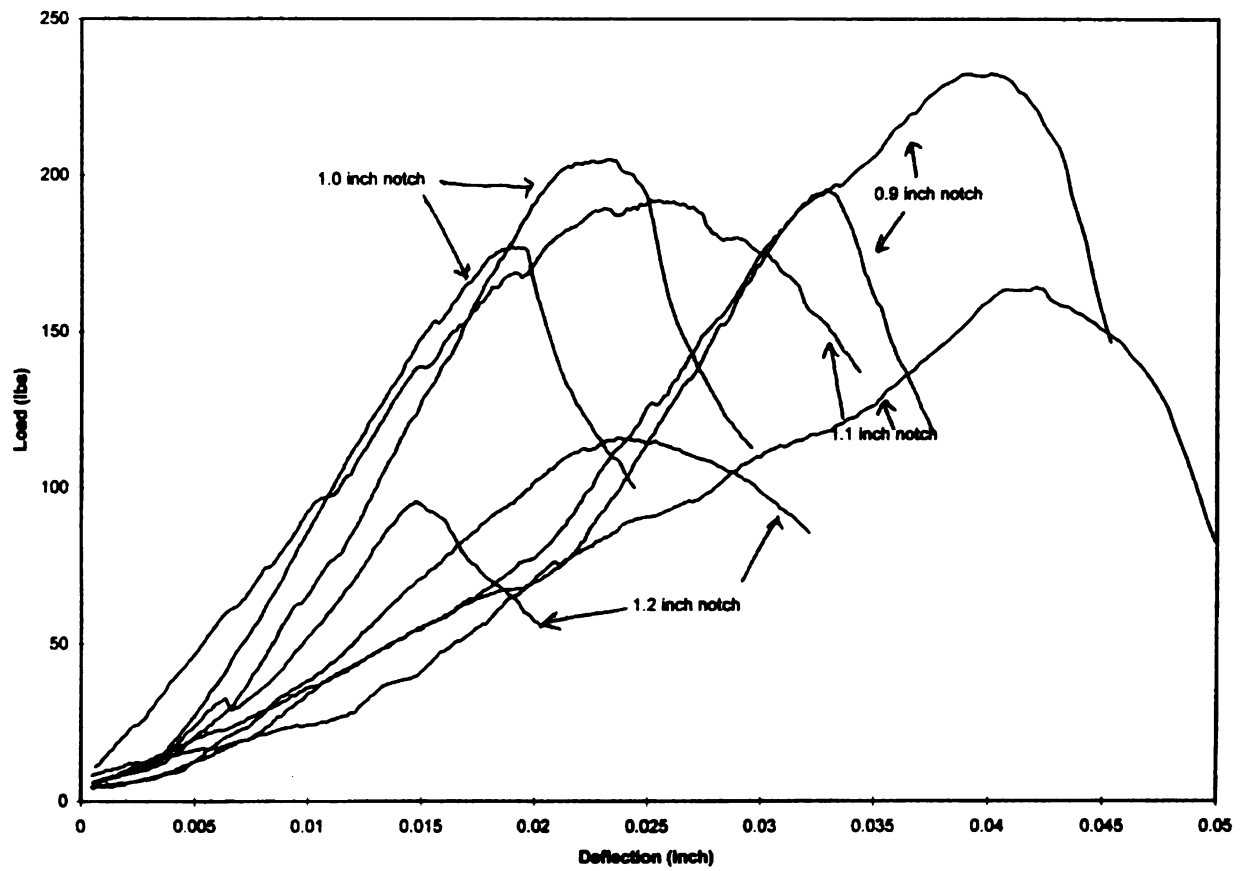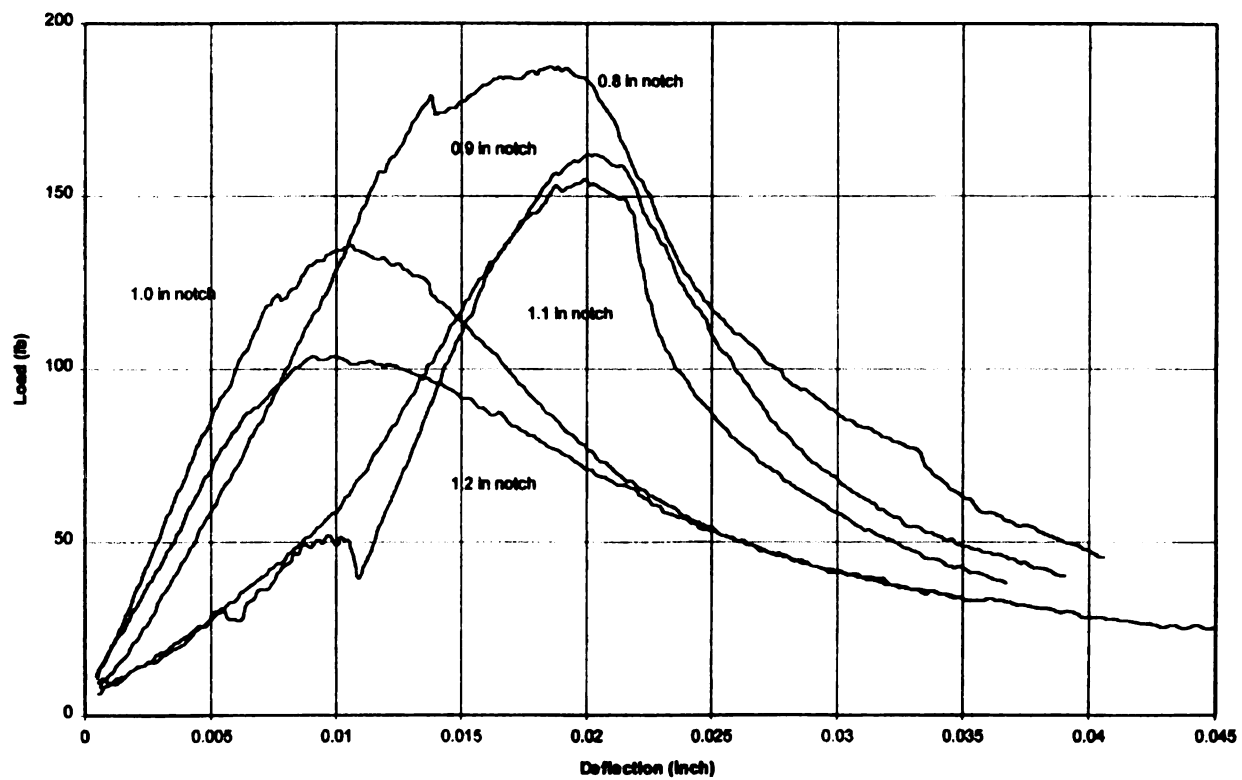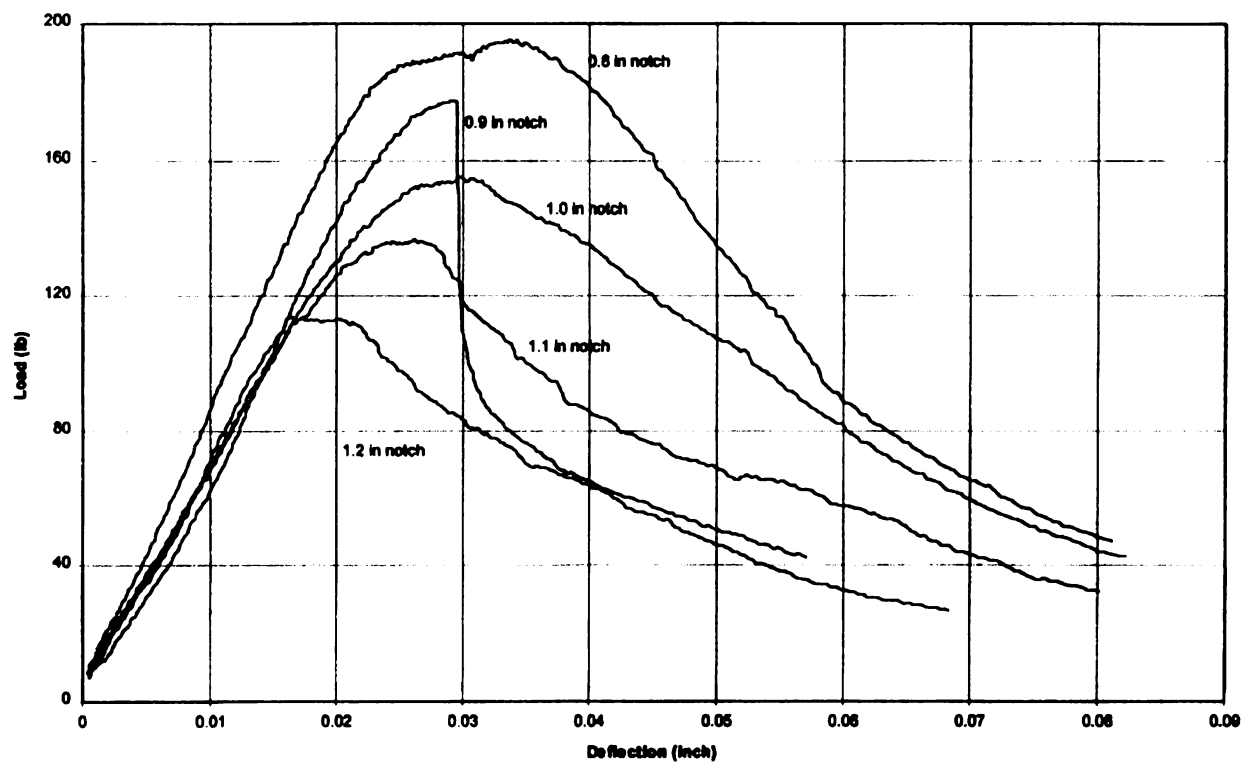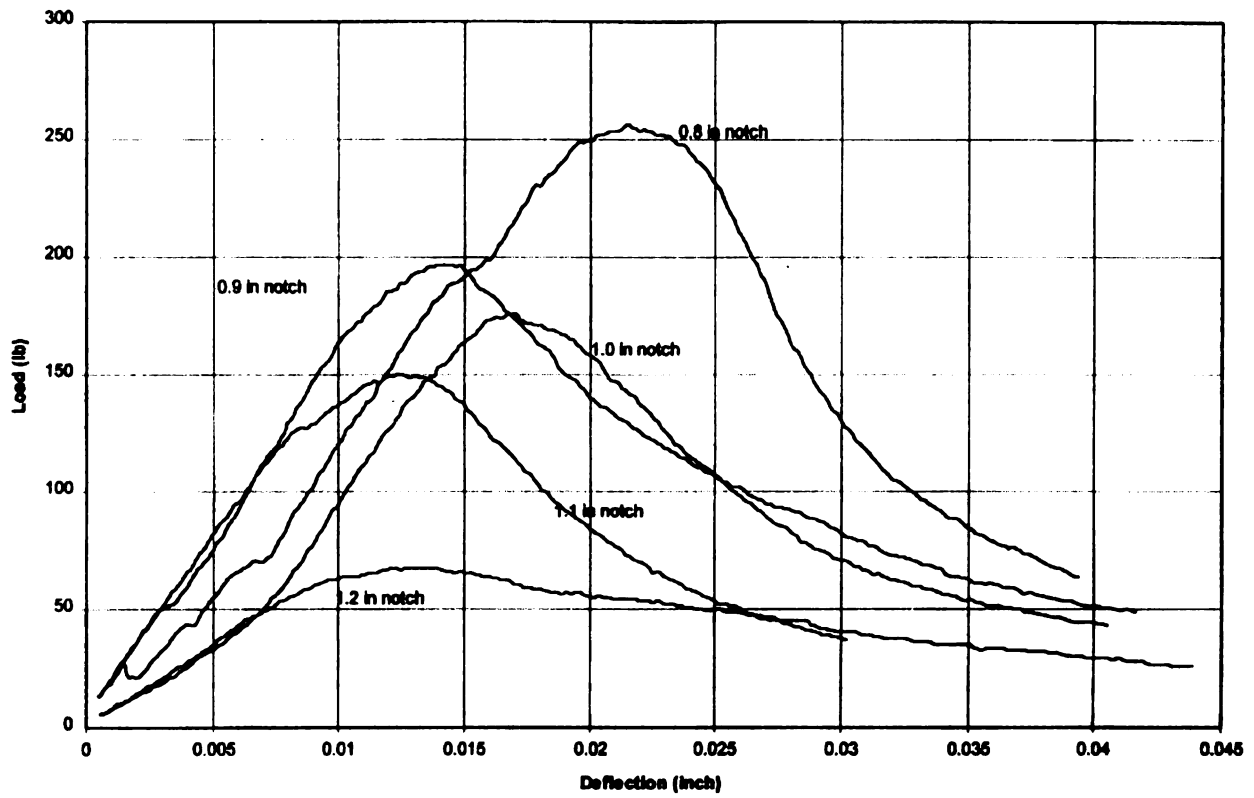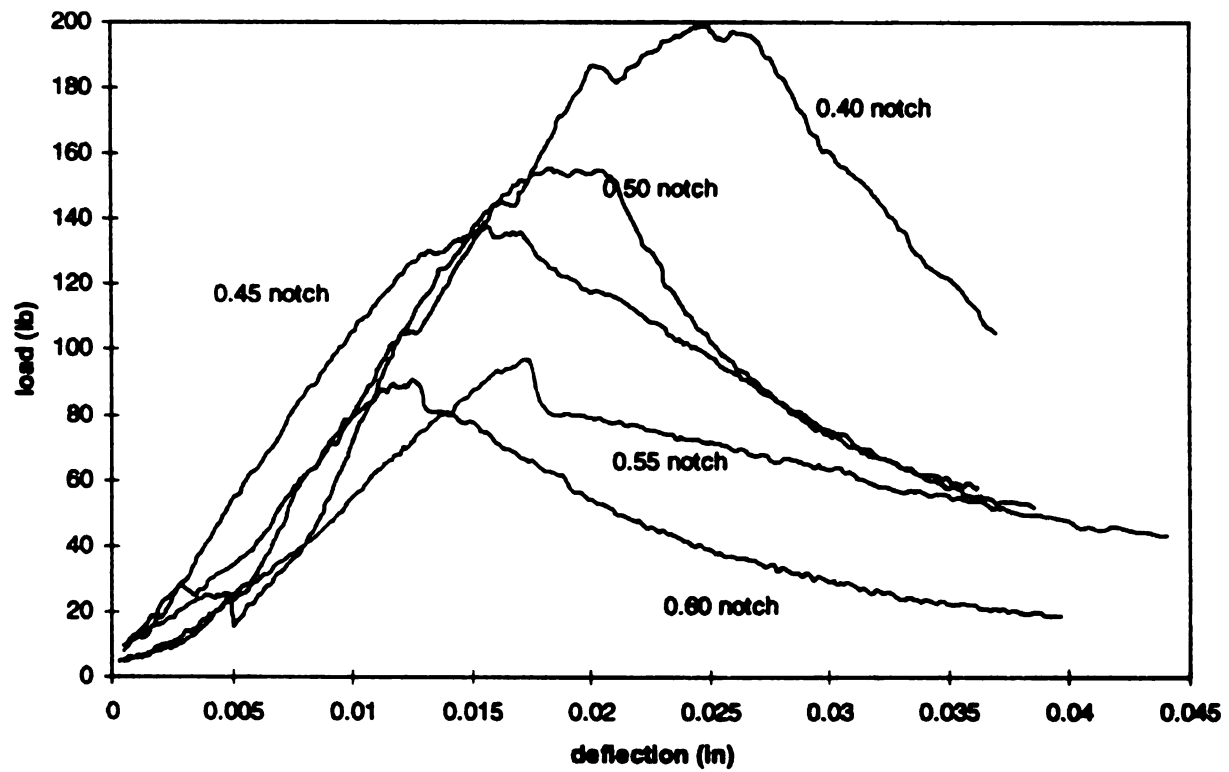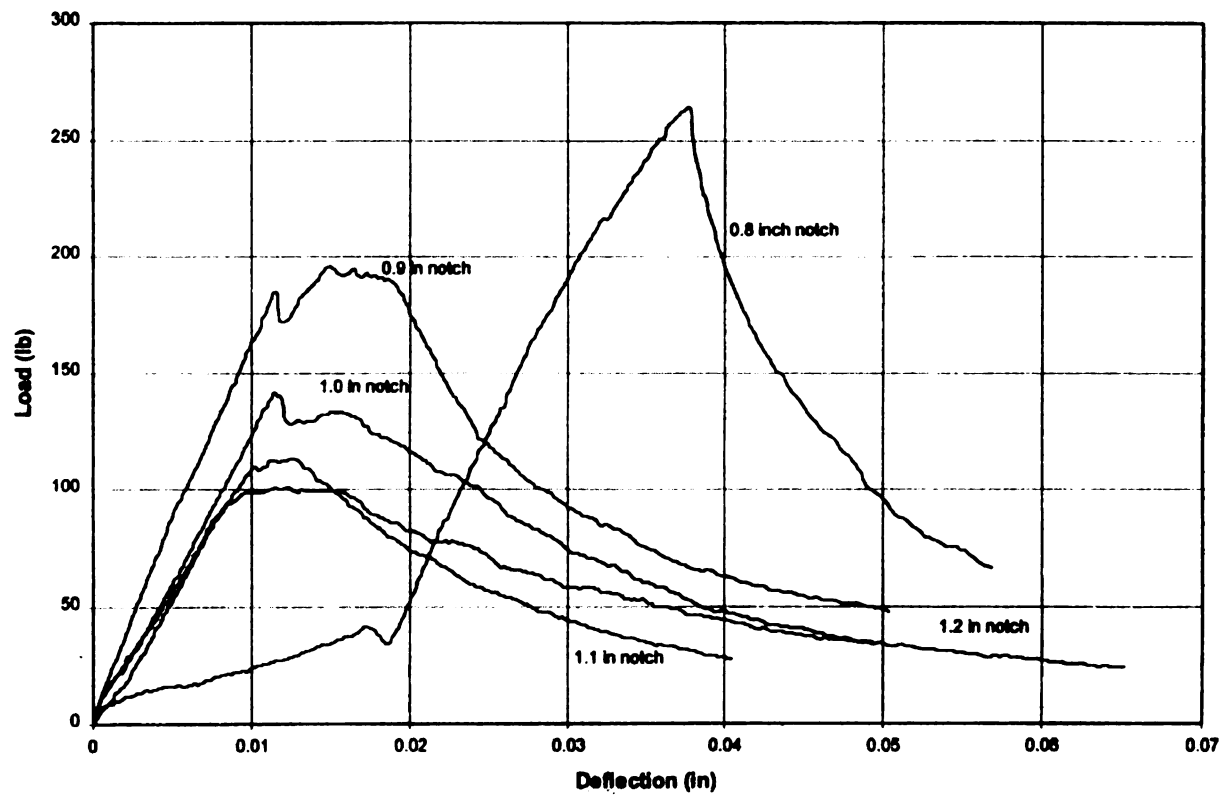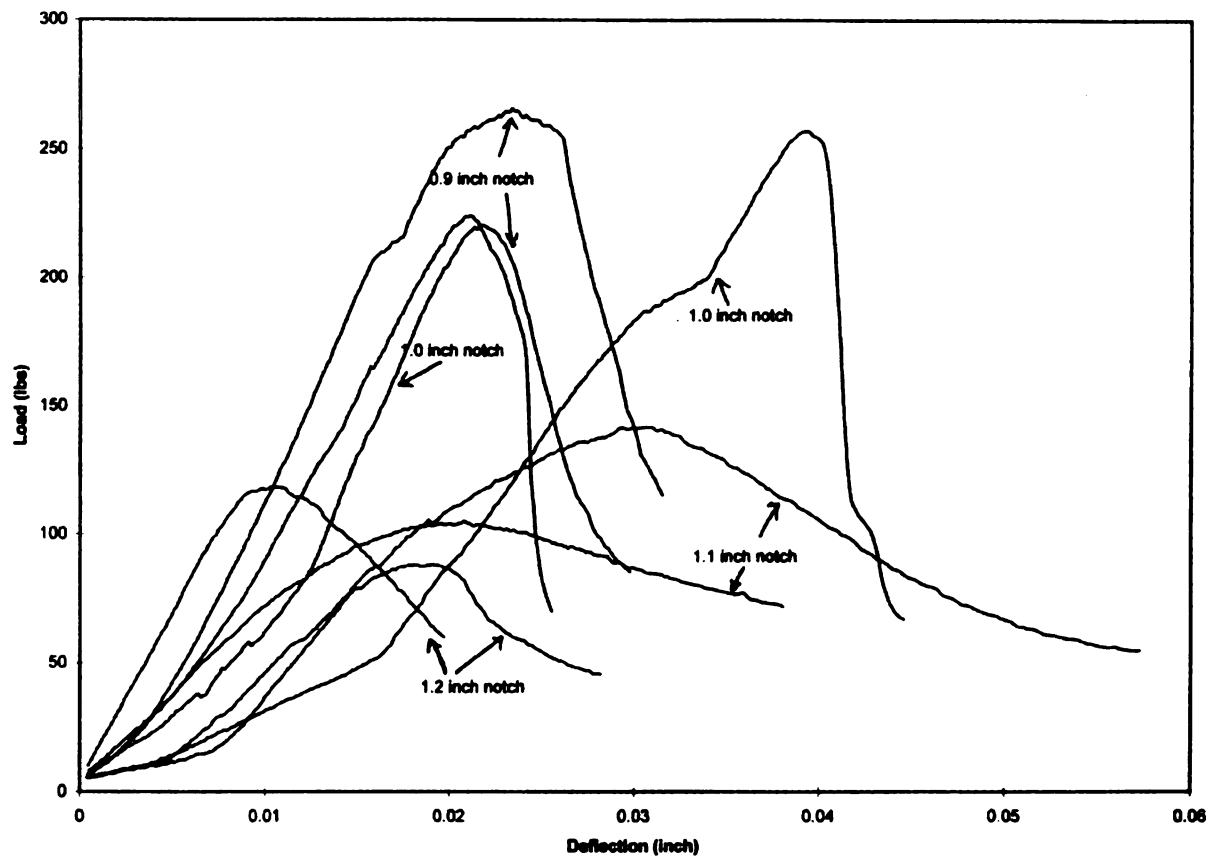
**Figure A.15 Load-deflection curves for AC5 10% Crumb Rubber beam samples for various notch lengths at -10°C**

# APPENDIX B

# LAP-SHEAR TEST RESULTS FOR FRESH ASPHALT

# Table B.1 Lap shear strength and displacement of SBS and SEBS modified asphalt with granitic rock substrate.

| TEST SPECIMEN | | TEST CONDITION → | ULTIMATE LAP SHEAR STRENGTH(N) & DISPLACEMENT(mm) | | | | | | | | | |
|---|---|---|---|---|---|---|---|---|---|---|---|---|
| | | | 20°C | | 10°C | | 0°C | | -10°C | | -20°C | |
| AC-5 VS. GRANITIC ROCK | SBS wt% | 0 | 171<br>154 | 0.26<br>0.37 | 576<br>627 | 0.55<br>0.41 | 1389<br>- | 0.87<br>- | 1189<br>- | 0.33<br>- | 1851<br>1458 | 0.31<br>0.23 |
| | | 1 | | | 351<br>369 | 0.85<br>0.80 | | | 2300<br>2886 | 0.75<br>1.12 | 2195<br>- | 0.53<br>- |
| | | 2 | 85<br>77 | 0.45<br>0.41 | 380<br>496 | 0.80<br>0.44 | 1326<br>1290 | 0.60<br>0.71 | 1970<br>1189 | 0.49<br>0.33 | 1904<br>1760 | 0.49<br>0.25 |
| | | 3 | 54<br>109 | 0.58<br>1.16 | 493<br>498 | 1.38<br>1.20 | 1079<br>1101 | 0.87<br>1.12 | 686<br>1323 | 0.39<br>0.27 | 1626<br>2290 | 0.21<br>0.28 |
| | | 4 | 58<br>67 | 0.90<br>0.75 | 359<br>- | 0.41<br>- | 894<br>893 | 0.45<br>0.49 | 1482<br>- | 0.42<br>- | 2053<br>2004 | 0.27<br>0.25 |
| | | 5 | 90<br>87 | 1.62<br>1.10 | 481<br>440 | 0.28<br>0.37 | 980<br>1016 | 0.60<br>0.36 | 1777<br>920 | 0.50<br>0.25 | 1184<br>1636 | 0.16<br>0.19 |
| | SEBS wt% | 1 | | | 441 | 0.38 | | | 2617<br>1453 | 0.83<br>0.42 | 1365<br>1287 | 0.24<br>0.28 |
| | | 2 | 143<br>- | 0.59<br>- | 608<br>628 | 0.39<br>0.42 | 1443<br>1489 | 0.59<br>0.71 | 974<br>1209 | 0.52<br>0.49 | 2730<br>1355 | 0.34<br>0.21 |
| | | 3 | 85<br>97 | 0.28<br>0.20 | 550<br>484 | 0.42<br>0.43 | 1074<br>980 | 0.75<br>0.55 | 1428<br>1589 | 0.25<br>0.43 | 2127<br>1294 | 0.42<br>0.16 |
| | | 4 | 115<br>115 | 0.62<br>0.46 | 633<br>521 | 0.63<br>0.60 | 1289<br>1443 | 0.99<br>0.86 | 1033<br>1360 | 0.38<br>0.28 | 1580<br>1892 | 0.27<br>0.17 |
| | | 5 | 111<br>100 | 1.04<br>0.75 | 612<br>518 | 0.74<br>0.82 | 1248<br>1189 | 0.85<br>0.58 | 1489<br>- | 0.29<br>- | 1189<br>2351 | 0.14<br>0.38 |
| | | 6 | 123<br>134 | 1.06<br>1.00 | 640<br>648 | 0.85<br>1.23 | 1397<br>1406 | 0.76<br>0.92 | 1694<br>- | 0.58<br>- | 1272<br>1497 | 0.15<br>0.26 |
| AC-10 VS. GRANITIC ROCK | SBS wt% | 0 | 219<br>250 | 0.40<br>0.32 | 858<br>768 | 0.60<br>0.85 | 1621<br>1931 | 0.66<br>0.60 | 1106<br>- | 0.24<br>- | 1680<br>1111 | 0.15<br>0.13 |
| | | 2 | 98<br>99 | 0.21<br>0.29 | 671<br>515 | 0.79<br>0.27 | 1492<br>1484 | 0.95<br>1.37 | 1843<br>2078 | 0.26<br>0.32 | 684<br>1536 | 0.08<br>0.19 |
| | | 3 | 135<br>144 | 1.48<br>1.43 | 539<br>694 | 1.22<br>1.57 | 1414<br>1186 | 1.45<br>1.56 | 2202<br>- | 0.30<br>- | 2507<br>2273 | 0.36<br>0.22 |
| | | 4 | 173<br>162 | 1.24<br>1.20 | 697<br>687 | 1.49<br>1.18 | 1470<br>1550 | 1.04<br>0.91 | 1624<br>1265 | 0.36<br>0.43 | 1421<br>1091 | 0.34<br>0.21 |
| | | 5 | 144<br>157 | 1.01<br>1.14 | 636<br>668 | 0.39<br>0.36 | 1252<br>1342 | 0.58<br>0.44 | 1465<br>1082 | 0.25<br>0.18 | 1179<br>1067 | 0.16<br>0.15 |
| | | 6 | 174<br>164 | 1.55<br>1.67 | 686<br>617 | 1.03<br>1.10 | 1477<br>1467 | 0.87<br>0.90 | 1838<br>586 | 0.29<br>0.26 | 1641<br>1074 | 0.27<br>0.14 |
| | SEBS wt% | 2 | 140<br>101 | 0.28<br>0.21 | 609<br>669 | 0.34<br>0.45 | 1470<br>1748 | 0.85<br>0.92 | 867<br>1489 | 0.24<br>0.33 | 1233<br>1682 | 0.19<br>0.19 |
| | | 3 | 89<br>157 | 0.25<br>0.28 | 705<br>741 | 0.57<br>0.77 | 1602<br>1692 | 0.87<br>0.94 | 1252<br>1389 | 0.40<br>0.32 | 1882<br>1755 | 0.20<br>0.20 |
| | | 4 | 146<br>135 | 0.75<br>0.72 | 803<br>764 | 0.61<br>1.01 | 1655<br>1658 | 1.00<br>0.98 | 1318<br>1885 | 0.28<br>0.26 | 2036<br>1174 | 0.23<br>0.18 |
| | | 5 | 213<br>199 | 0.73<br>0.96 | 824<br>789 | 1.25<br>0.76 | 1592<br>1504 | 1.32<br>0.95 | 1350<br>1939 | 0.36<br>0.38 | 999<br>1655 | 0.17<br>0.19 |
| | | 6 | 185<br>204 | 1.30<br>1.07 | 838<br>913 | 0.79<br>1.06 | 1760<br>- | 0.9<br>- | 1277<br>1697 | 0.27<br>0.42 | 1260<br>1152 | 0.13<br>0.36 |

**Table B.2  Lap shear strength, and toughness of SBR modified asphalt with granitic rock substrate.**

| PROPERTIES | | Ult. Strength (N) | | Toughness (N-mm) | | Failure Mode | |
|---|---|---|---|---|---|---|---|
| COMPOSITION | | 0°C | -10°C | 0°C | -10°C | 0°C | -10°C |
| Granitic Rock uncoated | AC-5/ 0wt% SBR | 1440 1523 | 2356 1873 | 2597 2550 | 394 342 | COH: LT4&5 | ADH: LT6 |
| | AC-5/ 5wt% SBR | 967 1057 | 2795 2983 | 3741 3465 | 3204 3091 | COH: LT4 | COH: LT4 |
| Granitic Rock coated with 5g/95g (SBR/H$_2$O) Solution (1~3 micron thick) | AC-5/ 0wt% SBR | 924 844 | 1191 2338 | 4100 3200 | 145 663 | COH: LT5 | ADH: LT6 |
| | AC-5/ 5wt% SBR | 678 629 | 1166 1244 | 2100 390 | 145 197 | COH: LT4 | ADH: LT6 |
| Granitic Rock coated with 10g/90g (SBR/H$_2$O) Solution (3~7 micron thick) | AC-5/ 0wt% SBR | 1421 1338 | 2852 3044 | 2718 2345 | 3731 2941 | COH: LT4 | ADH: LT6 |
| | AC-5/ 5wt% SBR | 1030 911 | 1505 1671 | 2900 3000 | 940 450 | COH: LT2&4 | ADH: LT6 |
| Granitic Rock coated with 30g/70g (SBR/H$_2$O) Solution (5~10 micron thick) | AC-5/ 0wt% SBR | - - | 1465 2327 | - - | 740 1800 | - | ADH: LT6 |
| | AC-5/ 5wt% SBR | - - | 2459 2341 | - - | 2800 2360 | - | P.ADH: LT6 |
| Greenstone coated with 5g/95g (SBR/H$_2$O) Solution (1~3 micron thick) | AC-5/ 0wt% SBR | 859 1000 | ·2338 927 | 3850 1700 | 857 153 | COH: LT4&5 | ADH: LT6 |
| | AC-5/ 5wt% SBR | 575 644 | 1698 1894 | 3600 3000 | 4500 4400 | COH: LT4&5 | COH: LT4&5 |

171

**Table B.3  Lap shear strength, strain energy and toughness of Elvaloy modified asphalt with granitic rock substrate.**

| PROPERTIES → COMPOSITION ↓ | | | Ultimate Strength (N) | | | | Elastic Strain Energy (N-mm) | | | | Toughness (N-mm) | | | |
|---|---|---|---|---|---|---|---|---|---|---|---|---|---|---|
| | | | 10°C | 0°C | -10°C | -20°C | 10°C | 0°C | -10°C | -20°C | 10°C | 0°C | -10°C | -20°C |
| AC-5 vs. Granitic Rock | Elvaloy wt % | 0 | 478 468 | 1425 1435 | 1640 1904 | 1269 1069 | 140 130 | 900 390 | 435 440 | 225 160 | 2040 1885 | 3530 2000 | 435 440 | 225 160 |
| | | 1 | 165 253 | 1303 1440 | 3368 2402 | 805 2485 | 25 35 | 365 315 | 1800 950 | 110 670 | 210 200 | 1375 945 | 2100 950 | 110 670 |
| | | 2 | 419 439 | 1371 1391 | 1718 2182 | 1069 1977 | 85 85 | 370 375 | 345 535 | 325 750 | 1830 1650 | 3000 3120 | 345 535 | 325 750 |
| | | 3 | 351 370 | 1142 1088 | 2699 2685 | 1264 1635 | 350 280 | 855 760 | 1190 890 | 270 415 | 2600 1850 | 1430 2665 | 2230 890 | 270 415 |
| AC-10 vs. Granitic Rock | Elvaloy wt % | 0 | 800 815 | 1845 1781 | 1562 1186 | 820 531 | 195 190 | 600 515 | 320 215 | 95 50 | 1900 1630 | 875 515 | 320 215 | 95 50 |
| | | 1 | 741 702 | 1571 1537 | 1249 1659 | 517 844 | 180 195 | 540 985 | 215 275 | 70 105 | 1620 1760 | 1440 2120 | 215 275 | 70 105 |
| | | 2 | 487 531 | 1532 1869 | 1322 2294 | 1239 1015 | 120 120 | 700 1280 | 270 870 | 190 170 | 1660 1430 | 1850 2260 | 270 870 | 190 170 |
| | | 3 | 839 439 | 2221 1777 | 2343 1811 | 751 1313 | 340 100 | 1680 820 | 775 415 | 100 215 | 890 1425 | 2420 3080 | 775 415 | 100 215 |

172

# Table B.4 Lap shear strength, strain energy and toughness of Crumb rubber modified asphalt with granitic rock substrate.

| PROPERTIES → | | | Ultimate Strength (N) | | | | Elastic Strain Energy (N-mm) | | | | Toughness (N-mm) | | | |
|---|---|---|---|---|---|---|---|---|---|---|---|---|---|---|
| COMPOSITION ↓ | | | 20°C | 0°C | -10°C | -20°C | 20°C | 0°C | -10°C | -20°C | 20°C | 0°C | -10°C | -20°C |
| AC-5 vs. Granitic Rock | Crumb Rubber wt % | 0 | 82<br>72 | 1244<br>1811 | 2089<br>2289 | 1010<br>1923 | 15<br>30 | 820<br>1600 | 1600<br>1900 | 190<br>820 | 575<br>520 | 1940<br>1875 | 2150<br>1900 | 190<br>820 |
| | | 5 | 53<br>53 | 1034<br>1274 | 1322<br>981 | 1679<br>1508 | 50<br>20 | 750<br>600 | 510<br>260 | 390<br>480 | 85<br>250 | 1200<br>950 | 510<br>260 | 390<br>480 |
| | | 10 | 58<br>63 | 1117<br>1000 | 2011<br>2221 | 1698<br>1635 | 5<br>35 | 590<br>360 | 1030<br>1330 | 495<br>515 | 135<br>110 | 950<br>680 | 1290<br>1670 | 495<br>515 |
| | | 15 | 53<br>58 | 1181<br>1108 | 2626<br>2494 | 1889<br>2319 | 15<br>35 | 670<br>580 | 2040<br>1710 | 500<br>745 | 250<br>600 | 1350<br>1210 | 2430<br>3180 | 500<br>745 |
| | | 20 | 92<br>82 | 1303<br>1161 | 1768<br>2153 | 1557<br>2177 | 25<br>25 | 820<br>550 | 1150<br>2020 | 490<br>645 | 275<br>185 | 1340<br>1170 | 1700<br>2550 | 490<br>645 |
| AC-10 vs. Granitic Rock | Crumb Rubber wt % | 0 | 97<br>87 | 1674<br>1860 | 1220<br>1196 | 1689<br>961 | 20<br>20 | 850<br>1200 | 325<br>365 | 415<br>180 | 500<br>700 | 3000<br>1480 | 325<br>365 | 415<br>180 |
| | | 5 | 82<br>58 | 1586<br>1474 | 2861<br>1044 | 1015<br>1191 | 25<br>15 | 785<br>480 | 2900<br>310 | 380<br>450 | 200<br>140 | 1375<br>1100 | 2900<br>310 | 380<br>450 |
| | | 10 | 72<br>77 | 1674<br>1430 | 2455<br>2597 | 1279<br>1318 | 25<br>60 | 1050<br>860 | 1140<br>1170 | 315<br>280 | 250<br>700 | 1550<br>1370 | 1140<br>1170 | 315<br>280 |
| | | 15 | 126<br>131 | 1576<br>2362 | 2675<br>1752 | 1703<br>1181 | 40<br>40 | 850<br>1580 | 1700<br>660 | 400<br>255 | 450<br>280 | 1400<br>2000 | 2075<br>660 | 400<br>255 |
| | | 20 | 131<br>116 | 1493<br>1542 | 1650<br>1054 | 1376<br>1191 | 50<br>45 | 785<br>860 | 685<br>420 | 380<br>250 | 410<br>345 | 1390<br>1485 | 800<br>420 | 380<br>250 |

**APPENDIX C**

**LAP-SHEAR TEST RESULTS FOR AGED ASPHALT**

**Table C.1  Lap shear strength and displacement of aged
SBS modified asphalt with granitic rock substrate.**

| Binder System | | LAP-SHEAR STRENGTH, N | | | | | ELASTIC STRAIN ENERGY, N-mm | | | | |
|---|---|---|---|---|---|---|---|---|---|---|---|
| | | 20°C | 10°C | 0°C | -10°C | -20°C | 20°C | 10°C | 0°C | -10°C | -20°C |
| AC-5/ | 1 wt% | 160 | 450 | 1350 | 1400 | 1000 | 30 | 100 | 350 | 150 | 110 |
| SBS | 3 wt% | 200 | 400 | 1000 | 1400 | 1200 | 150 | 90 | 320 | 200 | 200 |
| | 6 wt% | 190 | | 1100 | | 2300 | 175 | | 730 | | 740 |
| AC-10/ | 0 wt% | 320 | 920 | 1300 | 900 | 850 | 145 | 260 | 210 | 70 | 130 |
| | 2 wt% | 230 | | 1200 | | 1000 | 120 | | 330 | | 60 |
| SBS | 3wt% | 300 | 570 | 1530 | 1200 | 1300 | 110 | 200 | 500 | 125 | 100 |
| | 5 wt% | 330 | | 1300 | | 1450 | 210 | | 375 | | 120 |
| | 6 wt% | 210 | | 1500 | | 1450 | 345 | | 340 | | 210 |

**Table C.2  Lap shear strength, and toughness of aged
SBR modified asphalt with granitic rock substrate.**

| PROPERTIES | | Ultimate Strength (N) | | | Toughness (N-mm) | | |
|---|---|---|---|---|---|---|---|
| COMPOSITION | | 0°C | -10°C | -20°C | 0°C | -10°C | -20°C |
| Aged AC-5/SBR<br><br>vs.<br><br>Granitic Rock | 0wt% | 1830<br>--- | 1552<br>1830 | 1576<br>1415 | 549<br>--- | 349<br>339 | 178<br>185 |
| | 1wt% | 1708<br>1713 | 1264<br>2118 | 1039<br>1264 | 1300<br>1400 | 163<br>453 | 192<br>158 |
| | 3wt% | 1322<br>1269 | 2817<br>2060 | 946<br>1342 | 1200<br>2100 | 2557<br>491 | 168<br>255 |
| | 5wt% | 1054<br>1078 | 2387<br>2475 | 3276<br>4233 | 1500<br>1800 | 1880<br>2074 | 1909<br>2960 |
| Aged AC-10/SBR<br>vs.<br>Granitic Rock | 0wt% | 1737<br>2001 | 1391<br>1957 | 844<br>912 | 690<br>895 | 167<br>420 | 75<br>161 |

## Table C.3 Lap shear strength, strain energy and toughness of aged Elvaloy AM modified asphalt with granitic rock substrate.

| PROPERTIES → COMPOSITION ↓ | | Ultimate Strength (N) | | | Strain Energy (N-mm) | | | Toughness (N-mm) | | |
|---|---|---|---|---|---|---|---|---|---|---|
| | | 10°C | 0°C | -10°C | 10°C | 0°C | -10°C | 10°C | 0°C | -10°C |
| Aged AC-5/ Elvaloy vs. Granitic Rock | 0 wt% | 927 942 | 1469 1899 | 934 901 | 365 470 | 260 475 | 100 90 | 1645 2475 | 260 475 | 100 90 |
| | 1 wt% | 854 805 | 1630 1889 | 1912 1483 | 735 740 | 540 1500 | 500 195 | 2335 1820 | 540 1500 | 500 195 |
| | 2 wt% | 751 771 | 1673 1850 | 1608 1886 | 245 390 | 700 745 | 270 290 | 700 625 | 900 745 | 270 290 |
| | 3 wt% | 1015 610 | 1461 2001 | 996 963 | 785 95 | 290 1075 | 190 240 | 1335 295 | 290 1320 | 190 240 |
| Aged AC-10/ Elvaloy vs. Granitic Rock | 0 wt% | 1000 1064 | 1249 1269 | 751 765 | 150 210 | 175 160 | 50 55 | 150 210 | 175 160 | 50 55 |
| | 1 wt% | 1288 1112 | 1747 1562 | 762 1216 | 330 420 | 320 235 | 65 130 | 1055 1040 | 320 235 | 65 130 |
| | 2 wt% | 1152 1913 | 1864 1371 | 857 1036 | 540 610 | 395 330 | 85 145 | 815 770 | 395 330 | 85 145 |
| | 3 wt% | 1049 1156 | 1381 1928 | 1260 883 | 755 825 | 215 490 | 160 175 | 1745 1690 | 215 490 | 160 175 |

177

**Table C.4 Lap shear strength, strain energy and toughness of aged Crumb rubber modified asphalt with granitic rock substrate.**

| PROPERTIES → COMPOSITION ↓ | | | Ultimate Strength (N) | | Elastic Strain Energy (N-mm) | | Toughness (N-mm) | |
|---|---|---|---|---|---|---|---|---|
| Binder | Condition | wt % | 0°C | -10°C | 0°C | -10°C | 0°C | -10°C |
| AC-5/ CRM vs. Granitic Rock | Stored @ 350°F for 0 hours | 0 | 1248 1811 | 2089 2289 | 820 1600 | 1600 1900 | 1940 1875 | 2150 1900 |
| | | 10 | 1117 1000 | 1322 981 | 590 360 | 1030 1330 | 950 680 | 1290 1670 |
| | Stored @ 350°F for 5 hours | 0 | 1440 1332 | 1108 1313 | 1020 1360 | 345 445 | 1470 1990 | 345 445 |
| | | 10 | 1220 1327 | 2143 1864 | 645 715 | 605 490 | 1140 1150 | 605 490 |
| | Stored @ 350°F for 24 hours | 0 | 1205 1191 | 512 1181 | 475 405 | 80 305 | 475 405 | 80 305 |
| | | 10 | 1401 1923 | 810 878 | 360 450 | 180 300 | 795 450 | 485 395 |
| AC-10/ CRM vs. Granitic Rock | Stored @ 350°F for 0 hours | 0 | 1674 1860 | 1220 1196 | 850 1200 | 325 365 | 3000 1480 | 325 365 |
| | | 10 | 1674 1430 | 2455 2597 | 1050 860 | 1140 1170 | 1550 1370 | 1140 1170 |
| | Stored @ 350°F for 5 hours | 0 | 1318 1586 | 1508 1503 | 1630 1190 | 515 480 | 2140 1190 | 515 480 |
| | | 10 | 1415 1293 | 1586 346 | 1210 975 | 620 40 | 1550 1250 | 620 40 |
| | Stored @ 350°F for 24 hours | 0 | 712 815 | 986 1112 | 170 450 | 290 325 | 170 450 | 290 325 |
| | | 10 | 238 1440 | 190 --- | 40 720 | 20 --- | 135 1100 | 20 --- |

# LIST OF REFERENCES

179

# LIST OF REFERENCES

1. Lewandowski L.H.., *Polymer Modification of Paving Asphalt Binders*, Polymers in Asphalt, Rubber Chemistry and Technology, Vol. 67, pp. 447-480, 1994.

2. Report, *SHRP-A/IR-90-015, Strategic Highway Research Program*, National Research Council, Washington, D.C., 1990

3. Newcomb, D.E., M. Stroup-Gardiner and J.A. Epps, *Laboratory and Field Studies of Polyolefin and Latex Modifiers for Asphalt Mixtures*, Polymer Modified Asphalt Binders, ASTM STP 1108, American Society for Testing and Materials, Philadelphia, 1992.

4. Rogge, D.F., R.L. Terrel and A. J. George, *Polymer Modified Hot Mix Asphalt - Oregon Experience*, Polymer Modified Asphalt Binders, ASTM STP 1108, American Society for Testing and Materials, Philadelphia, pp. 151-172, 1992.

5. Khosla, P.N., *Effect of the Use of Modifiers on Performance of Asphaltic Pavements*, Transportation Research Record, 1317, TRB, National Research Council, Washington D.C., pp. 10-22, 1992.

6. Baladi G.Y., *Fatigue Life and Permanent Deformation Characteristics of Asphalt Concrete Mixes*, Transportation Research Record 1227, TRB, National Research Council, Washington D.C., 1989

7. Baladi G.Y., R.S. Harichandran and R.W. Lyles, *Asphalt Mix Design - An Innovative Approach*, Transportation Research Record 1227, TRB, National Research Council, Washington D.C., 1989

8. Baladi G.Y., *Integrated Material and Structural Design Method for Flexible Pavements*, Final Report RD-88-109 and 110, FHWA, USDOT, 1987.

9. Stuart K. D., *Asphalt mixtures Containing Chemically Modified Binders*, Report, Federal Highway Administration, FHWA-RD-92-101, 1991.

10. Goodrich, J.L., *Asphalt and Polymer Modified Asphalt Properties Related to the Performance of the Asphalt Concrete Mixes*, Proceedings of the Association of the Asphalt Paving Technologists, Vol. 57, 1988.

11. Little, D. N., Button, J. W., White, R. M., Ensley, E. K., Kim Y., Ahmed S. J., *Investigation of Asphalt Additives*, Report, Federal Highway Administration, 1987.

12. Shuler, T.S., Collins, H.J., and Kirkpatrick, J. P., *Polymer Modified Asphalt Concrete Properties Related to Asphalt Concrete Performance,* ASTM STP 941, O.E. Brisco, Ed. 1987.

13. Button, J.W., Little, D.N., Kim, Y., and Ahmed, J., *Mechanistic Evaluation of Selected Asphalt Additives,* Proceedings of the Association of the Asphalt Paving Technologists, Vol. 56, 1987.

14. Khattak, M. J., and Baladi, G. Y., *Engineering Properties of Polymer Modified Asphalt mixtures,* Transportation Research Record 1638, TRB National Research Council, Washington, D.C., 1998.

15. Bhurke A.S., E.E. Shin, S.Rozeveld, P. Vallad and L.T.Drzal, *Effect of Polymer Modification on the Properties of Asphalt Concrete,* Proc. of the 20$^{th}$ Annual Adhesion Society, pp. 671-673, 1997

16. Bhurke A.S., E.E. Shin, P. Vallad and L.T.Drzal, *Polymer Modified Asphalt-Aggregate Adhesion Measurement and Characterization,* Proc. of the 19$^{th}$ Annual Adhesion Society, pp. 203-206, 1996

17. Bhurke A. S., E.E. Shin, S.J. Rozeveld, P. Vallad and L.T.Drzal, *Polymer Modified Asphalt-Aggregate Adhesion Measurement and Characterization - II,* Proc. of the 20$^{th}$ Annual Adhesion Society, pp. 603-605, 1997

18. Shin, E. E., A.S. Bhurke, E.B. Scott, S.J. Rozeveld, and L.T. Drzal, *Microstructure, Morphology and Failure Modes of Polymer Modified Asphalts,* Transportation Research Record 1535, TRB, National Research Council, Washington D.C., pp. 61-73, 1996.

19. Bhurke A.S., E.E.Shin, and L.T.Drzal, *Fracture Morphology and Fracture Toughness of Polymer Modified Asphalt Concrete,* In Transportation Research Record, TRB Paper # 970942 , National Research Council, Washington D.C., 1997.

20. Wei, J.B., J.C. Shull, Y. Lee and M.C. Hawley, *Characterization of Asphalt Binders Based on Chemical and Physical Properties,* Int. Journal of Polymer Analysis & Characterization, Vol. 3, pp. 33-58, 1996.

21. Lee, Y., L.M. France and M.C. Hawley, *The Effect of Network Formation on the Rheological Properties of SBR Modified Asphalt Binders,* Rubber Chemistry & Technology, Vol. 70, pp. 256-263, 1997.

22. Bouldin, M.G. and J.H. Collins, *Wheel Tracking Experiments with Polymer Modified and Unmodified Hot Mix Asphalt,* Polymer Modified Asphalt Binders, ASTM STP 1108, American Society for Testing and Materials, 1990.

23. Tayebali A.A., *Influence of Rheological Properties of Modified Asphalt Binders on the Load Deformation Characteristics of the Binder/Aggregate Mixtures in Polymer Modified Asphalt Binders*, ASTM STP 1108, American Society for Testing and Materials, 1992.

24. Bouldin, M.G., J.H. Collins and A. Berker, *Rheology and Microstructure of Polymer/Asphalt Blends*, Rubber Chemistry and Technology, Vol. 64, No.4, pp. 577-600, 1991.

25. Scott, E.B., *Polymer/Fiber Modified Asphalt Fracture Mechanisms and Micristructure Relationships To Distresses and Environmental Factors*, MS Thesis, Michigan State University, 19993

26. Liang R. Y. and S. Lee, *Short-Term and Long-Term Aging Behavior of Rubber Modified Asphalt Paving Mixture*, Transportation Research Record 1530, TRB, National Research Council, Washington, D.C., pp. 11-17, 1996

27. Drzal L.T., *Composite Interphase Characterization*, SAMPE Journal, Vol. 19, Iss. 5, pp. 7-13, 1983

28. Hayakawa K., T. Soshiroda, *Effects of Cellulose Ether on Bond Between Matrix and Aggregate in Concrete*, Adhesion Between Polymers and Concrete, pp. 22-31, Chapman & Hall, London, London, 1986.

29. Mlodecki J., *Adhesion Forces of Polymer Modified Concrete and Plain Concrete to Steel in Moulds and in Reinforced Concretes*, Adhesion Between Polymers and Concrete, pp. 22-31, Chapman & Hall, London, London, 1986.

30. Adamson A., *Physical Chemistry of Surfaces*, 5th Ed., pp.113-115, Wiley, NY, 1994

31. Shull J.C., *An Investigation of the Fundamental Chemical, Physical and Thermodynamic Properties of Polymer Modified Asphalt Cement*, MS Thesis, Michigan State University, 1995.

32. France L.M., *Chemical, Physical and Thermodynamic Properties of Neat and Polymer Modified Asphalt Binders*, MS Thesis, Michigan State University, 1997.

33. Khattak M.J., *Engineering Characteristics of Polymer Modified Asphalt Mixtures*, Doctoral Dissertation, Michigan State University, 1999.

34. *Material Reference Library Asphalt Data*, Strategic Highway Research Program, National Research Council, Washington D.C., 1992.

35. Whiteoak, D, *The Shell Bitumen Handbook*. Shell Bitumen U.K., Surrey U.K., 1990.

36. Altgen K.H. and O.L. Harle, *The Effect of Asphaltenes on Asphalt Viscosity.* Industrial and Engineering Chemistry, Product Research and Development, Vol. 14, pp. 240-247, 1975.

37. Brodnyan, J.G., F.H. Gaskins, W. Philippoff, W. and E. Thelen, *The rheology of asphalts. III. Dynamical mechanical properties of asphalts*, Trans. Soc. Rheology, Vol. 4, pp. 279-296, 1960.

38. Heithaus J. J., *Measurement and significance of asphaltene peptization*, J. Inst. of Petroleum, Vol. 48, pp. 45-53, 1962.

39. Simpson, W.C., R.L. Griffin and T.K. Miles, *Relationship of Asphalt Properties to Chemical Constitution*, J. Chem. Eng. Data, Vol. 6, pp. 426-429, 1961.

40. Hawley, M., L.T. Drzal, and G.Y. Baladi, *Polymers in Bitumous Mixtures, Phase II*, Michigan Department of Transportation (MDOT) Quarterly Progress Report, June 16, 1994 - Sept. 15, 1994.

41. Bull A. L. and W.C. Vonk, *Thermoplastic Rubber/Bitumen Blends for Roof and Road*, Thermoplastic Rubbers Technical Manual, 2$^{nd}$ Edition, Shell Elastomers, Shell Chemical Co., 1988.

42. Troy K., P.E. Sebaaly and J.A. Epps, *Evaluation Systems for Crumb Rubber Modified Binders and Mixtures*, Transportation Research Record 1530, TRB, Nationsl Research Council, Washington, D.C., pp. 3-10, 1996

43. Jacobs M.M., P.C. Hopman and A.A. Molenar, *Characterization of Fracture in Asphalt Mixes Based on a Molecular Approach*, Transportation Research Record 1535, TRB, Nationsl Research Council, Washington, D.C., pp. 22-28, 1996

44. Alkins A.G. and Y-W Mai, *Elastic and Plastic Fracture*, pp. 29-69, Wiley, NY, 1985

45. Azimi H.R, R.A. Pearson and R.W. Hertzberg, *Fatigue of Hybrid Epoxy Composites: Epoxies Containing Rubber and Hollow Glass Spheres*, Polymer Engineering and Science, Vol. 36, No. 18, pp. 2352-2365, 1996

46. Sorushian P., L.T. Drzal, S. Ravanbakhsh, A.S. Bhurke and E.E. Shin, *Recycling of Automobile Plastics in Concrete Coinstruction: A Research and Demonstration Project*, Report MSU-ENGR-001-96, Michigan State University, 1996.

47. Hawley M., L.T. Drzal and G.Y. Baladi, *Polymers in Bituminous Mixtures, Phase II*, Michigan Department of Transportation (MDoT) Final Report, 1997.

48. Rozeveld S.J., E.E. Shin, A.S. Bhurke, L. France, L.T. Drzal, *Network Morphology of Straight and Polymer Modified Asphalt Cements*, Microscopy Research and Technique, Vol 3., Iss 5, pp. 529-543, 1997.

49. Eriksen K., *Summary Report on Specimen Preparation*, Strategic Highway Research Program Symposium, Washington D.C., 1990.

50. Eriksen K. and A. Neidel, *Air Void Characteristics in Asphalt-Concrete Samples from Compaction Study*, Strategic Highway Research Program, National Research Council, 1992.

51. Eriksen K. and A. Neidel, *Thin Sections of Asphalt Concrete Preparation Techniques*, Strategic Highway Research Program Symposium, Washington D.C., 1990.

52. ASTM D792-86, *Standard Test Methods for Specific Gravity (Relative Density) of Plastics by Displacement*, Annual Book of ASTM standards, Vol 08.01, pp 293-296, 1990.

53. Alkins A.G. and Y-W Mai, *Elastic and Plastic Fracture*, pp. 105, Wiley, NY, 1985.

54. Lu M., K. Chiou, F. Chang, *Fracture Toughness Characterization of a PC/ABS Blend Under Different Strain Rates by Various J-Integral Methods*, Polymer Engineering and Science, Vol. 36, No. 18, pp 2289-2295, 1996.

55. Wu J. and Y. Mai, *The Essential Fracture Work Concept for Toughness Measurement of Ductile Polymers*, Polymer Engineering and Science, Vol. 36, No. 18, pp 2275-2288, 1996.

56. Aglan H., *Polymeric Additives and Their Role In Asphaltic Pavements. Part I: Effect of Additive Type on the Fracture and Fatigue Behavior*, Journal of Elastomers and Plastics, Vol. 25, pp. 307-321, 1993.

57. Roberts F. L., P.S. Kandhal, E.R. Brown, D. Lee, T.W. Kennedy, *Hot Mix Asphalt Materials, Mixture Design and Construction*, 2nd ed., NAPA Education Foundation, MD, pp. 169-170, 1996.

58. Roberts F. L., P.S. Kandhal, E.R. Brown, D. Lee, T.W. Kennedy, *Hot Mix Asphalt Materials, Mixture Design and Construction*, 1st ed., NAPA Education Foundation, MD, pp. 151-153, 1994.

59. Adedeji A., T. Grunfelder, F.S. Bates, C.W. Macosko, M. Stroup-Gardiner and D.E. Newcomb, Asphalt Modified by SBS Triblock Copolymer: Structures and Properties, Polymer Engineering and Science, Vol. 36, Iss 12, pp. 1707-1723, 1996.

60. Ho R.M., A. Adedeji, D.W. Giles, D.A. Hajduk, C.W. Macosco and F.S. Bates, Microstructure of Triblock Copolymers in Asphalt Oligomers, Journal of Polymer Science Part B - Polymer Physics, Vol. 35. Iss 17, pp 2857-2877, 1997.

61. Rouge N., C. Dubois, C. Vermillet and A. Chambaudet, *Characterization of the Open Porosity of Brake Pads. I. Development of 2-D Porosity Image Analysis Techniques*, Science and Engineering of Composite Materials, Vol. 4, No. 4, 1995.

62. Rouge N., C. Dubois and C. Vermillet, *Characterization of the Open Porosity of Brake Pads. II. Correlations Between Volume Porosity and Surface Area Porosity. Structural Modeling*, Science and Engineering of Composite Materials, Vol. 4, No. 4, 1995.

63. Rouge N., C. Dubois, L. Delage, *Characterization of the Open Porosity of Brake Pads. III. Analysis of the Effects of a Thermal Treatment on Porosity*, Science and Engineering of Composite Materials, Vol. 4, No. 4, 1995.

64. Williams T.M., F.P. Miknis, *The Effect of Antistrip Treatments on Asphalt-Aggregate Systems; An Environmental Scanning Electron Microscopy Study*, Journal of Elastomers and Plastics, Vol. 30, Iss 4, pp. 282-295, 1998.

65. *Ultracote UP-5000 Product Brochure*, Ultrapave, 1300 Tiarco Drive SW, Dalton, GA 37027.

66. Khattak M.J. and G.Y. Baladi, *Engineering Properties of Polymer-Modified Asphalt Mixtures*, Asphalt Mixtures Components, Transportation Research Record 1638, pp. 12-22, 1998.

67. Hawley M., L. T. Drzal, and G. Y. Baladi, *Polymers in Bituminous Mixtures, Phase II*, Final report, Michigan Department of Transportation (MDOT), 1997.

# GENERAL REFERENCES

# GENERAL REFERENCES

1.  Hawley M., L.T. Drzal, and G.Y. Baladi, *Polymers in Bitumous Mixtures, Phase II*, Michigan Department of Transportation (MDOT) Quarterly Progress Report, Jun. 16, 1994 - Sept. 15, 1994.

2.  Idem, Sept. 16, 1994 - Dec. 15, 1994.

3.  Idem, Dec. 16, 1994 - Mar. 15, 1995.

4.  Idem, Mar. 16, 1995 - Jun. 15, 1995.

5.  Idem, Jun. 16, 1995 - Sept. 15, 1995.

6.  Idem, Sept. 16, 1995 - Dec. 15, 1995.

7.  Idem, Dec. 16, 1995 - Mar. 15, 1996.

8.  Idem, Mar. 16, 1996 - Jun. 15, 1996.

9.  Idem, Jun. 16, 1996 - Sept. 15, 1996.

10. Idem, Sept. 16, 1996 - Dec. 15, 1996.

11. Idem, Dec. 16, 1996 - Mar. 15, 1997.

12. Idem, Mar. 16, 1997 - Sept. 15, 1997.

13. Hawley M., L.T. Drzal, and G.Y. Baladi, *Polymers in Bitumous Mixtures, Phase II*, Michigan Department of Transportation (MDOT) Final Report, March 16, 1994 - August 31, 1997.